2014•2015
FACULTEIT INDUSTRIËLE INGENIEURSWETENSCHAPPEN
master in de industriële wetenschappen: nucleaire technologie

Masterproef

Accident dosimetry with mobile phones: Real-time measurements by means of mobile phone applications & Post-accident dose reconstruction with SIM cards

Promotor :
De heer Luc LIEVENS

Promotor :
Mrs. LUANA DE FREITAS NASCIMENTO

Gezamenlijke opleiding Universiteit Hasselt en KU Leuven

Ruben Willems

Scriptie ingediend tot het behalen van de graad van master in de industriële wetenschappen: nucleaire technologie

2014•2015

Faculteit Industriële ingenieurswetenschappen

master in de industriële wetenschappen: nucleaire technologie

Masterproef

Accident dosimetry with mobile phones: Real-time measurements by means of mobile phone applications & Post-accident dose reconstruction with SIM cards

Promotor :
De heer Luc LIEVENS

Promotor :
Mrs. LUANA DE FREITAS NASCIMENTO

Ruben Willems

Scriptie ingediend tot het behalen van de graad van master in de industriële wetenschappen: nucleaire technologie

universiteit hasselt | KU LEUVEN

Acknowledgments

I would like to start with the inspiring quote *"Big things often have small beginnings* "which seems to suit the feeling that I have about my master's thesis. My "big thing" would refer to my master's thesis about radiation detection with mobile phones. And the "small beginnings" refers to my interests in radiation detection with smartphones.

It all started last academic year when I started a project for school. In this school project I developed an interest to detect ionising radiation with cameras and with the help of my mentor Luc Lievens I was able to conduct several experiments in which I investigated several camera properties and so my small thing started to develop into a project. But it was thanks to SCK•CEN, the Belgian nuclear research centre, that I was able to develop my project into my master's thesis. During my internship, my interests of using a mobile phone for radiation detection transformed itself to knowledge and experience and I was able to investigate other options than only using the camera.

With the help of my friends and mentors Dr. Luana F. Nascimento and Dr. Olivier Van Hoey, I was not only able to investigate the mobile phone's cameras but also their SIM cards and additionally also another external detector that was specially created for mobile phones.

I want to thank everyone who helped me to grow during this process, not only my small beginning but also myself.

I want to thank my school mentor Luc Lievens for his guidance through the whole project and also for playing an important role at the "small beginning".

I especially want to thank my SCK-CEN mentors, Dr. Luana F. Nascimento and Dr. Olivier Van Hoey, who helped me and my thesis to grow. I also want to thank them for their professional guidance, their support and also for their much-appreciated patience throughout the preparation of this thesis.

I also want to thank John-David Hendrickx (Proximus) and Nico van Houwelingen (Morpho) for their help regarding SIM cards and especially Morpho (Safran) for providing the SIM cards used in this study.

Last but not least, I want to thank all my friends, my colleagues and my family for sticking with me and supporting me during my thesis.

Table of Contents

Accident dosimetry with mobile phones:
Real-time measurements by means of mobile phone applications &
Post-Accident dose reconstruction with SIM cards

List of tables

List of figures

List of used abbreviations, symbols, units and definitions

Abbreviations

App(s)	Application(s) (software program on/for smartphones)
APS	Active Pixel Sensor
BSI	Back-illuminated sensor
CCD	Charge Coupled Device
CMOS	Complementary Metal Oxide Semiconductor
CW-OSL	Continuous Wave – Optically Stimulated Luminescence
DE	The (ambient) Dose Equivalent
DER	The (ambient) Dose Equivalent Rate
dp	Data point
GB	Giga Byte
GM	Geiger-Müller
IAEA	Internal Atomic Energy Agency
IR	Infra-Red
ISO	International Organization for Standardization
ITDB	Incident and Trafficking Database
LED	Light Emitting Diode
LNK	Laboratory for Nuclear Calibrations
MDD	Minimal Detectable Dose
MMD	Minimum Measurable Dose
MP	Mega Pixels
OSL	Optically stimulated luminescence
PMT	Photo Multiplier Tube
RDA	Research Dosimetric Applications
RDC	Radiation protection, Dosimetry and Calibration
SCK•CEN	Studiecentrum voor Kernenergie - Centre D'Etude de L'Energie Nucléaire (Belgian Nuclear Research Center)
SIM	Subscriber Identity Module
stdev	Standard deviation
TL	Thermo Luminescence
UHasselt	University of Hasselt
UV	Ultra-Violet
Var	Variance of the Polismart

Symbols

λ	Wavelength [m]
ε	Energy imparted [eV][J]
ϕ	Work function [eV]
D	Absorbed dose [Gy][J/kg]
DER	ambient Dose Equivalent Rate [Sv/h]
E	Energy [eV][J]
$E_{k,max}$	Maximum kinetic energy [eV][J]
E	Effective dose [Sv][J/kg]
H	Equivalent dose [Sv][J/kg]
h	Planck's constant [eV s]
$\dot{H}^*_{(10)}$	Ambient dose equivalent rate [Sv/h]
I	Current [A]
I_{OSL}	OSL intensity [Counts]
M	Dosimeter reading
m	Mass [kg]
Q	Dosimetric quantity
S(t)	OSL counts in function of time
v	Frequency [Hz] [s-1]
w_T	Tissue weighting factor
w_R	Radiation weighting factor

Units

A	Ampère
Bq	Becquerel, describes the number of disintegrations per second (s^{-1})
CPM	Counts per minute
eV	Electron Volt (1 eV = 1,602189 x 10^{-19} J)
GB	Giga byte
Gy	Gray
h	Hour
J	Joule
kg	Kilogram
m	Metre
mm	Millimetre (10^{-3} m)
MP	Mega pixels
m/s	Metre per second
nm	Nanometre (10^{-9} m)
s	Second
Sv	Sievert
TBq	Tera becquerel (10^{12} Bq)

Definitions

Apps

Front camera:
The camera located at the screen of the phone.

Back camera:
The camera located at the back of the phone. For our iPhone 4S this is the side with the Apple logo.

Polismart

Plateau (Polismart):
The plateau contains all data points excluded the ones before & after irradiation or where the variation is larger than 10%.

Variation (Polismart):
An on-screen value of the Polismart used to indicate uncertainties.

$$Variation = \frac{200}{\sqrt{detected\ pulses}}$$

Equation 0-1: Variation calculation of Polismart [1]

OSL

OSL counts - S(t):
This is the number of counts (luminescence) that the Riso Reader registered at a certain moment of time *t* while preforming an OSL measurement.

POSL - Posl:
Peak value of the OSL measurement.

$$\text{Posl} = \left\lfloor \sum_{t=0}^{0.2} \frac{\text{S}(t)}{4} \right\rfloor - \left\lfloor \sum_{t=20}^{25} \frac{\text{S}\,(t)}{100} \right\rfloor$$

Equation 0-2: Posl calculation

Abstract in Dutch

In deze masterproef werden smartfoon applicaties geëvalueerd op hun inzetbaarheid tijdens een ongeval met ioniserende straling. Tevens werden ook SIM-kaarten onderzocht voor retrospectieve dosis reconstructies bij de bevolking.

De applicaties werden getest in het kalibratie laboratorium van SCK•CEN met ^{60}Co en ^{137}Cs bronnen, ook werden er testen uitgevoerd met X-stralen. De SIM kaarten werden gekarakteriseerd m.b.v "*continuous wave optically stimulated luminescence"* (CW-OSL), hiervoor werd een *"TL/OSL Reader"* (Risø) gebruikt waarbij er bestraald werd met een ^{90}Sr/^{90}Y β^- bron en uitgelezen m.b.v blauwe LEDs.

De experimenten toonden aan dat de app's een lange stabilistaitetijd hebben van minstens 10 min en zelfs langer voor natuurlijke achtergrond straling. Deze eigenschap beperkt ten sterkste het gebruik van app's tijdens ongevallen. Ook werd een GM buis voor smartfoons getest (Polismart PM1904), deze vertoonde een veel snellere stabilisatietijd, accuratere metingen en een betere dosistempo lineariteit.

Bij de SIM-kaart testen werd er een relatief vlakke dosis respons (getest tot 4 Gy) en een significant verschil in de gevoeligheid van de verschillende kaarten gevonden. Het OSL signaal is reproduceerbaar met een afwijking van 10%. De kaarten kunnen gebruikt worden om dosissen boven 10 mGy te reconstrueren. Maar de sterkste limiterende eigenschap is signaalvervaging. Wanneer ze een paar uur, een dag of weken na het ongeval worden uitgelezen zal de signaalsterkte respectievelijk met 50%, 75% en 90% gedaald zijn.

Abstract in English

In this work we investigate the use of smartphone applications to evaluate dose rates in case of incidents/accidents with ionizing radiation and the use of SIM cards for retrospective assessment of doses received by the public.

The performance of the applications was tested in the calibration laboratory of SCK•CEN with ^{60}Co and ^{137}Cs sources and additional tests with X-rays were performed while the SIM cards were characterised by performing continuous wave optically stimulated luminescence (CW-OSL) measurements on several types of SIM cards using a TL/OSL Reader (Risø). The samples were irradiated with a ^{90}Sr/^{90}Y β^- source and stimulated with blue LEDs inside the Reader.

The experiments showed that the apps have a long stabilisation time of at least 10 min and even longer for natural background levels. This clearly limits the use in emergencies. Also the Polismart PM1904, an add-on GM tube for smartphones, was tested. This dedicated detector exhibited a much lower stabilization time, more accurate readings and a better dose rate response.

Our SIM card tests showed a relative flat dose response up to 4 Gy and a significant difference in sensitivity between different cards. The OSL signals are reproducible within a deviation of about 10%. It was found that SIM cards can be used to reconstruct doses above 10 mGy. However, the strongest limitation is the fading of the OSL signal. Analysing a SIM card after a couple hours, a day or a few weeks will result in a signal drop of respectively 50%, 75% and 90%.

1 Introduction

When a person is exposed to ionising radiation, they might develop injuries. These injuries can be small things like sickness and burns, but when a person received a high level of radiation they can experience more severe and lethal injuries. A correct and fast medical response is there for very important. If the doctors know at what level of radiation the victim was exposed they know which injuries might develop and how they need to evaluate their patient's situation [2].

Persons working with ionising radiation are wearing dedicated dosimeters to determine their occupational dose. In case of an accident, if needed, the worker can be brought directly to the hospital and the doctors can be informed about their exposure thanks to the worn dosimeter. Members of the public don't wear any dedicated dosimeter, which makes a fast response in case of an accident very difficult. Therefore it is in the interest of the public heath to know the doses to which the public is exposed to.

In this study, we investigate the use of mobile phones to detect ionising radiation. The mobile phone, in this case more specifically smartphones, can be equipped with software that uses an external detector or its own camera to detect ionising radiation.

A mobile phone can also be used to assess the received dose after irradiation. Previous studies and research [3-5] found that several components are suitable for dose assessments; however for these components (e.g. resistors and screen glass [3, 6, 7]) it is first needed to destroy the phone and to remove the components manually. This is a very time consuming job however since most SIM cards are radio-sensitive and easily removable, we investigate how we should analyse these cards in case of a nuclear emergency.

The SIM card seems to be suitable for dose assessments however a fast working protocol is missing, making a fast read-out in case of an emergency difficult. To make a fast response possible, the SIM cards must be characterised and a working protocol must be created.

Not only was the mobile phone's hardware studied but also their software. These studies [8-10] investigated several smartphone applications and we will continue in this line of research in which we want to check these app's usefulness in case of a nuclear incident, such as the nuclear accident in Fukushima.

2 Dosimetry

2.1 Dosimetric units

In order to make dose assessments there is the need to express the amount of radiation that a person or object receives. This can be done with the quantity "*absorbed dose"*.

The absorbed dose is defined as the mean energy ($\bar{\varepsilon}$) that is imparted per unit of mass due to ionising radiation to the matter of mass m in a finite volume V.

$$D = \frac{\mathrm{d}\bar{\varepsilon}}{\mathrm{d}m}$$

Equation 2-1: Absorbed dose

The mean energy imparted ($\bar{\varepsilon}$) is calculated as the sum of all energy entering the volume (V) subtracted by all the energy leaving this volume and the mass-energy conversion within this volume has to be taken into account. The SI-unit of the absorbed dose is gray (Gy) where 1 gray resembles 1 joule per kilogram (J/kg) [2].

A quantity that takes the effect of the types (and energies) from ionising radiation into account is the "*equivalent dose*". The equivalent dose of a certain tissue (H_T) takes the harmfulness of each type of radiation into account by multiplying the absorbed dose (D_T) with a certain radiation weight factor (w_R). This weight factor differs per particle; X-rays, gamma-rays and electrons have a radiation weight factor of 1. When a particle has a higher w_R-value , e.g. alpha particles ($w_R = 20$), the ionisation events are much more closely spaced which leads to a higher probability for irreversible damage (to chromosomes) and a smaller chance of tissue repair.

The equivalent dose (H) of a tissue is defined as the sum of all absorbed doses (in that tissue by a certain radiation type R) multiplied with a corresponding radiation weighting factor (w_R). The equivalent dose is expressed in the SI-unit joule per kilogram and its name is sievert (Sv):

$$H_T = \sum_R w_R \, D_{T,R}$$

Equation 2-2: Equivalent dose

After correcting the absorbed dose for the particle type (Equation 2-2), an extra factor must be added to correct for the effect of different types of tissue. Some tissues are more sensitive to stochastic effects than others and this effect is taken into account by means of different tissue weighting factors (w_T). For example, the gonads ($w_T = 0.08$) will have a higher risk on stochastic effects than skin tissue ($w_T = 0.04$) [2].

The effective dose E is defined as the summation of all the tissue's equivalent doses each multiplied by a corresponding tissue weighting factor (w_T) and is expressed in joule per kilogram or sievert (Sv):

$$E = \sum_T w_T \, H_T$$

Equation 2-3: Effective dose

Certain dosimetric quantities cannot be measured directly which is a problem for calibrating radiation monitors. To solve this problem the ICRU has created some operational quantities, such as the ambient dose equivalent [11].

The ICRP 103 defines the *Ambient dose equivalent H**(10) as *"The dose equivalent at a point in a radiation field that would be produced by the corresponding expanded and aligned field in the ICRU sphere at a depth of 10 mm on the radius vector opposing the direction of the aligned field."[2] (p 17)* and is expressed in joule per kilogram or in sievert (Sv).

The ambient dose equivalent is used for environmental monitoring in contrast to the personal dose equivalent which is used for personal monitoring. The ambient dose equivalent *H**(10) is an isotropic quantity defined in such a way that for most radiation fields it gives a conservative estimation for the effective dose. Directional quantities *H*'(0.07) and *H*'(3) are defined such that they give conservative estimates of the equivalent dose of respectively the skin and the eye lens. The corresponding quantities for personal monitoring are *H*p(10), *H*p(0.07) and *H*p(3), which are all three directional quantities [2].

While calibrating a radiation monitor it is also important to know what kind of value they register. If they are placed in open air, they are registering the dose in air which is dissimilar to the dose in tissue.

2.2 Dosimetry for accidents

According to a report of the International Atomic Energy Agency (IAEA) a total of 2477 incidents took place in the period 1993-2013. These incidents were reported by member states and several non-participating states to the IAEA's database for Incidents and Trafficking (ITDB). More than half of the incidents involved unauthorized activities such as the discovery of uncontrolled sources and unauthorised disposal of radioactive materials. In about 27% of the cases theft or loss of radioactive material was involved and 17% of the incidents were linked with unauthorised possession of radioactive material (related to criminal activities) [12].

An example of an accident with ionising radiation is the Chile accident (2005). A radiographer used a nuclear source (^{192}Ir ~3.33 TBq) to study a welding. After completing the radiography, the man dismantled his equipment but didn't notice that the source had fallen out of its original place. The following day another worker found the mysterious object and examined it closely. He showed it to several co-workers and putted it into his pockets. Later he took the object to the office of his supervisor and while the source was in his supervisor's office, an electronic dosimeter alarm was activated in a neighbouring office. The object was left in a metal pipe lying in the yard near to the office building. A specialist measured the dose rate (~1 mSv/h at a distance of 2 m from the pipe) and was able to store the source safely. The three workers were first examined on site and later transferred to a hospital. A biodosimetry test was performed for 34 workers that were potentially exposed to doses higher than 100 mSv [13].

In case of a radiological incident, the TMT handbook [14] suggests that 5 additional teams next to the non-radiological teams are created. One of these teams is the monitoring team which contains e.g. staff from the first responder organisations. Another team is the dose assessment team which tries to estimate the received dose by means of biological changes, Monte Carlo simulations, physical dose reconstructions and clinical manifestations of overexposure.

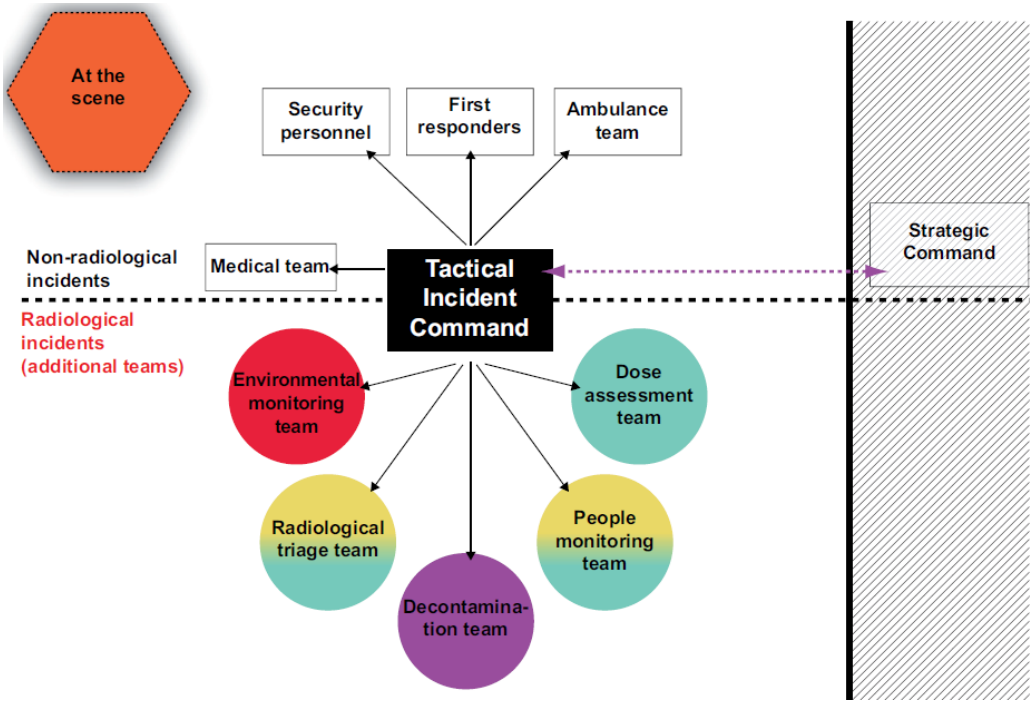

Figure 2-1: Schematic view of the different teams in case of a radiological incident [14] (p558)

The dose assessments team has to estimate the amount of energy that has been absorbed by individuals, this can be done by preforming clinical observations and by dosimetry, which is the art of measuring the absorbed dose delivered by ionising radiation and is applied in numerous situations and topics such as outer-space (space dosimetry) and biology (biological dosimetry).

In case of an incident with ionising radiation, retrospective dosimetry is often used to make dose assessments by using methods that measure persistent chemical, physical or biological changes in inert materials or biological tissues [15].

2.3 Dosimeters

A radiation detector is a device or system that measures radiation quantities or their variation in time on a direct or indirect way. A detector system has 3 functional parts; a detector medium to detect radiation, a reading mechanism and an output or interface; and must have at least one physical property that can be used for measuring dosimetric units.

Radiation detectors can also be divided into 2 categories; a first category, active detectors, contains all detectors that can display their recorded quantities in real-time. This is in contrast to passive detectors which are detectors that have a certain delay between irradiation and showing the measured quantity. This is mostly due the fact that the detector's medium and the reading- and display-mechanism are often separated.

Several of the oldest and most used detectors are gas-filled detectors. These detectors detect radiation by observing the effect of ionisation and excitation of gas molecules. These effects occur along the track from incident charged particles. The most known gas-filled detectors are ionisation chambers, proportional counters and Geiger tubes. These active detectors derives an electronic output signal originating from the created ion pairs, and can be read-out instantly [16].

A more modern type of detector is the Semiconductor Diode Detector (or sometimes called Solid State Detector) which is based on the collection electron-hole pairs from the conductor media such as silicon or germanium. When a charged particle passes the semiconductor, many electron-hole pairs are produced. In order to trap these pairs, an electrical field must be present so that both charge carriers are forced to drift in opposite direction. Once they arrive at an electrode they will generate a current pulse and this pulse is measured by an electronic circuit and thus can be displayed immediately [16]. Thanks to their small and compact size they are an interesting detector however their electronical and thermal noise should be minimalized.

When semiconductors (and insulators) are separated from any circuit they still can be used to measure the absorbed dose. This is due the fact of ionisation of the valence electrons and the creation of electron-hole pairs. The freed electron-holes are localised by pre-existing defects through non-radiative transitions. When an external energy source is applied, such as heat (TL) or light (OSL), the energy is absorbed by the freed electrons which will flowingly recombine, resulting in radiative emission and luminescence. These kind of semiconductors and insulators are used in TLDs (Thermo Luminescent Detectors) or in OSL detectors which are commonly used as a passive detector for radiation protection [17].

a. CMOS camera as Semiconductor Diode Detector

One of the tools that is equipped with semiconductor diodes is the CMOS-sensor in cameras and is dedicated to make pictures in the range of visible light.

Light can be seen as a wave and a particle since it has both properties (Einstein), it has a certain energy and wavelength which will define the light colour and intensity. So when a light particle hit the camera sensor it will transfer their energy to the sensor. This energy will be trapped in the sensor until the camera's software asks the stored energy to be read out in order to show the picture. When everything goes well, the device will show the picture as how its sensor perceived it.

Regarding ionising radiation (X-rays) as a form of light (photons) but with a specific colour X and that our camera can detect it. When we would remake the same picture we should see the same picture again with some pixels coloured with colour X but we can't really notice it through all the other colours. Since we know that light doesn't travel through black tape, and some ionising radiation does, we can easily discriminate the visible light from the ionising radiation by covering the camera with black tape. The sensor doesn't receive any visible light but only beams from the ionising radiation (with the X colour).

This X colour is coming from the ionising radiation which transfers energy to the sensor by ionisation events. The sensor will see this energy transfer as an incident light beam and will display this ionisation on the picture as normal light. If we didn't shield the camera from visible light before, we weren't able to discriminate between the signal coming from ionising radiation and the signal coming from visible light.

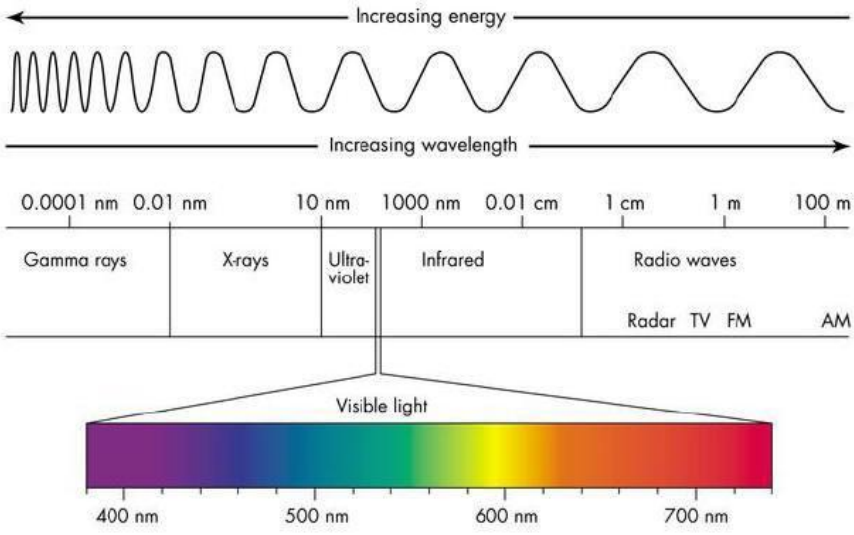

Figure 2-2: Colour wavelengths & perception [18]

Two sorts of digital cameras are used in the mobile phone sector. First there is the CCD-camera which stands for Capacity Coupled Device and secondly there is the Complementary Metal Oxide Semiconductor or CMOS. This last technology is based on the use of semiconductors (CMOS) to make pictures. These low power consuming sensors even have a higher integration for smaller components and outperform CCDs. Due to these properties, the CMOS-sensor is the most used camera sensor in mobile phone now a days [19].

The CMOS sensor is an Active Pixel Sensor (APS) and is an integrated circuit with a pixel matrix in which each pixel (~µm) holds one photodetector (for each main colour e.g. red, blue and green). Thanks to the APS architecture, the CMOS sensor is sensitive to incidence of visible or infrared light. When a light beam reaches a photodetector, a small current power is generated, which is related to the light intensity. This small current is later on amplified and send to the processor.

When the camera is exposed to alpha particles, the camera doesn't detect them since the particles don't penetrate the camera's lenses and filters. When beta particles are ionizing the sensor, they generate an electric current that is proportional to the beam energy:

$$E_{e^-} = I$$

Equation 2-4: Relationship electron energy and CMOS current [20]

If the sensor is exposed to photons (gamma radiation), the photons will create electrons inside the sensor (due to the photoelectric effect) and these will transfer their energy to the photodectectors [20]:

$$E_\gamma = hv = \phi + E_{k,max}$$

Equation 2-5: Relationship gamma energy and CMOS current through photoelectric effect [20]

Where

E_γ is the energy present in the incident photon equal to the product of Planck's constant (h) and the wave frequency (v). This energy is also related to the sum of the work function (ϕ) and the maximum kinetic energy of the ejected photon. ($E_{k,max}$). The work function is a certain energy [eV] that differs for each material and is needed to free an electron from that material [21].

As mentioned earlier, most applications are using a covered sensor to detect radiation. But is this really needed? Most people are using their camera to make pictures. This means that the camera wouldn't be covered with black tape. People will only tape off their cameras if they intentionally want to measure radiation. But is it needed to tape off the camera? Is there a possibility to use a program without taping off the camera?

This question has also been asked by Dosiek Luke and D. Schalk Patrick in a paper about passive radiation detection using optically active CMOS sensors. In their paper [22] they did a preliminary research to invest these question.

Their research was simplified and constricted to a known and calibrated ^{137}Cs source with an activity about 185 kBq. And they used a stationary web-camera to collected data by using video frames [22].

They succeed in proving that their algorithm (describe in their paper [22]) was able to distinguish particle impacts from noise in both, covered and uncovered circumstances. They noticed that their value for a radiation exposed pixel is dependent on the brightness of the ambient scenery. This makes it easier to detect radiation in dark scenes, but makes it difficult to detect radiation in light scenes [22].

b. Geiger-Müller tube

A Geiger tube or a Geiger-Müller (GM) counter is mostly a gas-filled metallic cylinder with an inner central electrode that has been insulated from the outer wall. Both the wall and the inner electrode are wired and a high voltage is applied to reach the GM counter region.

When a particle enters the GM-tube, it creates ions and electrons inside the outer wall and the gas. These electrons are attracted to the central electrode, which is positively charged and the ions will move to the outer wall, resulting in the production of a small current pulse in the connection wires. This pulse is counted and the charged ions become neutralised. After that the GM-tube can measure again [23].

GM counters also have some disadvantages; they have a strong energy dependence at low energies and they can become paralysed in very high radiation fields and display a zero reading [11].

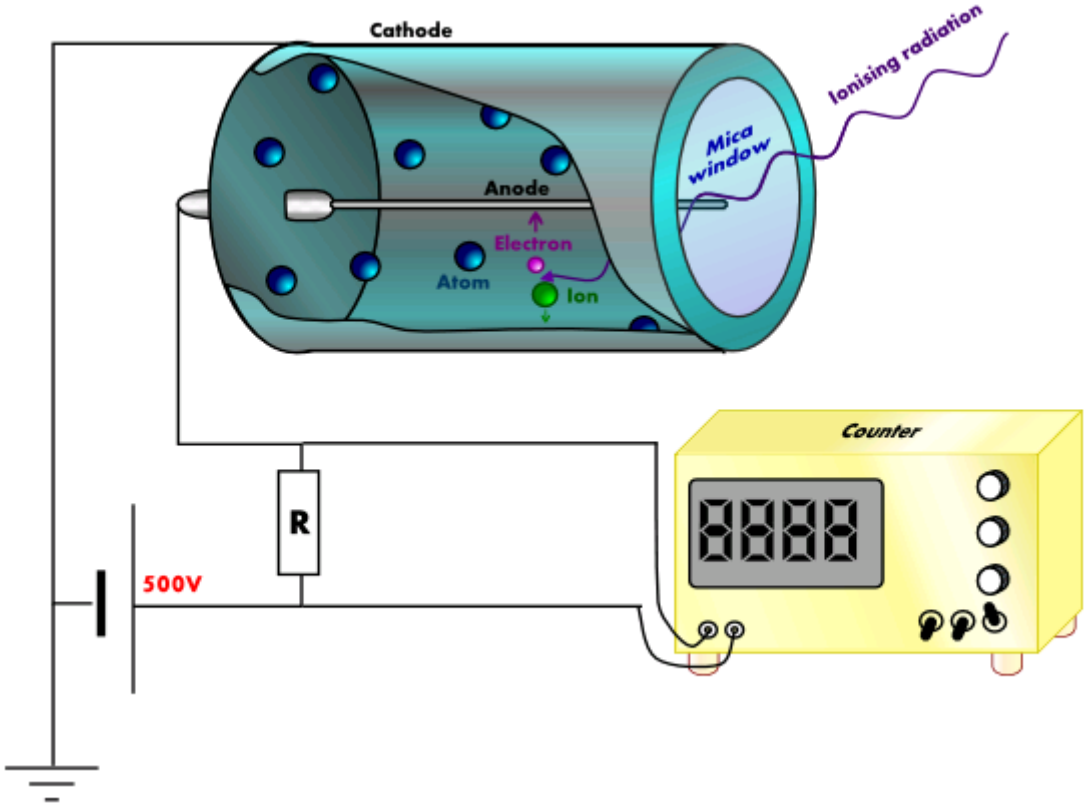

Figure 2-3: A Geiger-Müller detector [24]

In some cases the GM-tube is foreseen with a thin external metal layer such as lead or tin, in this case the detector is called an *energy compensated* Geiger-Müller tube. A bare tube will tend to have a too high efficiency at low X-ray energies (when compared with high energies) and this effect can be solved by applying this small layer. The metal layer filters low energetic X-rays and makes the detector's response more similar at different energies as can be seen in Figure 2-4 [16].

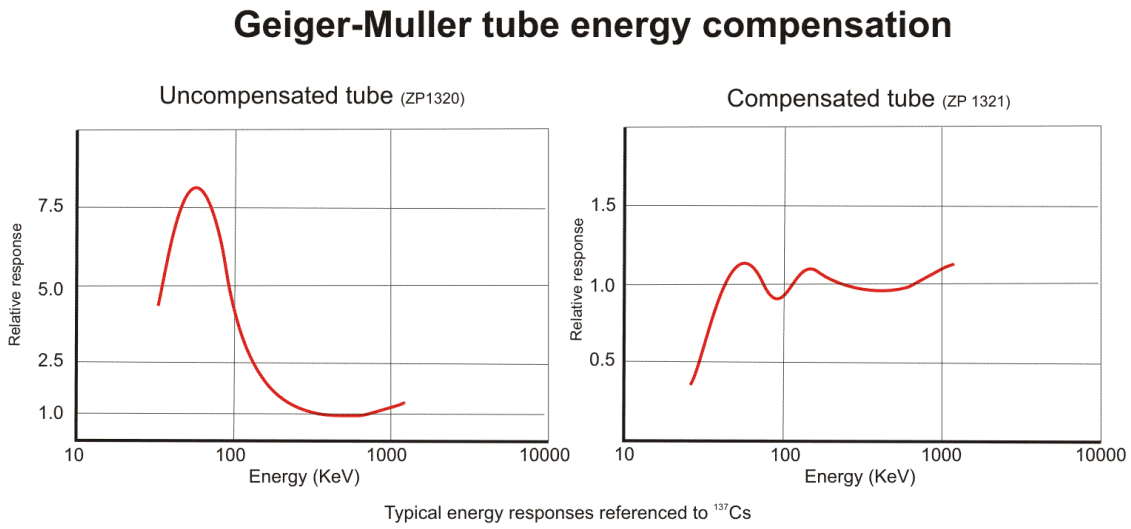

Figure 2-4: Effects of an energy compensated and non-compensated GM-tube [25]

c. Optically Stimulated Luminescence

Optically stimulated luminescence (OSL) is a technique that uses the emitted luminescence from an irradiated semiconductor or insulator, during exposure to light. The OSL intensity can be related to the dose of the absorbed radiation in a sample and therefor OSL can be used as a basis of a radiation dosimetry method.

When a sample is irradiated, valence electrons will be ionised and electron-hole pairs are created. Pre-existing defects within the sample will localise the free electron and holes through non-radiative trapping transitions. Subsequent illumination of the irradiated sample with light leads to absorption of energy by the trapped electrons, the electron will break free from the localised trap and moves through the conduction band into a luminescence centre. Here it will recombine with the localised holes leading to radiative emission occurrence, resulting in luminescence. This signal is also called the OSL signal and is proportional to the absorbed dose [26].

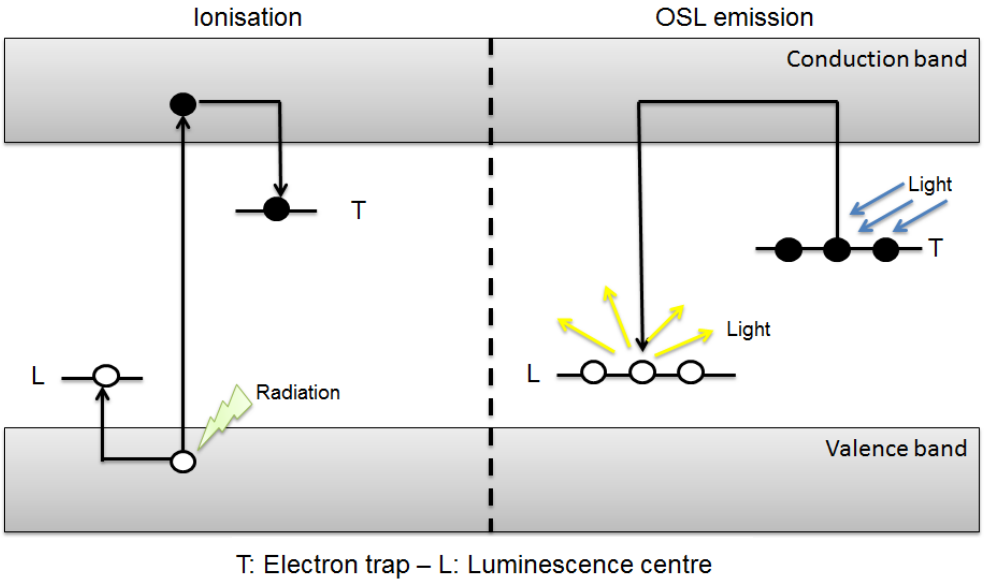

Figure 2-5: Creation of electron-hole pairs due to ionisations and the recombination of them (OSL) by adding external light

The absorbed dose is linked to the traps; the lower and upper limit of the traps will have its influence on the reconstructed dose. One of these limits is the ability to accumulate electron traps (lower limit) while the upper limit is reached when all traps are been filled [27].

In reality the model is more complex: After ionisation electrons situated in the conduction band can move to different traps. The first kind of trap is the shallow trap (level 1) into which electrons might be trapped during optical stimulation (downward arrow). From these shallow traps the electrons may be optically (or thermally) released (upward arrow). Secondly there are the dosimetry traps (level 2) in which trapped electrons can be optically released; and thirdly the deep traps (level 3) where the electrons remain localised. Next to the electron traps, there are also different sorts of recombination or luminescence centres: A radiative recombination centre (level 4) is such centre in which the recombination of electron-holes results in luminescence (OSL). However it is also possible that this recombination happens without luminescence in non-radiative recombination centres [26].

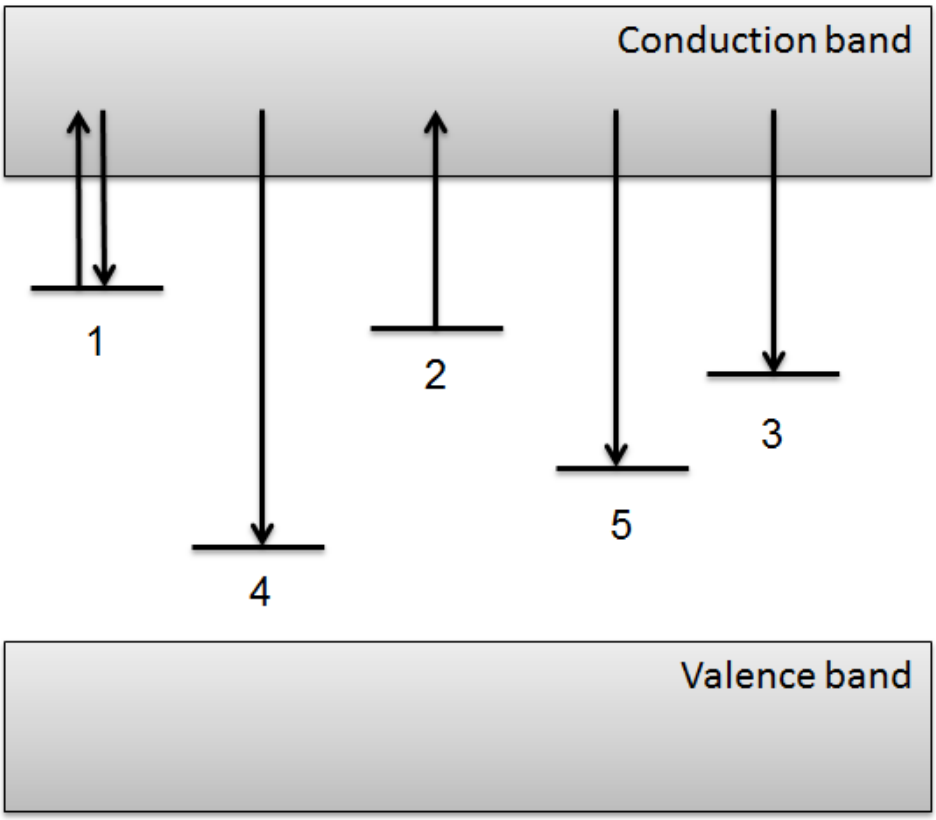

Figure 2-6: A model indicating different traps and recombination centres during optically stimulation [26]

3 Materials & Methods

a. LNK Calibration Laboratory

The LNK (Laboratory for Nuclear Calibrations) of SCK•CEN is a secondary calibration laboratory accredited[1] by the Belgian accreditation organisation BELAC. The lab is equipped with the infrastructure for sample and detector irradiations following national and international standards. The radioactive sources are characterized according to the international standards.[28]

The laboratory is equipped with a lot of different sources and apparatus, but during the study, samples were irradiated with following three devices. (Reference date 2013-10-01)

First, the laboratory has an horizontal set-up with 3 sources of ^{60}Co (labelled as P2, P3 and P4) and 3 sources of ^{137}Cs (Only P11 and P12 have been used). The set-up has a 20° beam opening. The air kerma for ^{60}Co and ^{137}Cs are respectively up to 1.5 mGy/h and 14.1 mGy/h (ISO 4037) [29].

Figure 3-1: The horizontal set-up with 3 sources of ^{60}Co and 3 sources of ^{137}Cs [29]

[1] Conform the ISO 17025 guidelines.

Next to this horizontal setup there is also a panoramic set-up which allows simultaneous irradiation of many dosimeters with a higher dose rate than the horizontal setup. This panoramic set-up has one ^{60}Co source (air kerma up to 33mGy/) and one ^{137}Cs source (with an air kerma up to 360 mGy/h). And thirdly there is a dual X-ray tube generator with energies up to 320 kV [29].

Figure 3-2:The panoramic setup inside the bunker [29]

Figure 3-3: X-ray generator with automatic filter wheel [29]

b. Smartphone apps

With the current technology, individuals and companies are able to turn their own smartphone into an active dosimeter by simply installing an app. These apps requires to tape off the smartphone's camera in order to detect ionising radiation.

Modern smartphones are equipped with one or several cameras. These cameras are mostly equipped with a CMOS sensor accompanied with signal processing hard- and software to make pictures. Since light is a form of radiation, there is the idea that cameras could be used to detect ionizing radiation. In prior research [9, 10, 30], SCK•CEN studied several iPhone 4S applications. These apps are using the build-in camera (front or back camera), which is covered with several layers of tape, to determine the dose rate. We will continue to investigate these apps with the same iPhone 4S devices.

The sensitivity of the smartphones app is related to their hard- and software. Differences in software such as detection algorithms can lead to different readings with the same phone. As for hardware it is the sensitivity of the CMOS sensor that determines the app's sensitivity. These CMOS sensors are not identically and can give significant different values mainly due to the electrical-components and due to differences in the production process.

With the aim to use a commonly used smartphone we decided to use the Apple iPhones 4S, on which we will test several applications[2]. During the measurement the cameras were covered with 3 layers of black tape to prevent exposure to visible light.

The applications iRad[3], Radioactivity Counter[4] and WikiSensor[5] were installed and tested at the calibration laboratory (LNK) at SCK•CEN.

The applications are tested by delivering a reference ambient dose equivalent rate with a ^{60}Co-source (Table 0-1) and additional irradiations of the Radioactivity Counter app are performed with a ^{137}Cs source (Table 0-1).

[2] Version information can be found in Table 0-4 and Table 0-5
[3] Application interface: Figure 3-4 p38
[4] Application interface: Figure 3-5 *p38*
[5] Application interface: Figure 3-6 *p38*

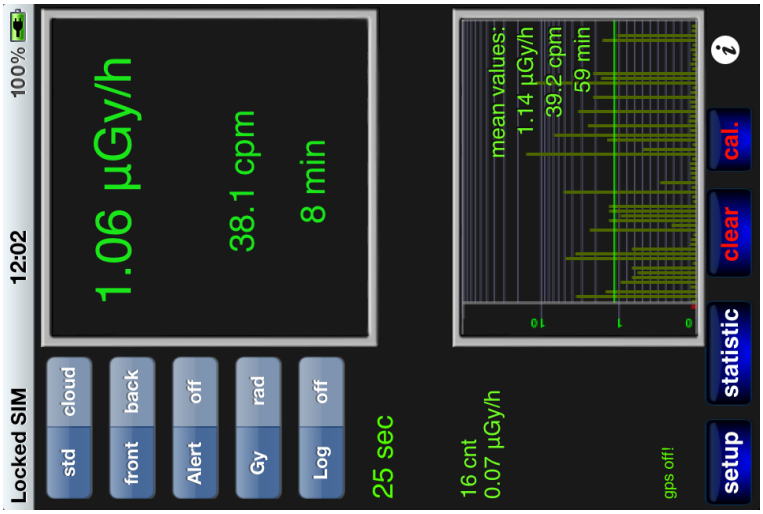

Figure 3-4: Interface of the Radioactivity Counter application

Figure 3-5: Interface of the WikiSensor application

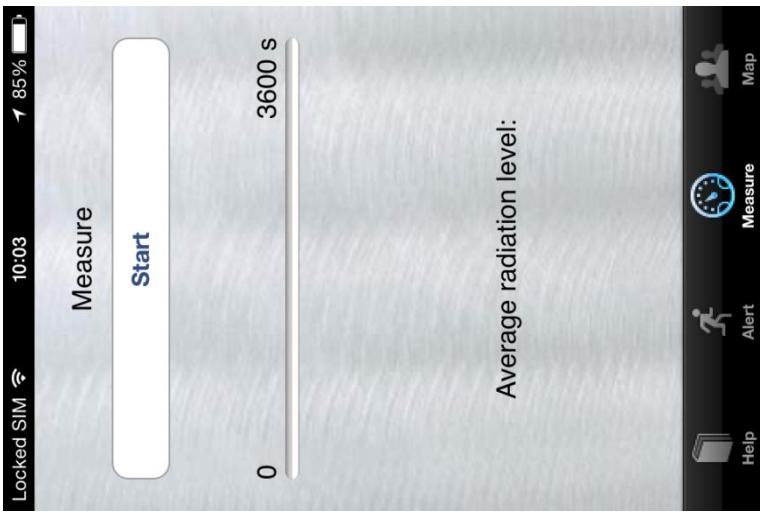

Figure 3-6: Interface of the iRad application

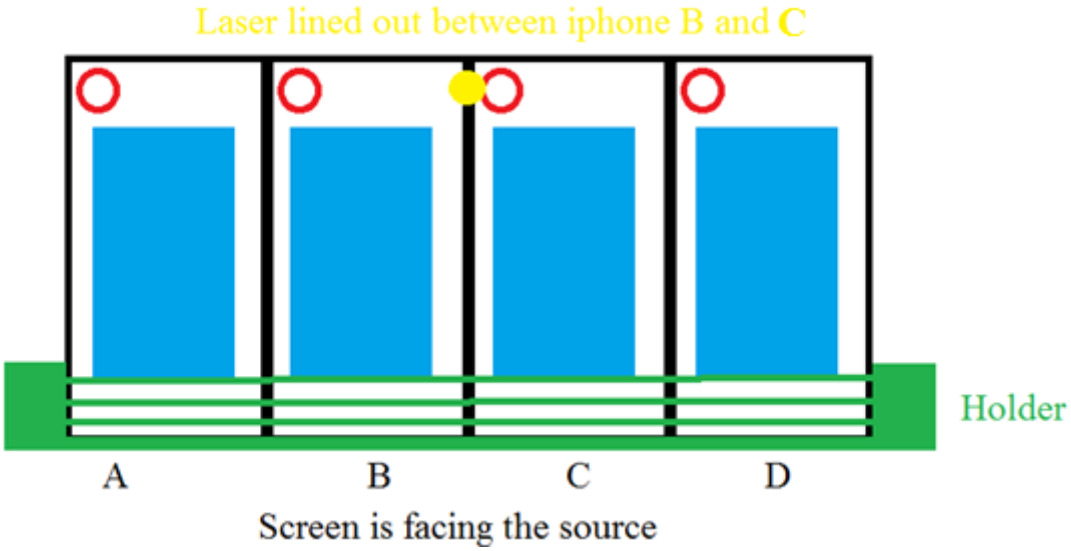

Figure 3-7: Schematic view of the alignment of iPhones during irradiations (Note: Cameras are taped off with 3 layers of black tape)

Figure 3-8: Experimental set-up for irradiations (smartphone apps)

c. Polismart

The *PM1904 Polismart II* (produced by Polimaster®) is an energy compensated Geiger-Müller detector, which can be attached to the iPhone. The detector is designed to measure ionizing radiation from photon emitting sources. To interact with the *PM1904* it is mandatory to install the Polismart application and to attach the *PM1904* to the iPhone [31] .

Figure 3-9: The PM1904 Polismart II [32]

The Polismart Geiger-Müller detector was tested and characterised at the Calibration Laboratory of SCK•CEN by using ^{60}Co and ^{137}Cs β^- sources (Table 0-1) and ISO Narrow series X-ray beams (Table 4-6). The used detector is the Radiation detector PM1904 Polismart® II with serial number 130555 and is connected with an iPhone 4S (Serial number DNXHCM1WDTC0, intern labelled as iPhone D) with operating system firmware version 5.4.00.

The Polismart app (version 1.3.2 by Polimaster Inc.) was installed on the iPhone and was used to log the dose rate. The app's settings were adjusted in order to display metric units and readings in sieverts.

For saving several data points on a regular basis it is better to use the "Track"-option. When selecting the Track Settings (at track screen) it is possible to make a measurement with a certain sample rate. In our case we used a sample rate of 1 data point per second.

The results are exported by using the History-screen by selecting the data set and by sharing it as an email. The email contains a table which can easily be used in excel for further analyses.

Technical information

The PM1904 is accompanied with a short manual that describes several characteristics of the detector, as shown in Figure 3-10. In some cases, the Polismart also determine the statistical error. This is done with the variation and is calculated by Equation 3-1 where n is the quantity of pulses [1].

Detector type	Geiger-Müller tube
DER Measurement range Limits of permissible main relative DER measurement error	0.01 µSv/h – 13 mSv/h; ± 20% in the range 1.0 µSv/h – 10 mSv/h
DE Measurement range Limits of permissible main relative DE measurement error	1 µSv – 10 Sv ± 20 %
Energy range Energy response relative to 0.662 MeV (^{137}Cs), no more than	(0.06 – 1.33) MeV; ± 30 %

Charge time	Up to 4 hours over micro USB
Batterv lifetime at average background < 0.3 µSv/h	2200 hours
Data collection	500 data points
Environmental: temperature range humidity	0 to +50 °C; up to 95 % at +30 °C
Ingress protection	IP30
Drop Test	0.7 m onto concrete surface
Dimensions – Weight	59 x 45 x 15 mm 30 g

Figure 3-10: Technical specifications PM1904 Polismart® II [32]

$$\text{Variation} = \frac{200}{\sqrt{n}}$$

Equation 3-1: Variation calculation of Polismart [1]

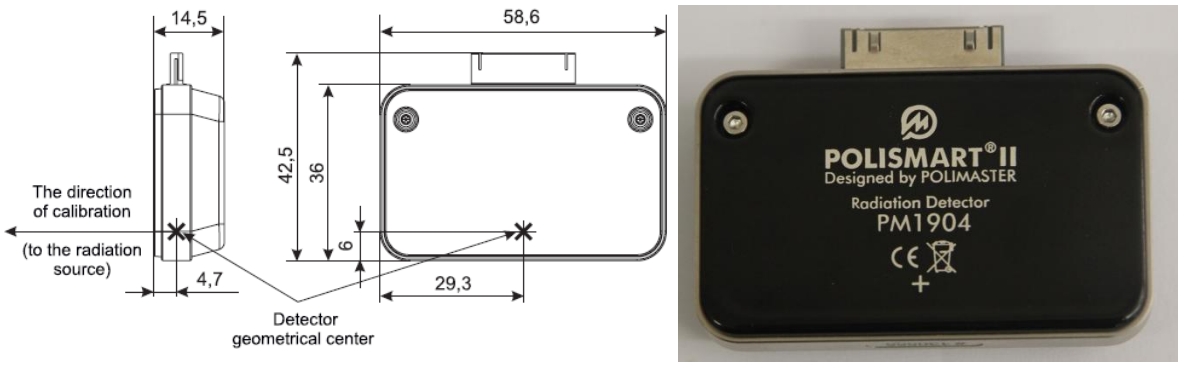

Figure 3-11: Dimensions of the PM1904 Polismart II [32]

d. SIM cards

Several components of the mobile phone such as glass, resistors and capacitors can be used as a passive dosimeter [5]. Removing such components often requires time and handwork, but one component can be extracted quickly and easily: The SIM card.

The SIM card has a radio-sensitive epoxy used to protect and encapsulate the chip module underneath the golden contacts. J.H. Barkyoumb discovered that "*... the radiation sensitivity of the epoxy is due to the silica used as the 'filler' for controlling the thixotropic properties of the epoxy used for 'glob top' or 'dam-and-fill' encapsulation"[33]*. This epoxy can either be transparent or painted black.

Silica (Silicium Oxide (SiO_2) or quartz) is a known radio-sensitive material that can be read-out by means of Optically Stimulated Luminescence (OSL) [26]. Another option is to read these particles by Thermo Luminescence (TL) but with an unknown melting temperature for each epoxy, the reader can easily been contaminated by vaporised particles, which can influence the results of future measurements and is an undesired effect.

In previous studies it was noticed that non-transparent epoxies (e.g. painted black) give bad results during OSL, this is due to the fact that the black coating prevents the optical stimulation and the observation of the resulting luminescence [34].

In this research the OSL-signal will be observed and tested with the Risø TL/OSL Reader, model *DA-20* from DTU Nutech (Figure 3-12).

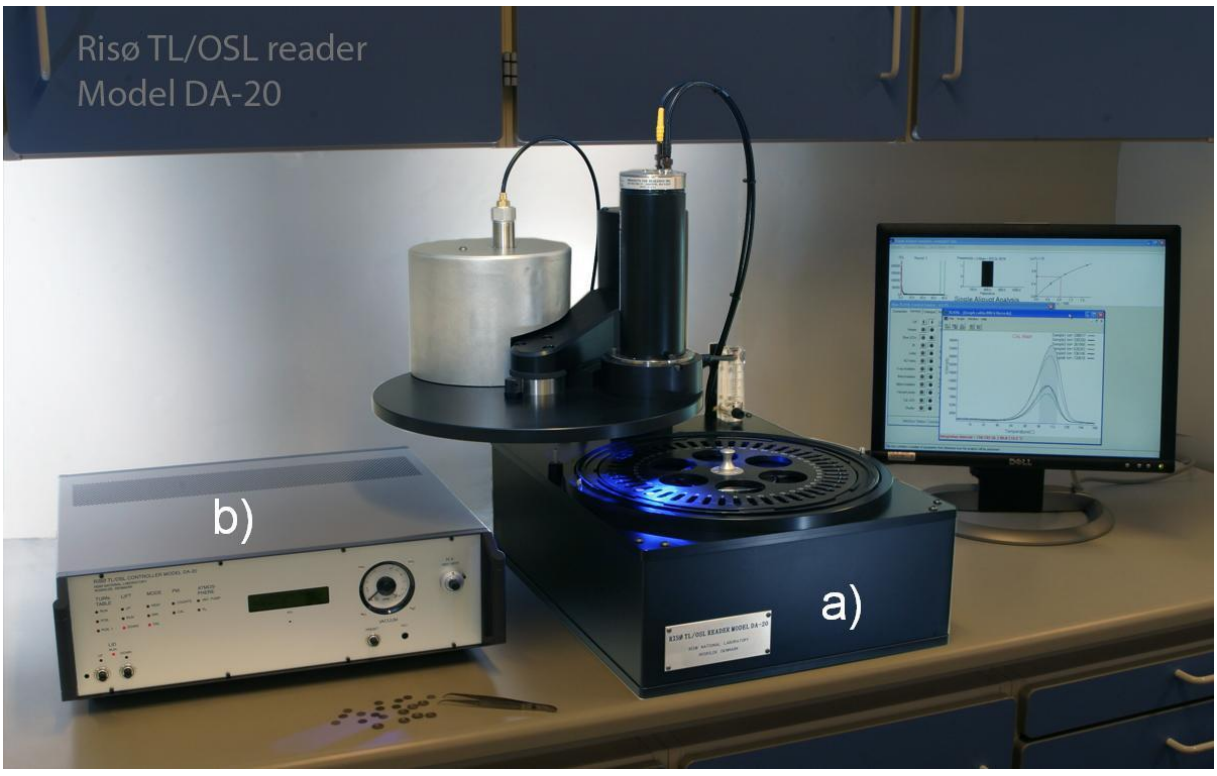

Figure 3-12: The Risø TL/OSL reader, model DA-20 from DTU Nutech [35]

The Risø TL/OSL reader

The Risø TL/OSL reader is an apparatus dedicated to measuring TL and OSL signals. The reader is placed in a dark room equipped with red lights; this has been done to minimalize the signal reduction of light sensitive samples (OSL).

The Risø consists of several parts, the first part is the controller-unit (marked with *b* on Figure 3-12), secondly the Reader-unit (marked with *a* on Figure 3-12) and thirdly a fully equipped computer.

The computer communicates with the controller and the controller sends the commands to the reader-unit. The commands are used to control the light detection system, the TL/OSL-system, the irradiation sources and several other components in the reader-unit. The light detection system uses several detection filters and a photon multiplier tube (PMT) while the TL/OSL-system contains a heating element and an optical stimulation unit. The Risø is able to contain an alpha source, a beta source and an X-ray tube. However the used Risø at the lab is only equipped with a $^{90}Sr/^{90}Y$ β^- source (Table 0-1) for sample irradiation. Figure 3-13 shows these various components of the reader-unit [35].

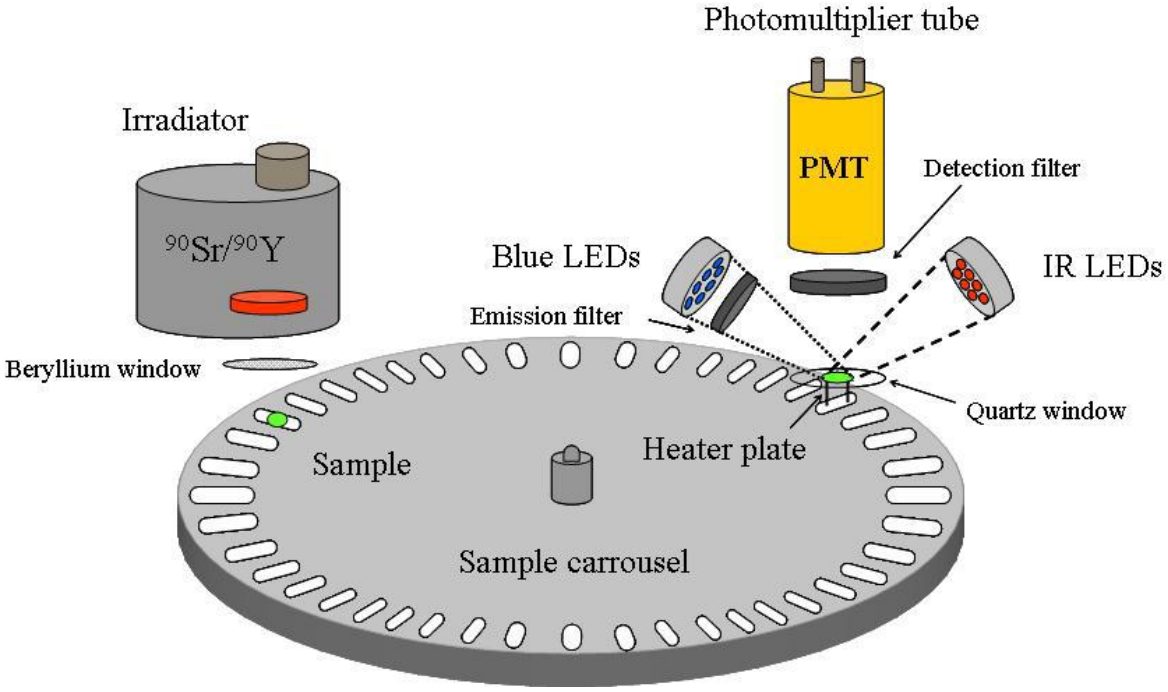

Figure 3-13: Schematic drawing of the Risø TL/OSL reader [35]

The samples are placed into cups (stainless steel discs about 9.7 mm) and put onto the sample carrousel. The Risø is equipped with a motor to rotate the sample carrousel while an opto-electronic system keeps track of the carrousel position. When the sample is placed at the TL/OSL system's position, the cup will be lifted up by the heating element, which also functions as an elevator and placed in the correct position to be illuminated with the LED's.

The samples are analysed with blue LEDs (470 nm) at 40.5 mW/cm² (90% of their optically power) by Continuous Wave OSL (CW-OSL). This means that the light source illuminate the sample with a constant intensity and simultaneously monitor the luminescence [26, 35].

The Risø reader has a light detection system containing a filter (*Hoya U-340*) and a photomultiplier tube (*bialkali EMI 923QB* PMT). The photomultiplier tube has a maximum detection efficiency in the range of 200-400 nm and operates in "photon counting" mode (counting charged pulses at the anode). According to the Risø-manual, many samples are weakly luminescent and in order to optimise the light collection, the sample-detector distance is about *55* mm [35].

Quartz (Silica) has a strong emission centre near UV at a wavelength about 365 nm but to detect these we need to filter out the stimulation light (470 nm) by using Hoya U-340 filter (Figure 3-14).

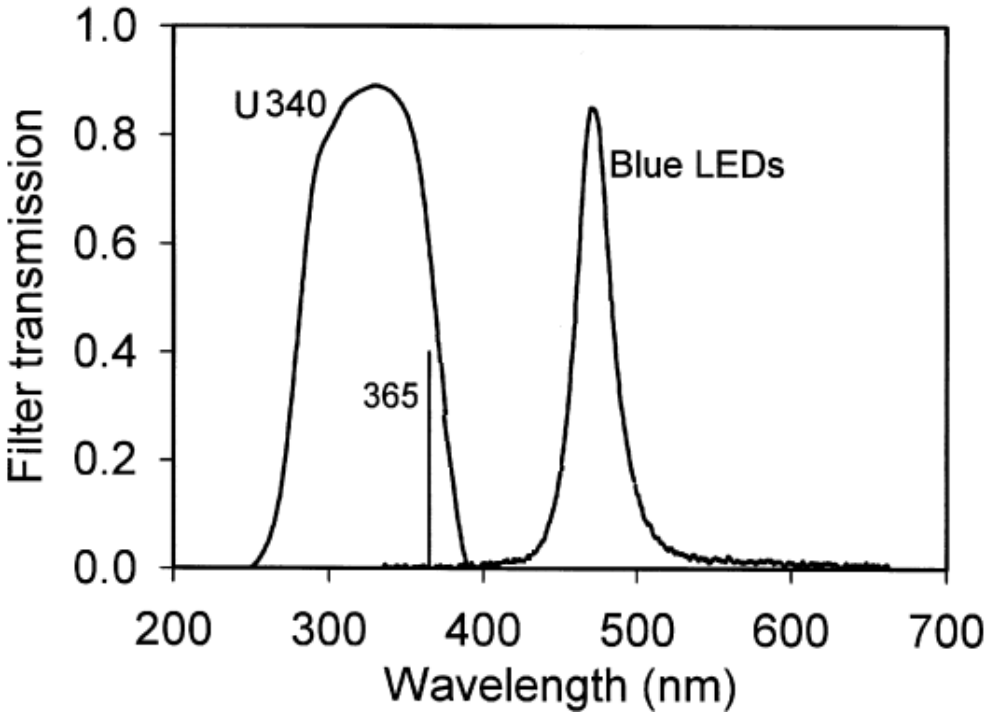

Figure 3-14: Characteristics for the Hoya U-340 filter in the Risø OSL detection system and the blue LEDs emission, the line at 365 nm shows the peak emission for OSL at room temperature [36]

Remark: The used beta radiation of $^{90}Sr/^{90}Y$ is probably not strong enough to irradiate significantly the SIM cards inside a mobile phone. Therefor we assume that the SIM cards have been irradiated and next we characterise the SIM card by using this source.

Signal settings & processing

The OSL intensity derived from the Risø is given in function of a record number. To transform this record number to time, we have to multiply it with the sample rate which is 0.05 (seconds per data point) in our case. The OSL signal will be analysed in excel by using the Peak value of the OSL measurement (Posl) and is calculated as the average of the first 0.2 second signal minus the background.

$$\text{Posl} = \text{P} - \text{B}$$

Equation 3-2: Posl calculation

With P the signal's peak:

$$\text{P} = \left\lfloor \sum_{t=0}^{0.2} \frac{\text{S}(t)}{4} \right\rfloor$$

Equation 3-3: Peak signal calculation

And with B the signal's background, which is the average of the 20-25 seconds of the signal:

$$\text{B} = \left\lfloor \sum_{t=20}^{25} \frac{\text{S}\,(t)}{100} \right\rfloor$$

Equation 3-4: Background calculation

These intervals are based on previous work of Vanessa Cauwels ([7]), the peak signal interval is chosen based on the time window in which the fast component is most explicitly represented (in our case the first 0.2 seconds) and a background signal between 20-25 seconds to make sure the recorded signal is not due the fast component.

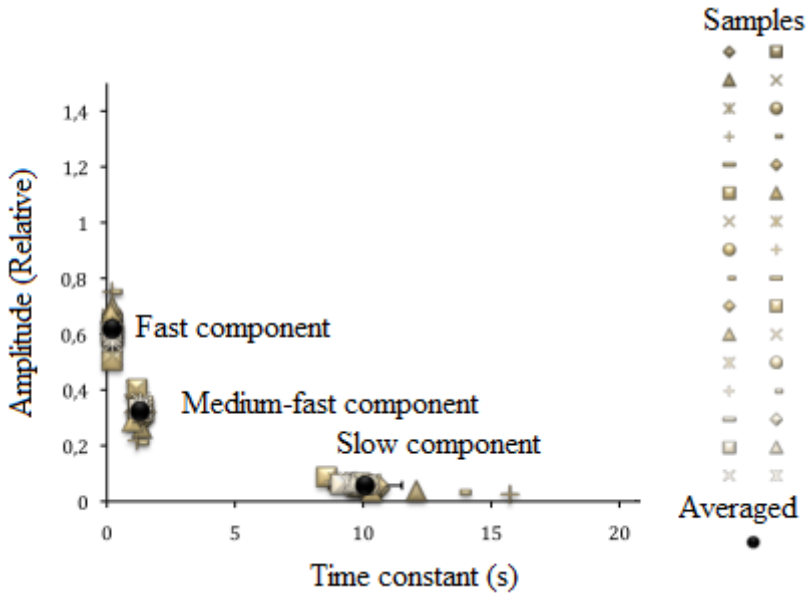

Figure 3-15: The different OSL components of SIM cards [7] (p59)

Next to the thesis of Vanessa Cauwels, we also compared our time window with results of an extended study ([37]) which studied the zero dose and the uncertainty on it. The findings of that study (Figure 3-16 and Figure 3-17) shows us that our integration window for Posl is good since it would minimalize the zero dose and their uncertainty.

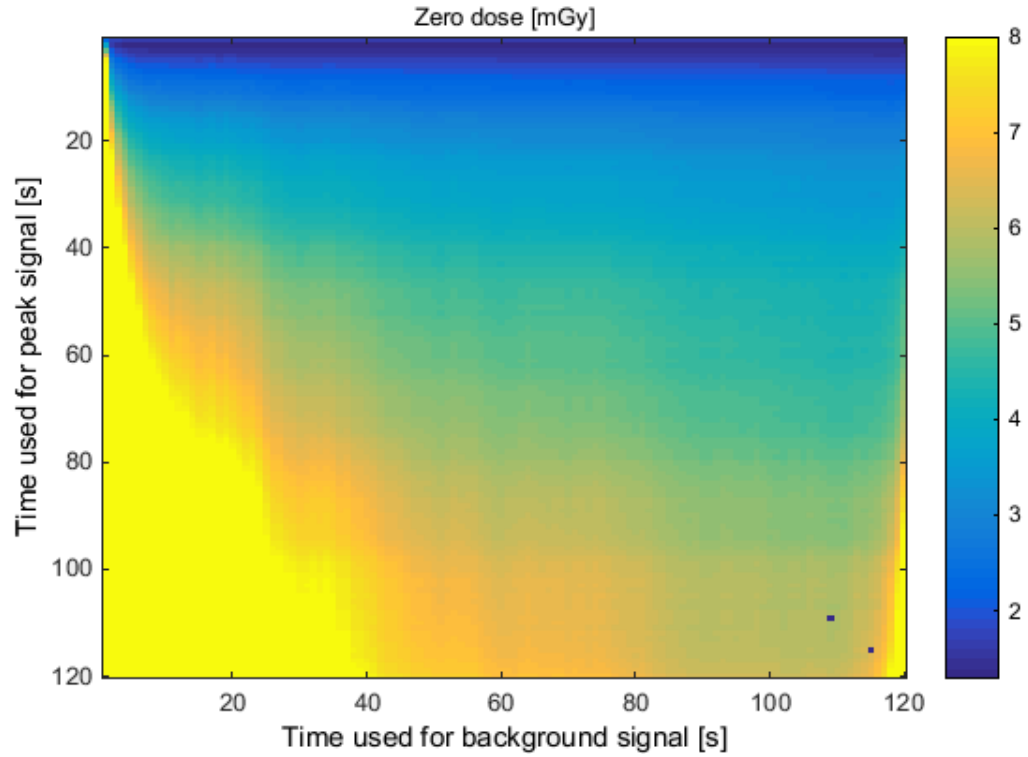

Figure 3-16: Zero dose calculation of SIM cards [37]

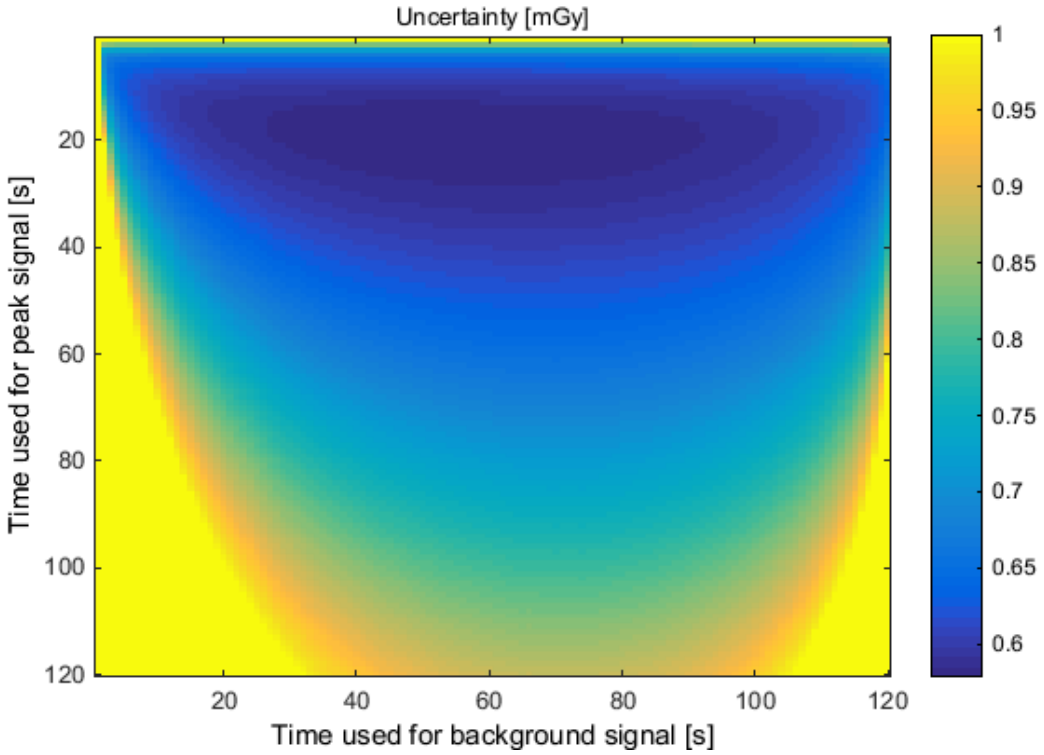

Figure 3-17: Uncertainty calculation for zero dose [37]

Samples

For our research we started with a bunch of chip cards (not SIM cards) from the company Unipas. After sampling this *SLE5542* chip card we noticed that there was no noticeable amount of epoxy applied on the chip module.

Figure 3-18: The SLE5542 card from Unipas.nl [38]

For practical reasons we want to investigate the SIM cards used in Belgium. We contacted two of the biggest telecom providers to request their help in this study. Proximus replied positively and brought us in contact with one of their SIM card suppliers: Morpho (Safran).

The people of Morpho (Safran) were so kind to give us a lot of usable samples. From the 8 different types[6] we received 4 different types of SIM cards[7] (Figure 3-19) and 4 types of chip modules[8] with different epoxies (Figure 3-20 and Figure 3-21).

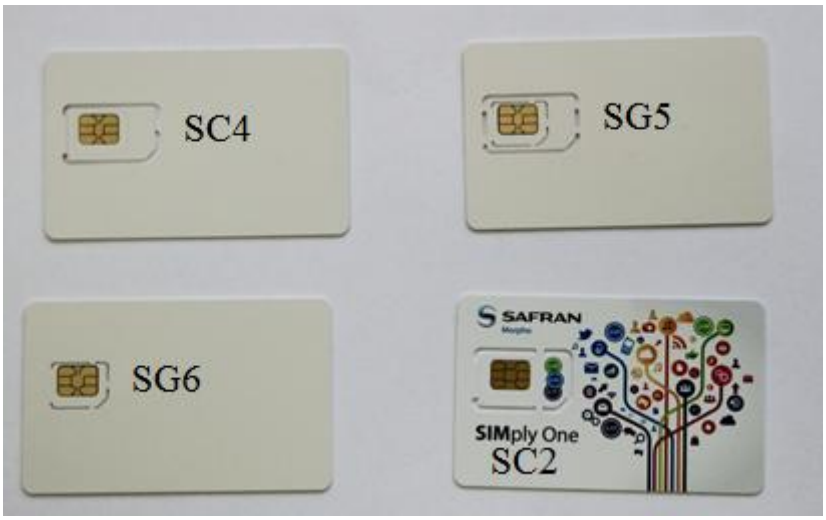

Figure 3-19: Morpho SIM cards [38]

[6] More technical data can be found in Annex A (Table 0-6 and Table 0-7).
[7] *SG6, SG5, SC4 and SC2.*
[8] Named after the used epoxies: *Delo 698/4670, Vitralit 1680, Loctite 3323/3327 and Delo 4670*.

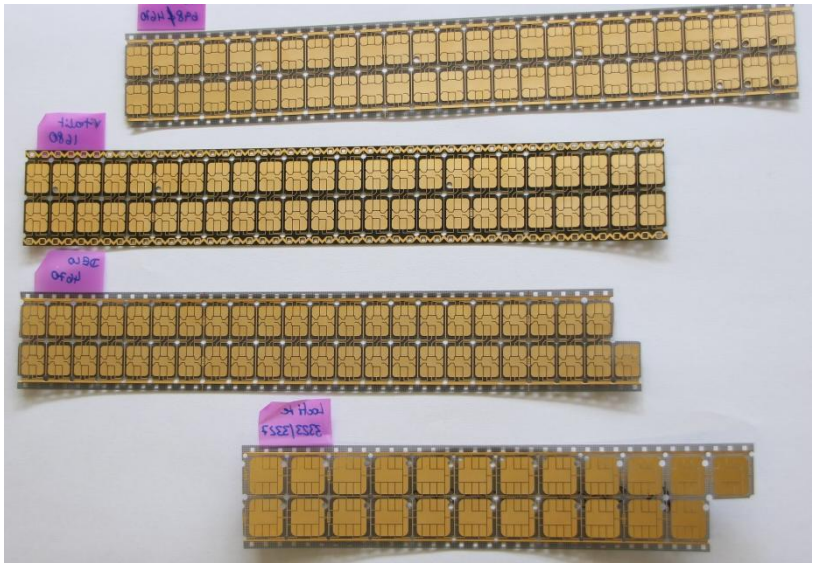

Figure 3-20: Morpho SIM card modules (front side);
from top to bottom: *Delo 689-4670; Vitralit 1680; Delo 4670; Loctite 3323-3327*

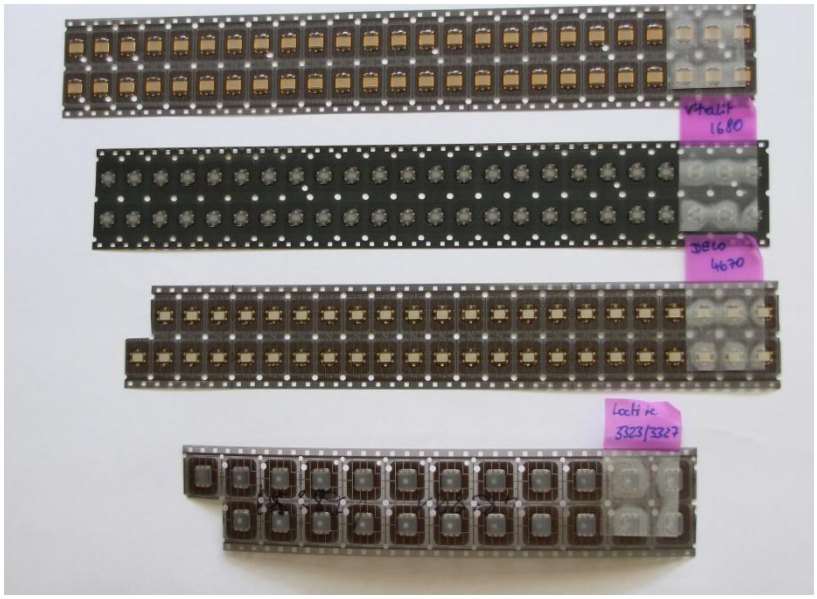

Figure 3-21: Morpho SIM card modules covered in epoxy (back side);
from top to bottom: *Delo 689-4670; Vitralit 1680; Delo 4670; Loctite 3323-3327*

Each sample is allocated to a certain set. A set is used for numbering samples. The first sample of each SIM card is allocated the number 1, the second sample is allocated the number 2 etc. So in total there will be 8 samples with number 1. These 8 samples are then collected in a set. Set 001 contains all the SIM card samples with number 1. Each set has 8 positions and the filling of these positions are based on the card's type. For example the 4th position in each set is filled in by a corresponding Delo 4670 sample.

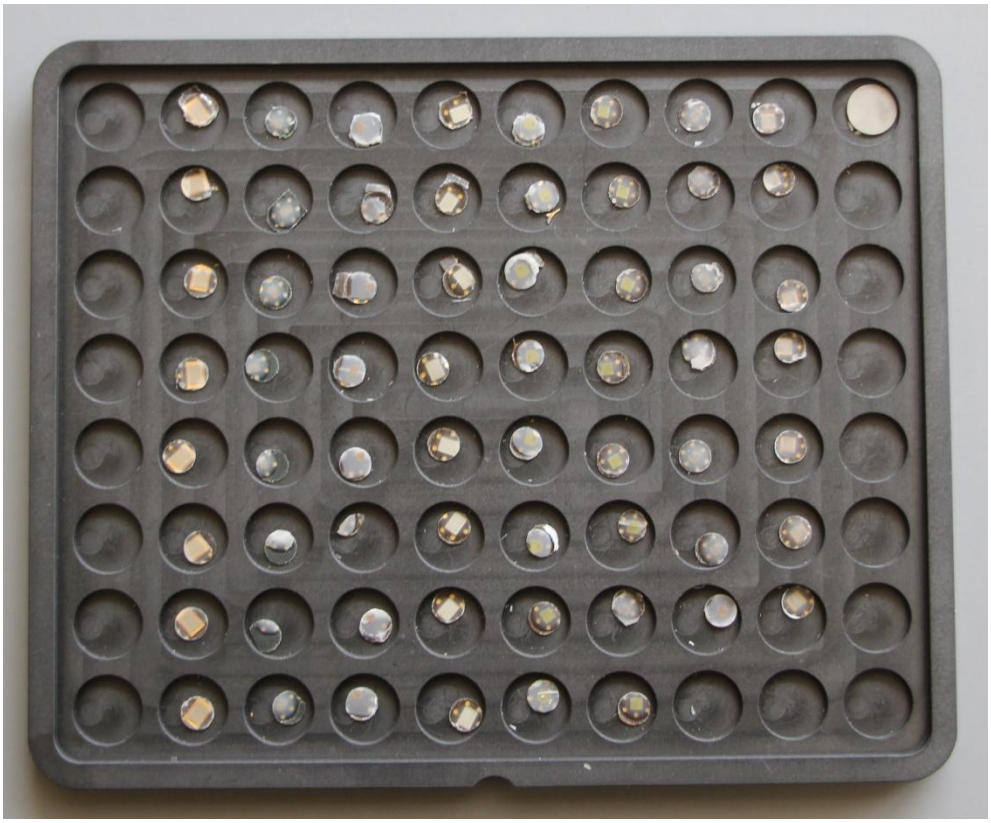

Figure 3-22: Samples arranged as a matrix, each row representing a different set and each column representing all the samples of a certain type. More samples than displayed are used

Remark: The samples have been sorted like this for practical reasons.

Sample preparation

In order to determine the absorbed dose it is required to analyse the cards. This is done with the Risø TL/OSL Reader. The Risø has a circular cup/sample holder of about *7-8* mm inner diameter and therefore the samples are punched out with a 6 mm punch as seen in Figure 3-23 and Figure 3-24. The punched sample will then be placed into cups (Figure 3-25), which are then placed in a carousel inside the Risø. This whole process is preformed inside the dark room under red light.

Figure 3-23: A punch (tool)

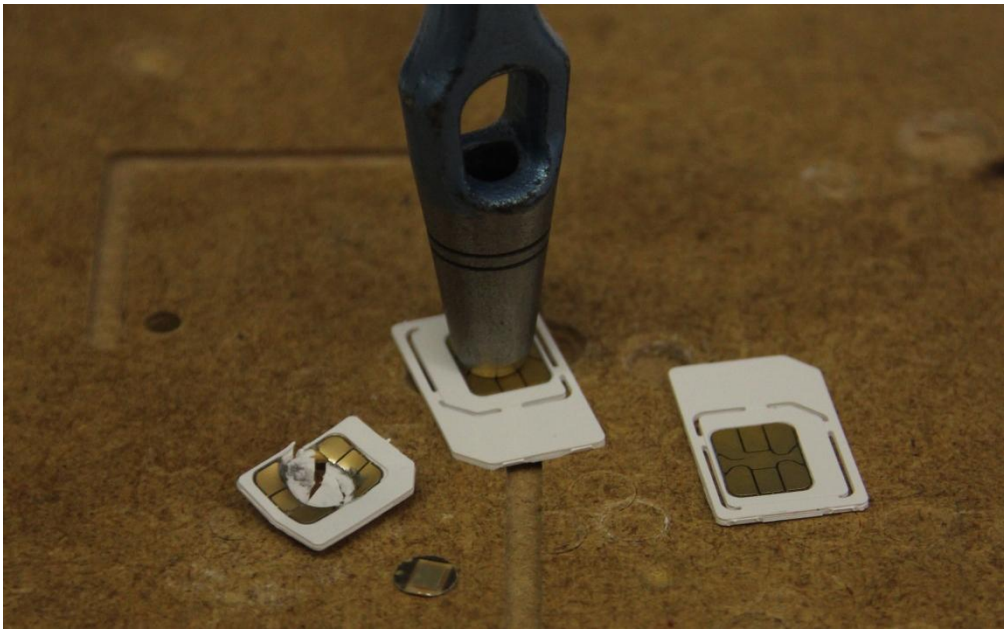

Figure 3-24: Punching SIM cards. Left: Punched SIM card and a sample. Middle: Punching a SIM card. Right: An unpunched card

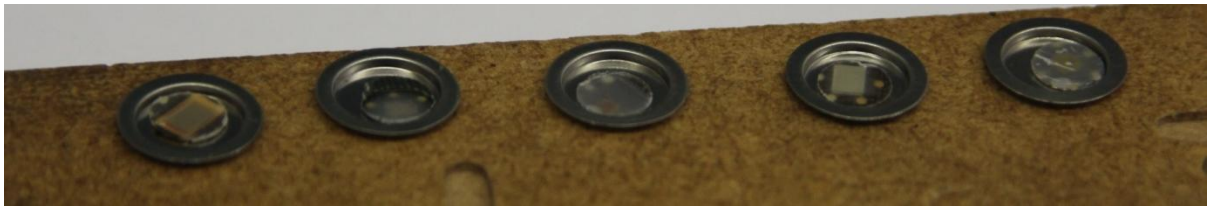

Figure 3-25: SIM card samples placed in cups

The cups used in our experiment have been studied before and didn't express any typical decay signal. There is no typical OSL decay signal but there is a noise signal of 3.46±2.45 counts per data point (average of 5 cups + their standard deviation) ([37]).

4 Experiments – Results

a. Smartphone apps

4.a.1 Radioactivity Counter - A first experiment

A first experiment[9] was conducted to simulate the situation how people will measure in reality during an accident. During this first study, the Radioactivity Counter was used on a single phone (iPhone C) which was exposed to a ^{60}Co source for about 10 minutes. The phone's camera was aligned with the source by using a positioning laser. The values were manually recorded by pointing a camera to the iPhone's screen and writing the on-screen values down. In this experiment the dose rate and the count rate values inside the upper box were written down.

Figure 4-1: Monitoring the iPhone

After the experiment the readings at several dose rates were plotted as a normalised value (measured dose rate over the reference ambient Dose Equivalent Rate ore DER) and plotted in Figure 4-2. By looking at this graph it can be noticed that the readings are unstable during the first few minutes, and can overestimate the measured dose rate up to a factor of 5; whilst the stabilised readings (at the end of the 10 min measurement) are overestimating the reference dose with maximum a factor 2. When the iPhone was exposed to a low dose rate ($\dot{H}^*_{(10)}$= 6 µSv/h), the app tends to underestimate the dose and failed to give a correct reading when a DER of 2.4 µSv/h was delivered.

[9] The doses were delivered as air kerma and are transformed to ambient dose equivalent rate by use of a conversion factor of 1.2 (defined by ISO 4037-3) (only in this experiment).

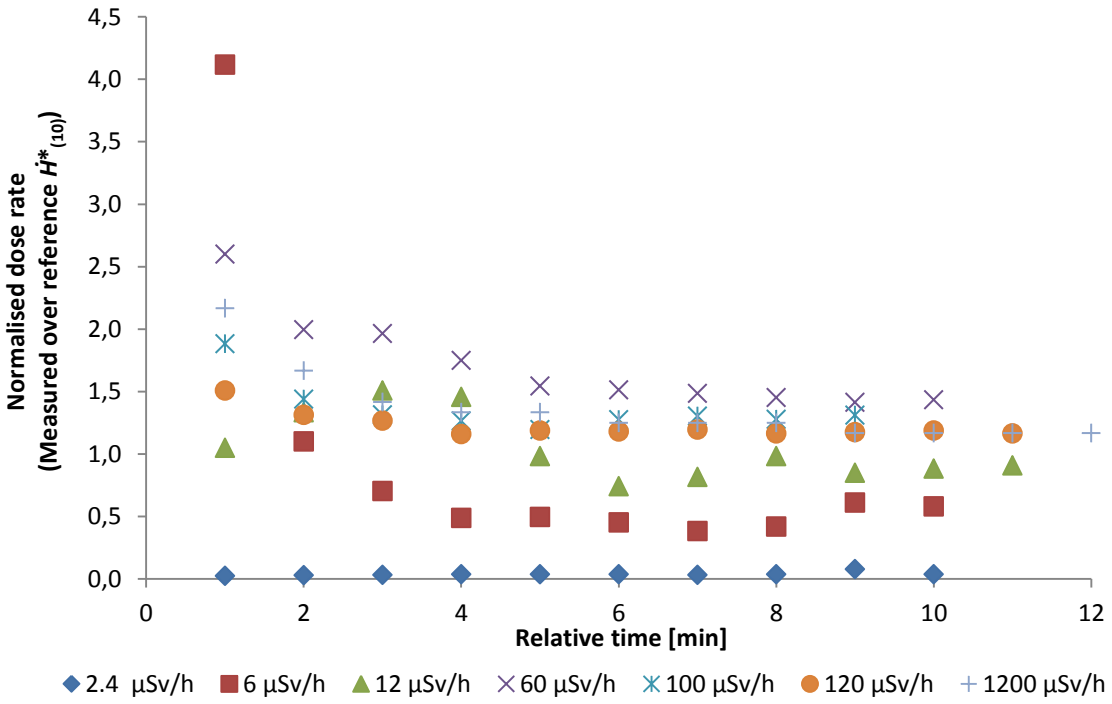

Figure 4-2: The evolution of the normalised dose rate (upper box) measured by iPhone C's Radioactivity Counter for ^{60}Co

We also looked at the effect of averaging the measured dose rates during respectively the whole measurement, the first 2 minutes and the last 5 minutes. When averaging over the whole experiment we noted that the dose rate is overestimated with a factor 1-2 with a large uncertainty (standard deviation) except for 2.4 µSv/h where the app failed to register a correct dose rate. Most members of the public won't measure for 10 minutes but they tend to do a quick measurement, assuming they only make a measurement for 2 minutes, it can be seen in Figure 4-3 that the dose is overestimated with a factor 1.4-3.1 excluding uncertainties.

The most precise measurements (readings & uncertainty) are recorded when the application had some time to stabilise (in this case 5 min). The overestimation for doses going from 12 µSv/h up to 1.2 mSv/h are smaller (1.0 – 1.75) and give good results for a non-dedicated detector (Figure 4-3).

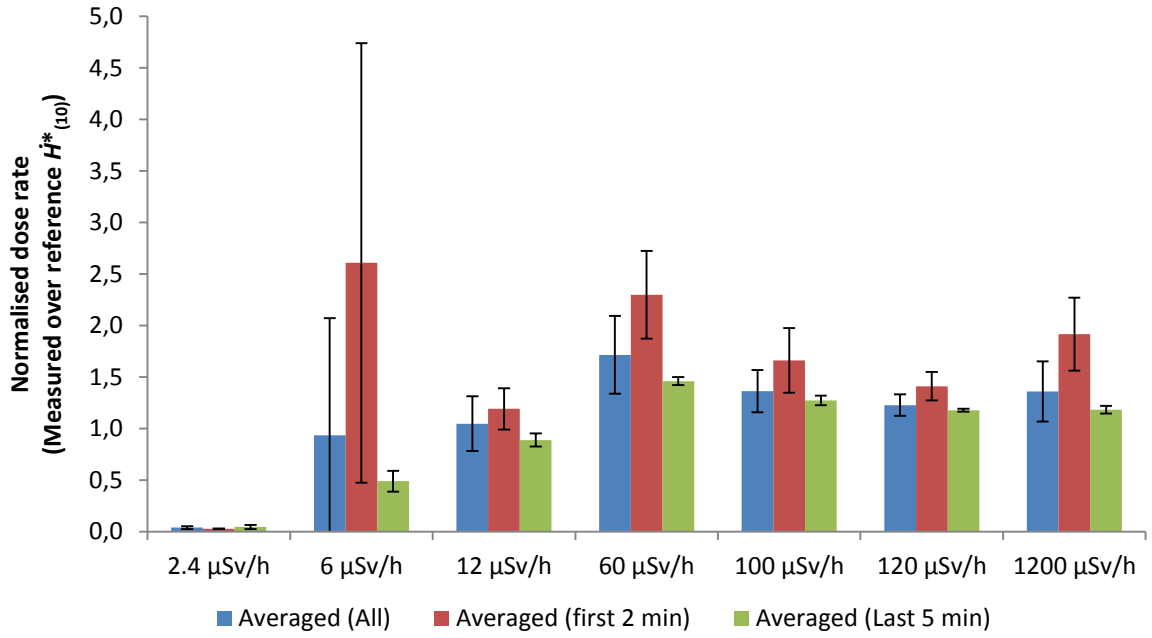

Figure 4-3: Averaged normalised dose rate and their standard deviation (error bars) for ^{60}Co

Another value that was recorded is the count rate; the count rate is an interesting value since the dose rate is derived from the count rate after a calibration. Comparing the smartphone's count rate with the phone's dose rate enables us to evaluate the calibration and its conversion algorithm. The count rate was plotted (Figure 4-4) and seems to follow the trend of the dose rate readings as shown before in Figure 4-2.

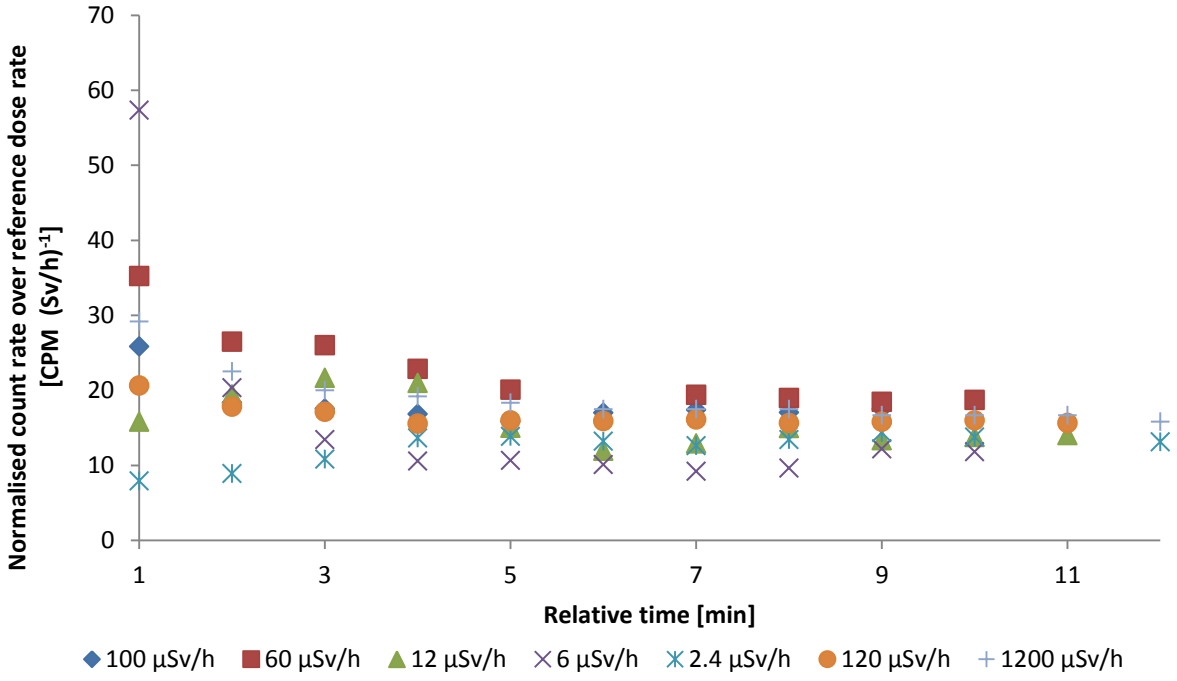

Figure 4-4: The evolution of the count rate (upper box), normalised over the reference dose rate, and measured by iPhone C's Radioactivity Counter for ^{60}Co

Analogue to the investigation of different time intervals for observing the averaged dose rate, we investigated the averaged count rate and constructed a calibration curve through the dataset. All calibration curves might seem to have a linear response (linear trend line with $R^2 < 0.98$) but the results using the last 5 min measurements tend to be more stable. However these datasets are collected in a short period of time which can lead to very variable results. It is advised to preform longer measurements to receive more stable results.

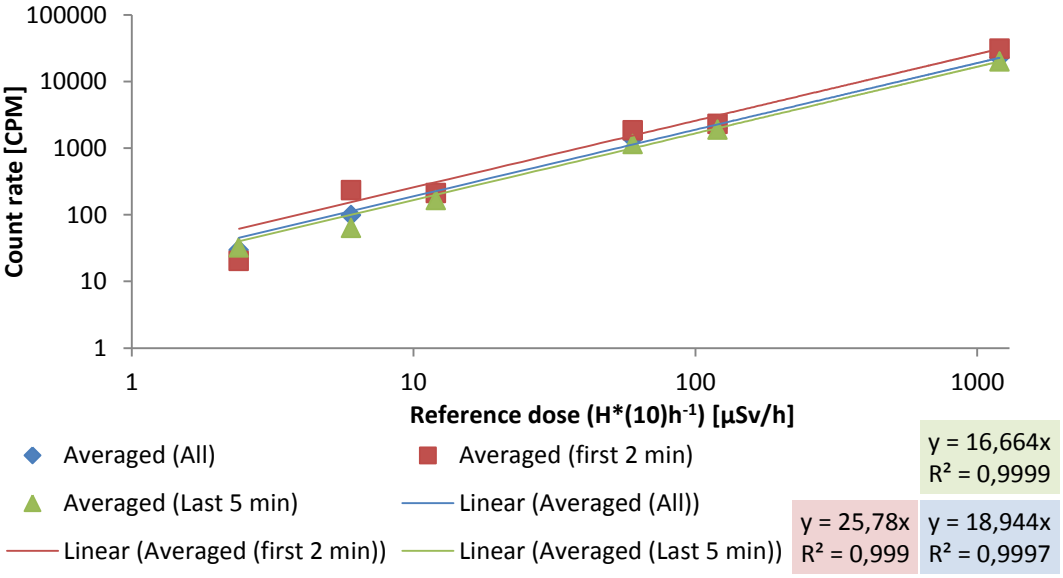

Figure 4-5: Averaged count rates for ^{60}Co and calibration curves

Using the calibration curves and the averaged count rates, we were able to convert the count rates into dose rates and we noticed that when using count rates and a calibration curve the over/underestimations are far more limited and closer to the reference value.

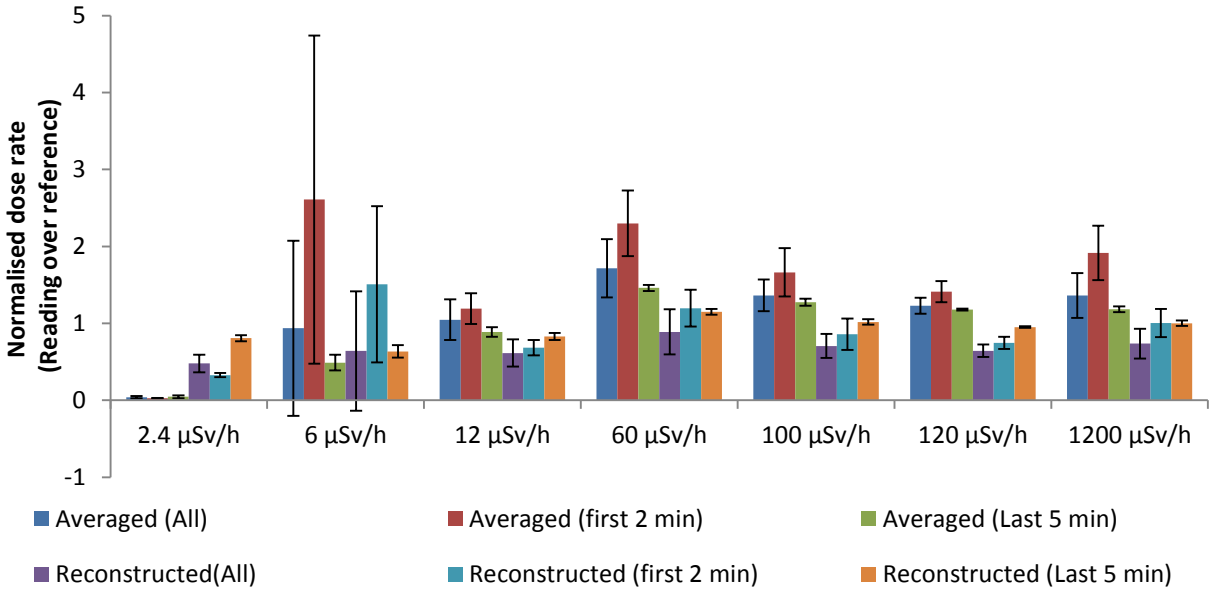

Figure 4-6: Normalised dose rate and their standard deviation (error bars) for ^{60}Co by averaging dose rate readings and reconstructing dose rates by using count rates and a calibration curve

Table 4-1: Results for normalised dose rates (measured over reference) and their standard deviation

	Normalised dose rates (Measured over reference)						
Dose rates	2.4 µSv/h	6 µSv/h	12 µSv/h	60 µSv/h	100 µSv/h	120 µSv/h	1200 µSv/h
Averaged (all)	0.04	0.94	1.05	1.72	1.36	1.23	1.36
Averaged (first 2 min)	0.03	2.61	1.19	2.30	1.66	1.41	1.92
Averaged (last 5 min)	0.05	0.49	0.89	1.46	1.27	1.18	1.18
Reconstructed(all)	0.48	0.64	0.61	0.89	0.70	0.64	0.74
Reconstructed (first 2 min)	0.33	1.51	0.68	1.20	0.86	0.75	1.00
Reconstructed (last 5 min)	0.81	0.63	0.83	1.15	1.02	0.95	1.00
stdev(measured all)	0.01	1.14	0.27	0.38	0.21	0.10	0.29
stdev(measured first 2 min)	0.00	2.13	0.20	0.43	0.31	0.14	0.35
stdev(measured last 5 min)	0.02	0.10	0.06	0.04	0.05	0.01	0.04
stdev(reconstructed all)	0.11	0.78	0.18	0.29	0.16	0.08	0.20
stdev(reconstructed first 2 min)	0.03	1.01	0.10	0.24	0.20	0.08	0.18
stdev(reconstructed last 5 min)	0.04	0.08	0.05	0.04	0.04	0.01	0.04

4.a.2 Radioactivity Counter - Stabilisation measurements

For this experiment, 3 out of 4 iPhones have been used (B, C and D). The iPhones were irradiated in the calibration laboratory of SCK•CEN where a ^{60}Co source (Tag "*P2*") was used to irradiate the samples with an Ambient dose equivalent rate $\dot{H}^*_{(10)}$ = 10.0 ± 0.4 µSv/h at room temperature.

An irradiation of ~1 hour was given and each minute the dose rate in the **upper box** was noted. As can be seen in Figure 4-7, the app sometimes didn't register any radiation and restarted the whole detection process leading to unstable measurements.

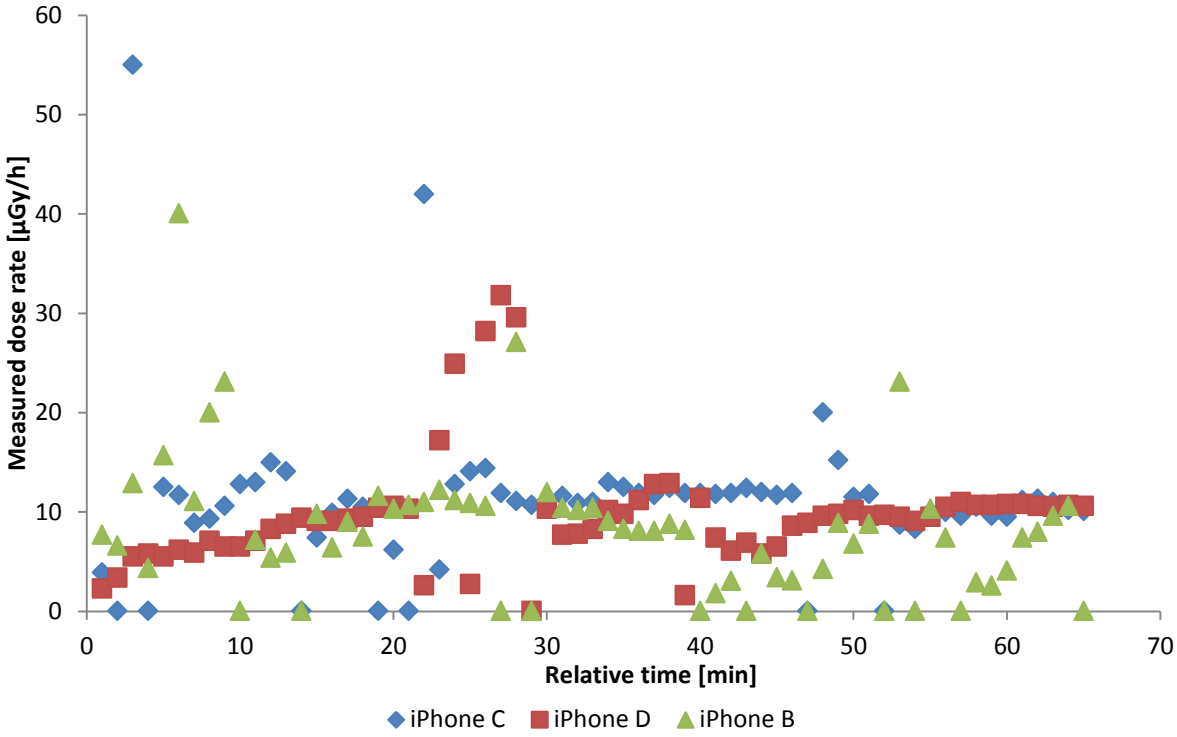

Figure 4-7: Stabilisation measurement for Radioactivity Counter, irradiated with H*(10) = 10.0 ± 0.4 µSv/h

After looking to the top box we now take a look at the **logged values** from the log file generated by the Radioactivity Counter. For this experiment all 4 iPhones are irradiated with a ^{60}Co with a dose rate of 1mSv/h ($\dot{H}^*_{(10)}$= 1001 ± 29 µSv/h). 2 iPhones measured a total time of 7 minutes and stopped measuring during an on screen system message. After this experiment we also conducted an irradiation with all 4 iPhones being irradiated with a reference dose rate of 10 µSv/h.

In Figure 4-8 and Figure 4-9 we can see that the logged values are having a more stable behaviour than the on-screen mean values (**lower box**). This can easily been explained that due the fact that on-screen values are making a mean value. They also include the background measurements in their calculation.

Since there is a short time between starting the measurement and the actual irradiation (due experimental set-up and due safety reasons) the mean value is low since it has one or several background readings at the beginning of the measurement. Over time, the mean value is

increasing to reach about 80% of the reference dose rate after 10 minutes. This same effect is also expressed in the on-screen mean count rate.

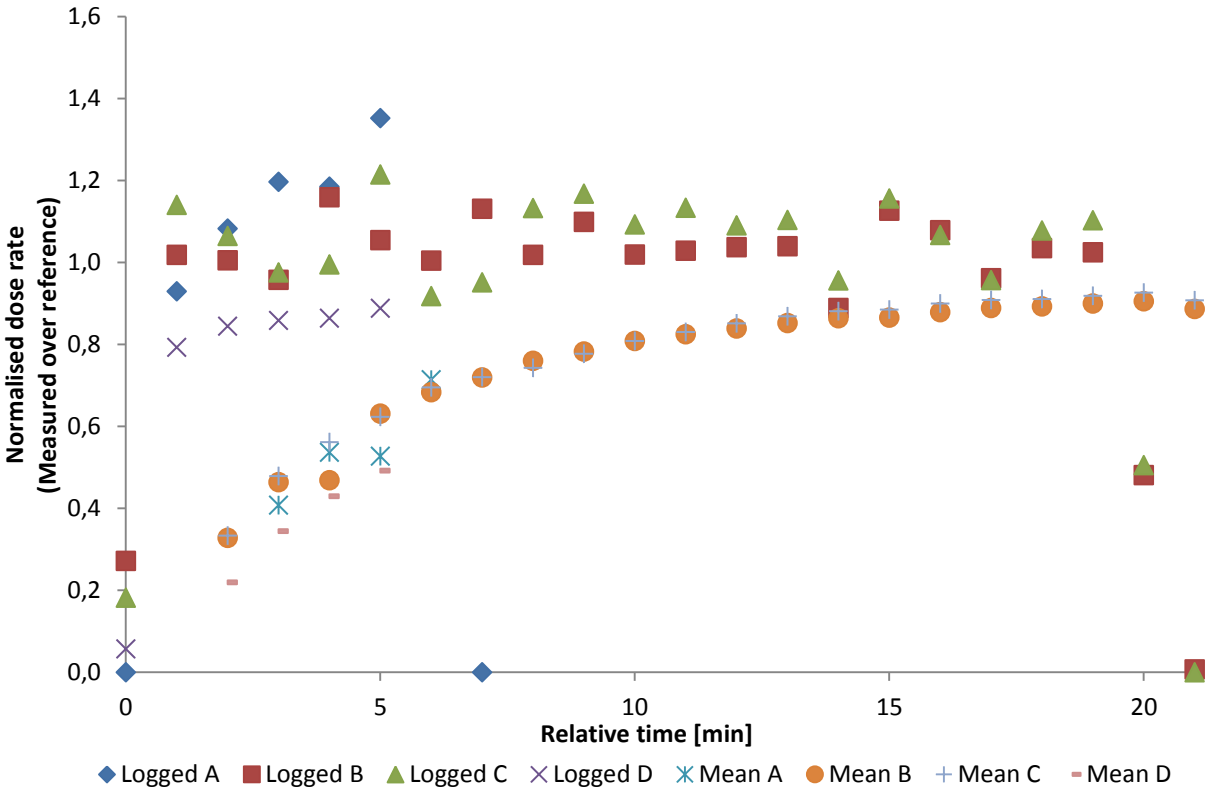

Figure 4-8: Normalised dose rates of the Radioactivity Counter (measured over reference) for logged and on-screen values (lower box) for the reference dose rate $\dot{H}^*_{(10)}$ = 1000 µSv/h. Values over factor 2 not displayed

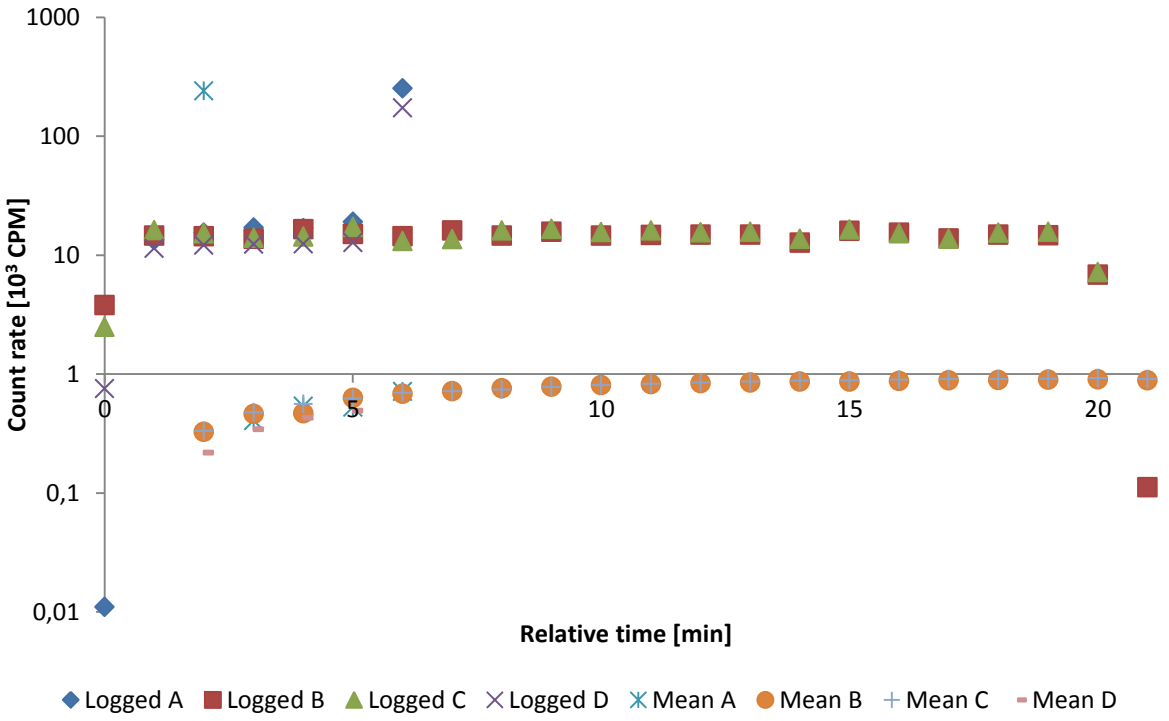

Figure 4-9: Count rates of the Radioactivity Counter for logged and on-screen values (lower box) for the reference dose rate $\dot{H}^*_{(10)}$ = 1000 µSv/h

We repeated the same experiment for a reference dose of 10 µSv/h and we noticed that the on-screen values of the lower box are stabilising in about 10 minutes while logged values keep varying over the whole measurement, this effect is due to the statistical aspect of radiation and are simply based on the count rates for that one minute.

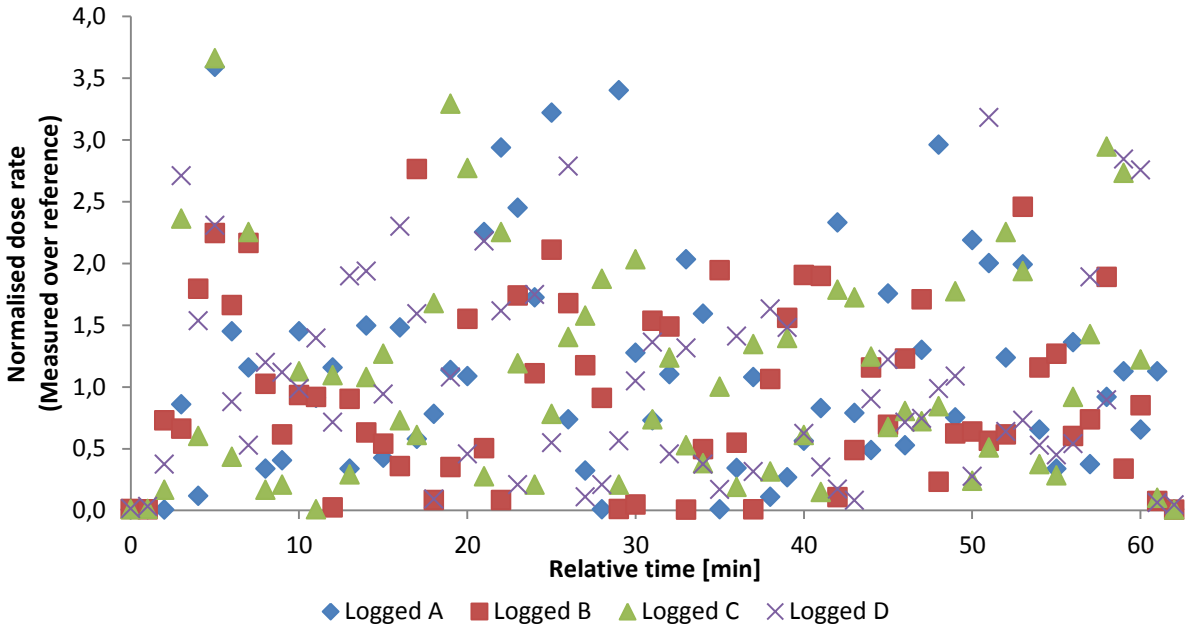

Figure 4-10: Normalised dose rates of Radioactivity Counter (measured over reference) for logged values at the reference dose rate $\dot{H}^*_{(10)}$ = 10 µSv/h

However the mean values (Figure 4-11) can be compared with the logged values by averaging these to calculate the mean value on a specific moment (Figure 4-12).

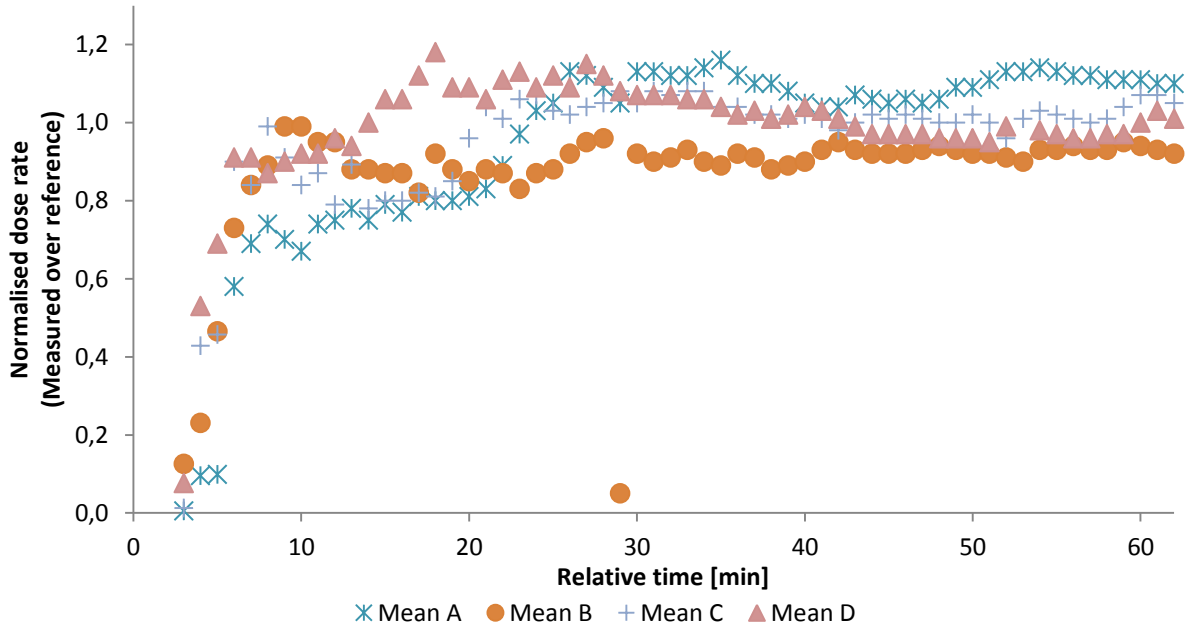

Figure 4-11: Normalised dose rates of Radioactivity Counter (measured over reference) for on-screen values at the reference dose rate $\dot{H}^*_{(10)}$ = 10 µSv/h

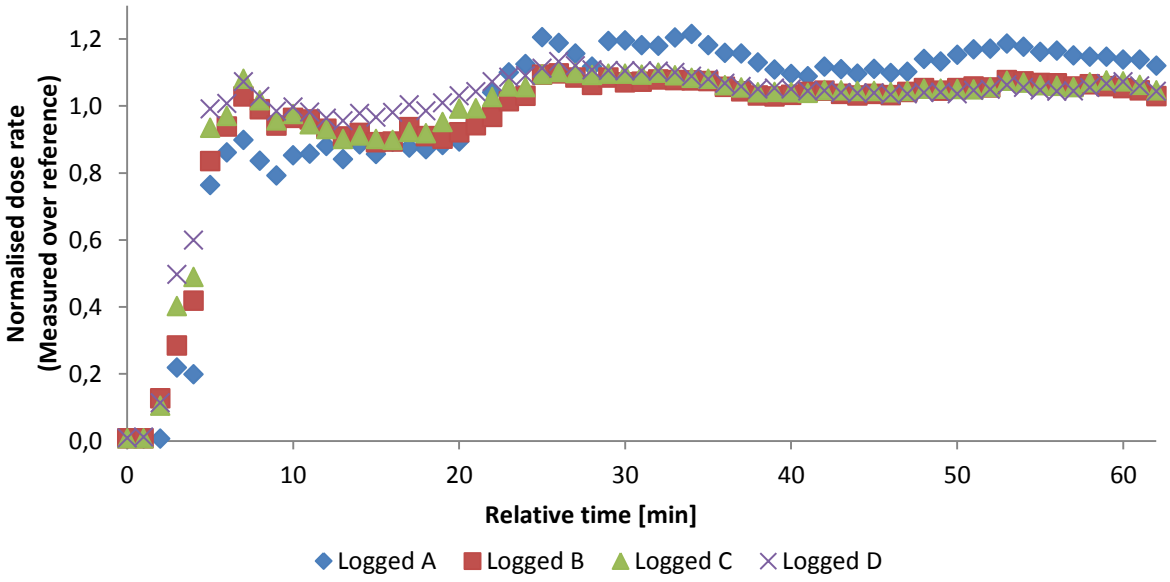

Figure 4-12: Reconstructing the mean values by use of the logged dose rates

4.a.4 Radioactivity Counter - Dose rate response & energy response

After the stabilisation measurements we investigated the dose rate response for different iPhones at different dose rates for ^{137}Cs and ^{60}Co. This experiment (for dose rates > 1 mSv/h) was conducted together with the testing of Polismart's dose rate response. The source was aligned with the Polismart detector and 2 iPhones were placed next to it. Both iPhones probably received slightly different results due beam-attenuations or scatter.

We used the option to log the values and measured for 10 minutes then the average and standard deviation of the logged dose rates were determined and plotted in following graphs (Figure 4-13 to Figure 4-17). We noticed that a higher reference dose rate will lead to a higher logged dose rate. The dose rate response is not ideally and over-and-under-estimations are made very easily.

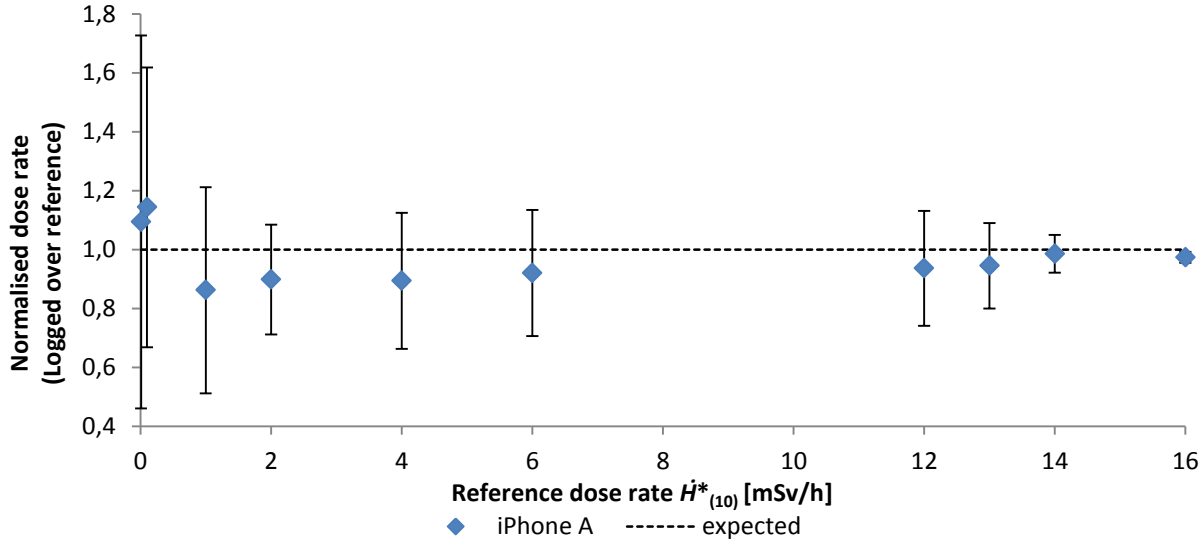

Figure 4-13: Dose rate response for ^{137}Cs Radioactivity Counter

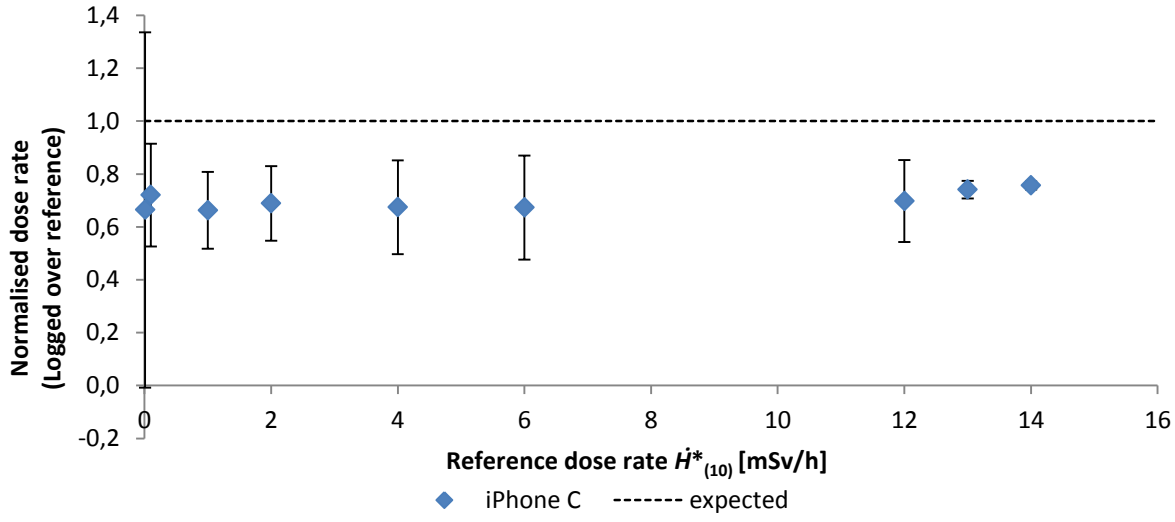

Figure 4-14: Dose rate response for ^{137}Cs Radioactivity Counter

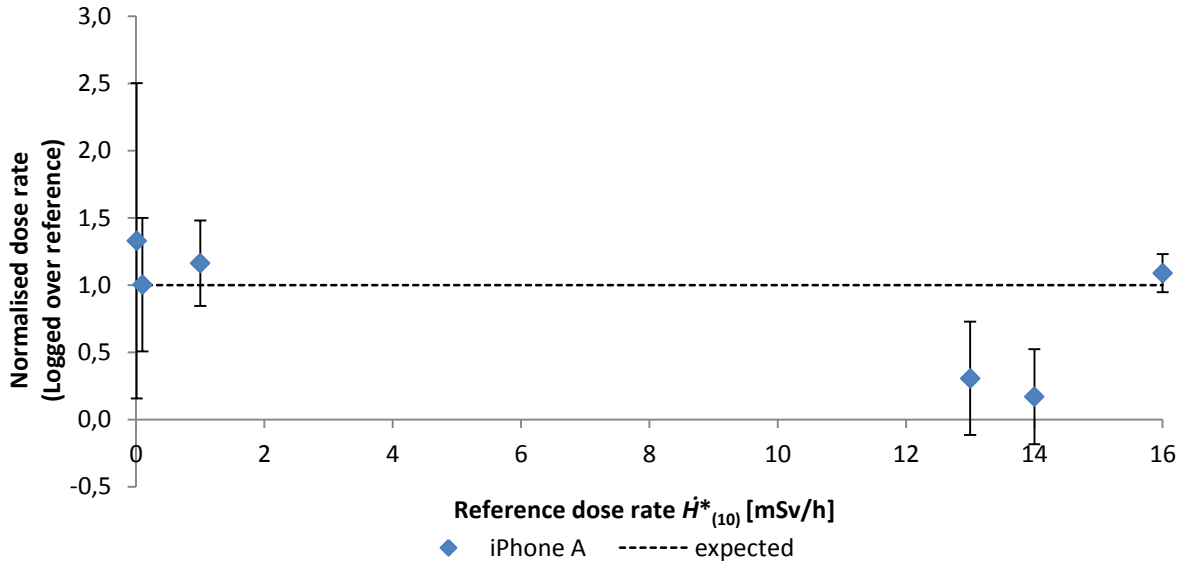

Figure 4-15: Dose rate response ^{60}Co for Radioactivity Counter

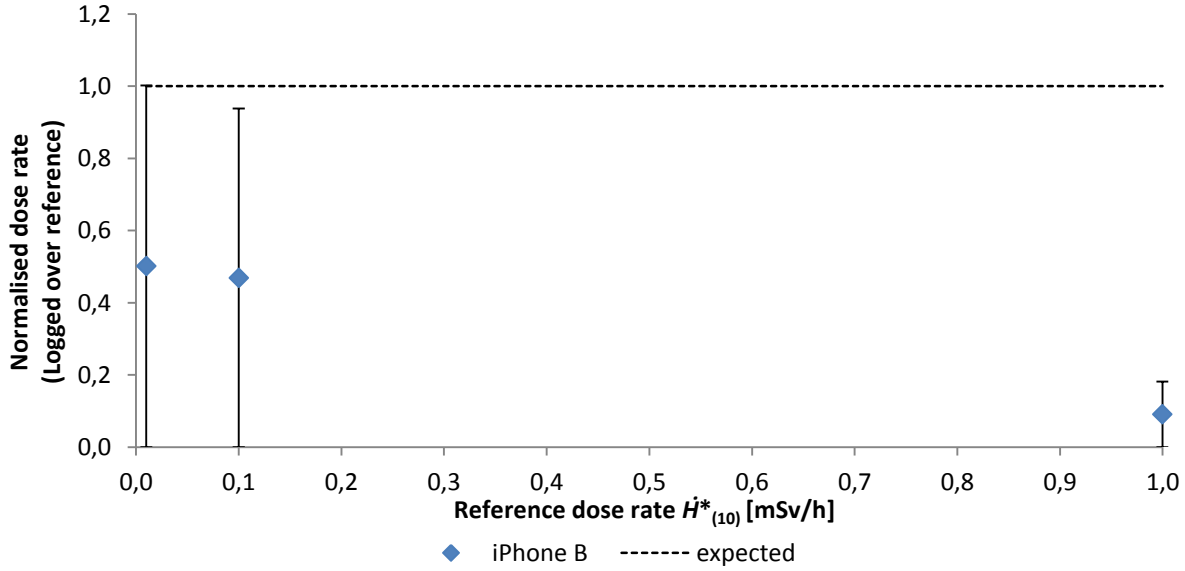

Figure 4-16: Dose rate response ^{60}Co for Radioactivity Counter

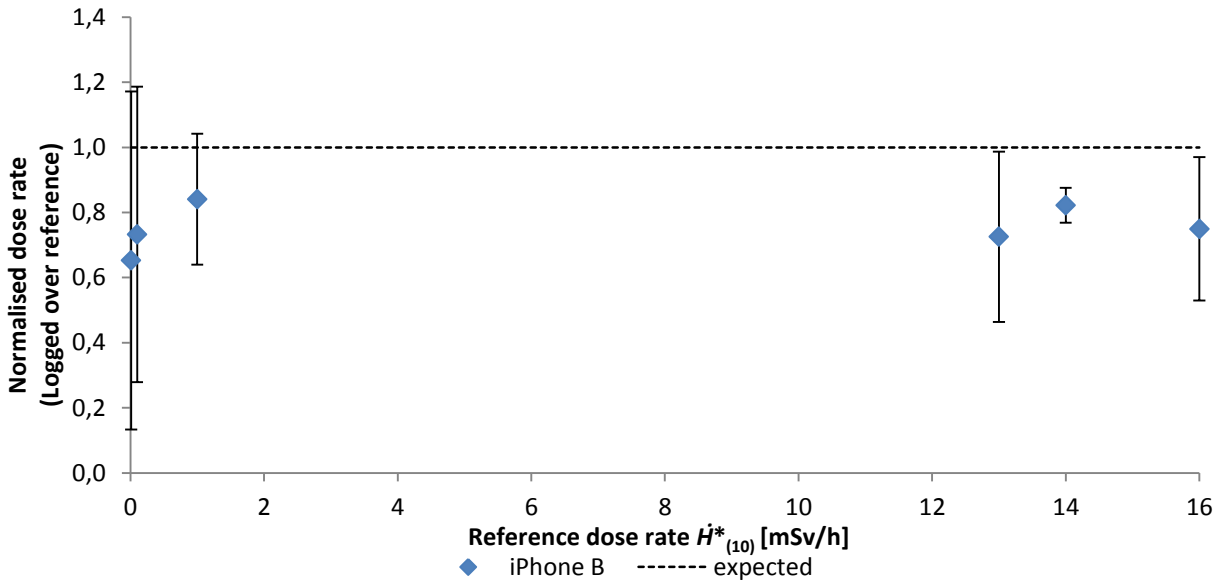

Figure 4-17: Dose rate response ^{60}Co for Radioactivity Counter

4.a.5 WikiSensor - Stabilisation measurements

This stabilisation experiment is analogue to the one of the Radioactivity Counter (4.a.2 Radioactivity Counter - Stabilisation measurements) but we used instead another app. The WikiSensor is tested in the same set-up (^{60}Co, $\dot{H}^*_{(10)}$ = 10.0 ± 0.4 µSv/h). The front camera was used to detect radiation with an integration time of 60 seconds. An external camera was placed to see the on-screen readings but due the camera properties, at first only the dose rate was recorded. Since other values were blurry and couldn't be distinguished. It can be noticed that the recorded dose is a not an averaged value over the measurement time but just the value of the last minute. This is why the dose rate doesn't stabilise in Figure 4-18, therefore the averaged or mean value has been calculated manually and are plotted in Figure 4-19.

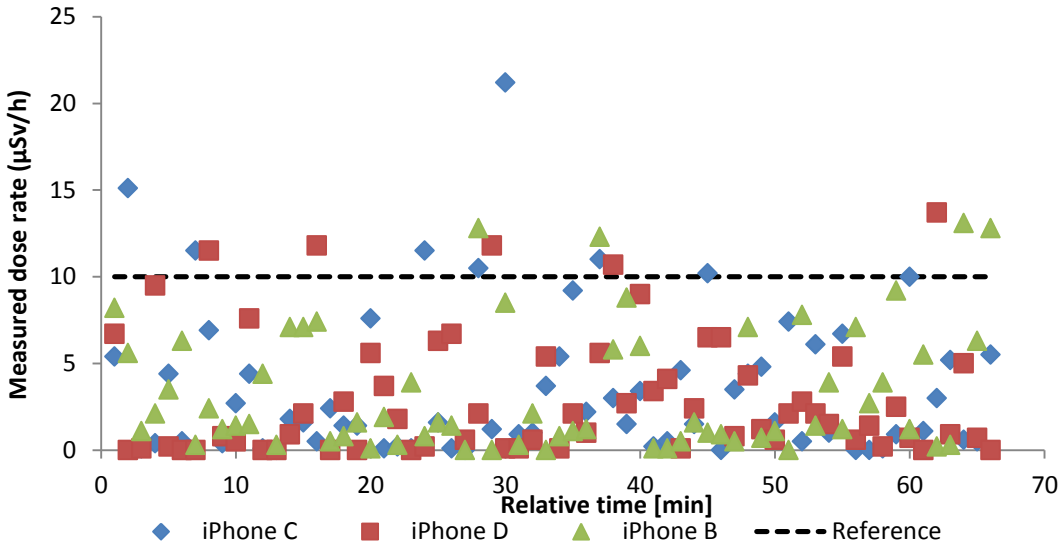

Figure 4-18: Stabilisation measurement for WikiSensor, irradiated with $\dot{H}^*_{(10)}$ = 10.0±0.4 µSv/h

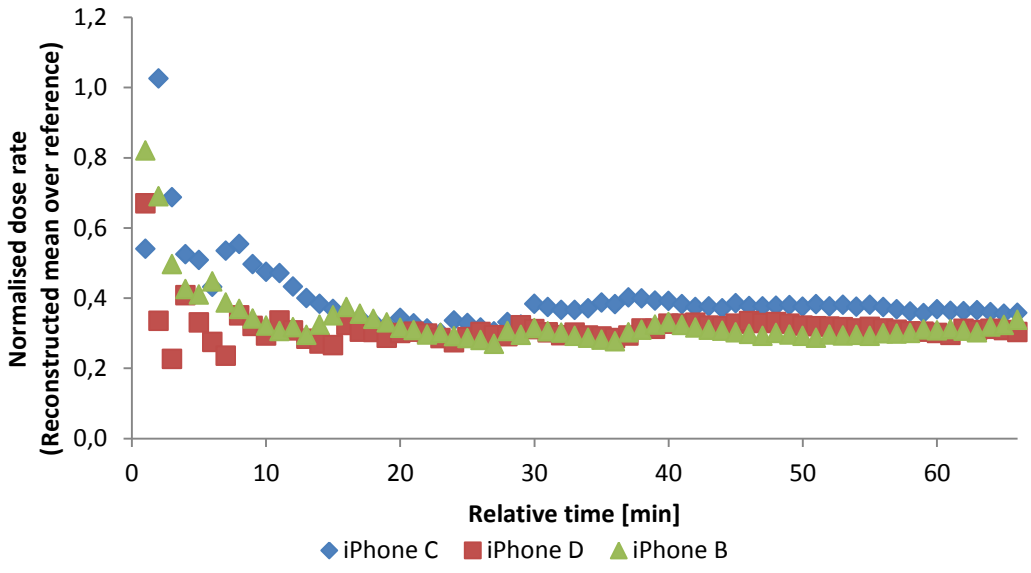

Figure 4-19: Stabilisation measurement for WikiSensor, irradiated with $\dot{H}^*_{(10)}$ = 10.0±0.4 µSv/h. The recorded dose rates are used to calculate a mean dose rate on a specific time and are normalised over the reference dose rate

As can be seen in Figure 4-18 and Figure 4-19, the WikiSensor's dose rate readings are underestimating the reality and only succeeds a few times to register the correct dose rate. A possible reason for this underestimation is a poor calibration. In order to test this, the same experiment was conducted but now the count rate (burned pixels per 60 seconds) was observed and linked to the reference dose rate ($\dot{H}^*_{(10)}$ = 10.0 µSv/h).

By using a one-point calibration[10] we were able to transform the count rates to dose rates and the results are shown below Figure 4-20 - Figure 4-23). Note that the experiment lasted about 70 minutes but some data points couldn't be recorded because an iPhone system message was covering the screen.

The reconstructed doses are closer to the reference dose than the measured values but the WikiSensor often keeps over- and underestimating the dose rates and it is unclear to tell when a stable signal has been reached.

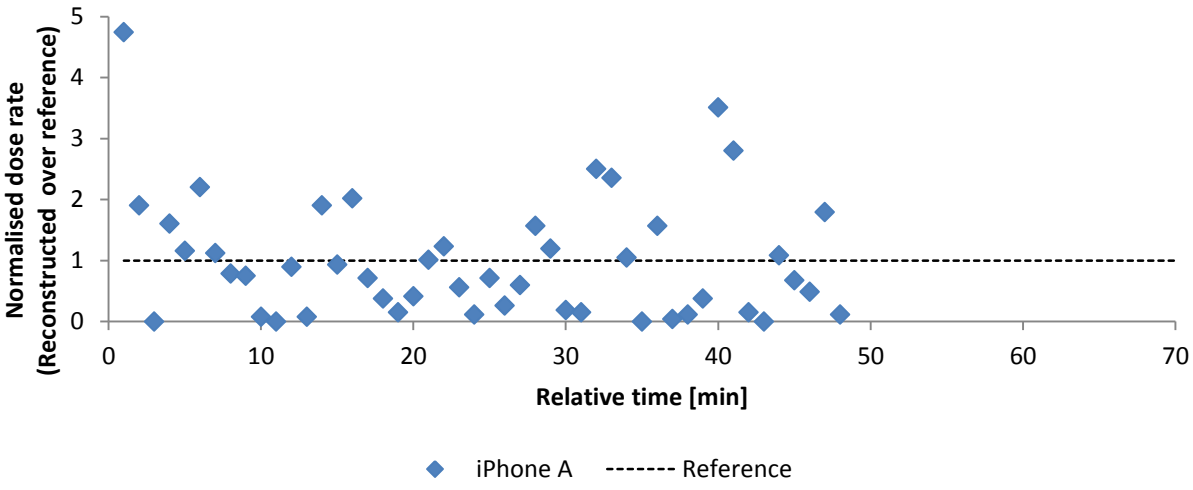

Figure 4-20: Normalised reconstructed dose rates for WikiSensor $\dot{H}^*_{(10)}$ = 10.0±0.4 µSv/h

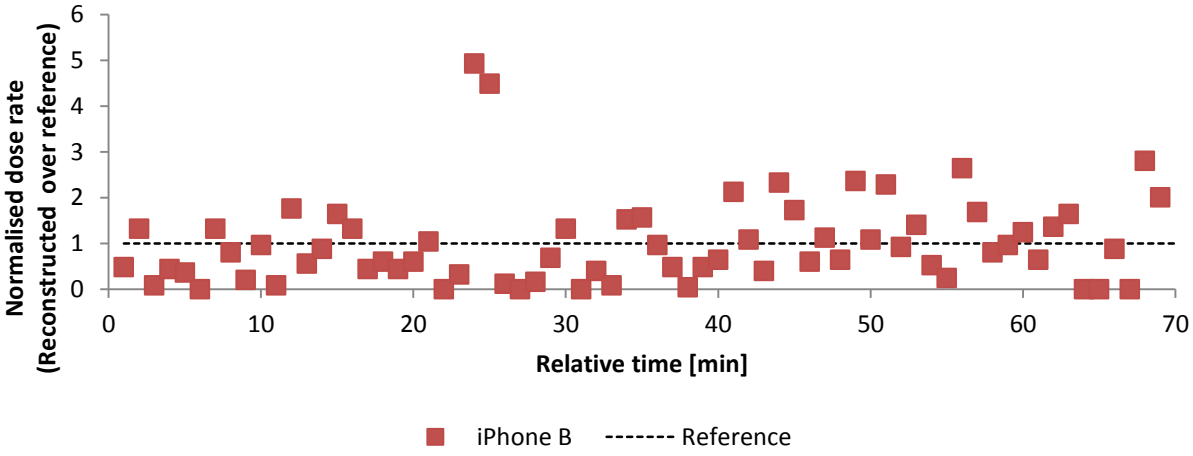

Figure 4-21: Normalised reconstructed dose rates for WikiSensor $\dot{H}^*_{(10)}$ = 10.0±0.4 µSv/h

[10] The calibration was constructed by dividing the reference dose with the averaged of count rate of the whole experiment.

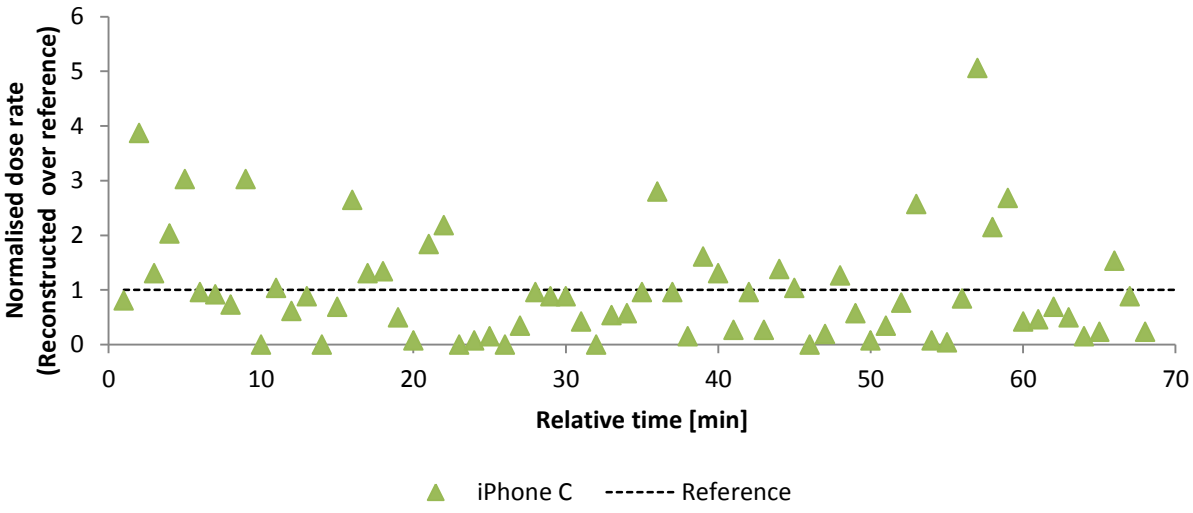

Figure 4-22: Normalised reconstructed dose rates for WikiSensor $\dot{H}^*_{(10)}$ = 10.0±0.4 µSv/h

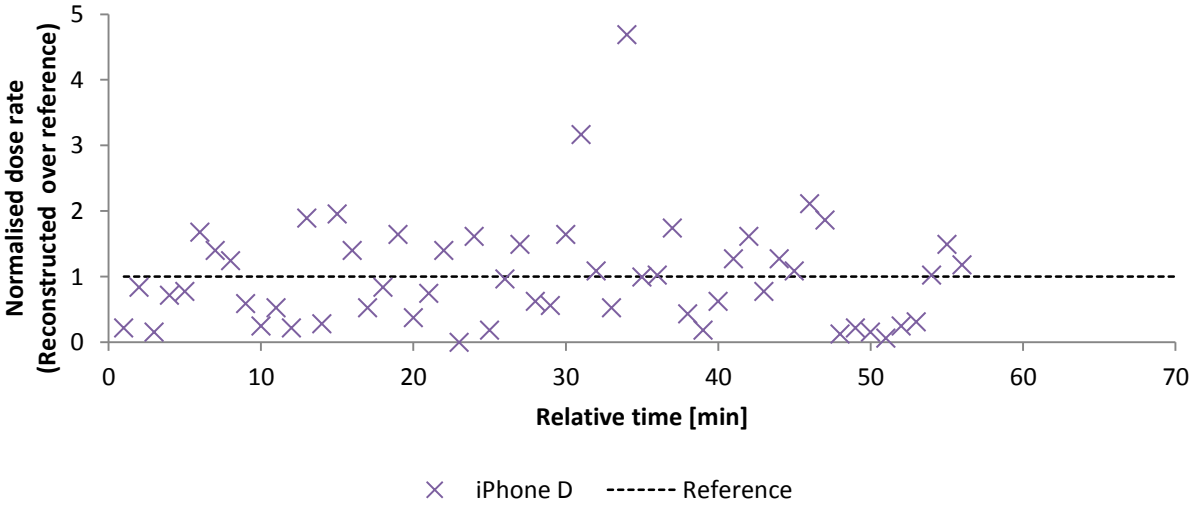

Figure 4-23: Normalised reconstructed dose rates for WikiSensor $\dot{H}^*_{(10)}$ = 10.0±0.4 µSv/h

4.a.6 WikiSensor - Stabilisation measurements – Integration window

The WikiSensor provides the option to choose an integration window; we investigated several integration values (1, 2, 5 minutes and 1 hour) in order to determine their recorded dose rates and burned pixels. All 4 iPhones have been irradiated with the same set-up as used in the other WikiSensor experiments (^{60}Co, $\dot{H}^*_{(10)}$ = 10.0 ± 0.4 µSv/h). The iPhones are placed as in Figure 3-7.

For small integration times, the second displayed value was recorded in order to eliminate the effect of placing the source in correct position. We also noticed that the application shut down during the 1 hour measurement on iPhone C.

In last section we noticed that the Wikisensor only shows the value at the end of the measurement time. For studying longer time, we had to change the time and restart the measurement. But since only the last measurement is displayed, we can't test the stabilisation time (on-screen) but we can increase the measurement time so that it will give the dose rate level during that time window. This has been done in Table 4-2 where the integration time (the time of one measurement) started with 1 minute and increased up to 60 minutes. Since we noticed a bad calibration in last study and therefore we investigate the burned pixels per minute but we didn't found any clear relationship between the integration time and the measured burned pixels per minute.

Table 4-2: Evolution of burned pixels per minute for increasing integration time for ^{60}Co, $\dot{H}^*_{(10)}$ = 10.0 ± 0.4 µSv/h

	Pixel Burned/min			
Integration time (min)	iPhone A	iPhone B	iPhone C	iPhone D
1	16.0	39.0	30.0	24.0
2	21.5	47.5	20.0	4.5
5	22.4	37.0	18.2	24.0
60	36.2	31.8		26.6

4.a.7 iRad - Stabilisation measurements

The last application that is being tested is iRad, this app is also tested with stabilisation measurements for ^{60}Co at a dose rate $\dot{H}^*_{(10)}$ = 10.0 ± 0.4 µSv/h. The iPhones C and D were placed with their screen facing away from the source and their back camera was used to register radiation.

As can be noticed in Figure 4-24, the stabilisation time is about 20-30 minutes and both apps are over estimating the reference dose rate.

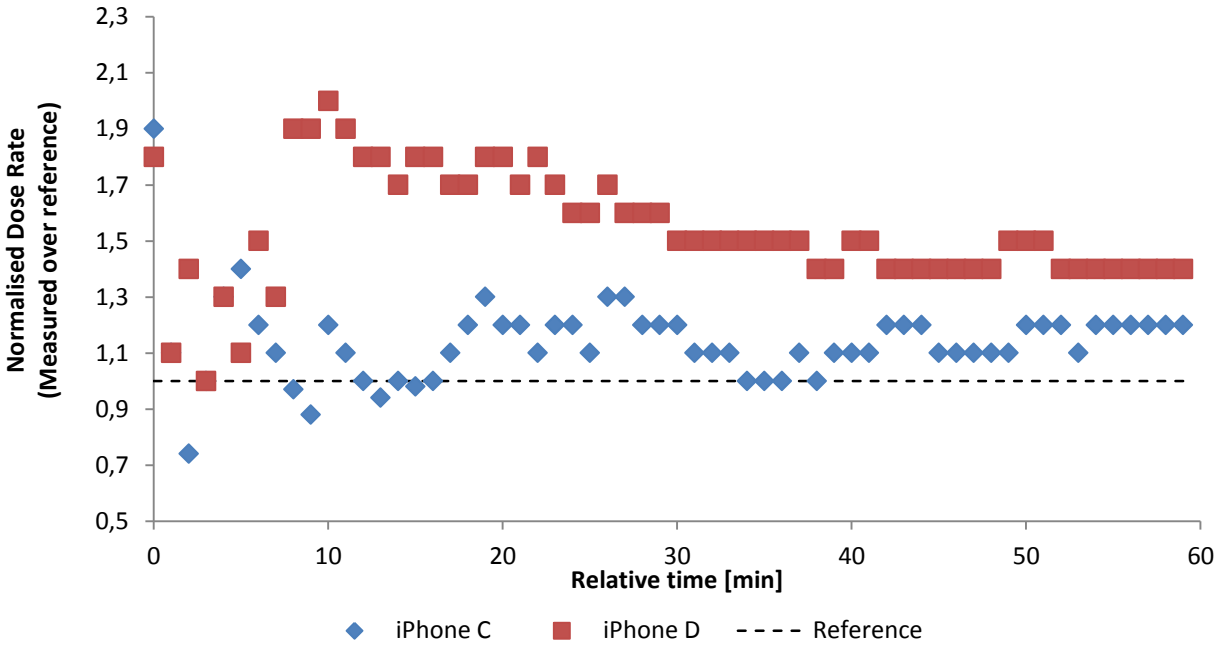

Figure 4-24: Stabilisation measurement for iRad, irradiated with $\dot{H}^*_{(10)}$ = 10.0 ± 0.4 µSv/h

b. Polismart

4.b.1 Background measurements

A first and easy test to perform is to measure background radiation. For this experiment the detector was placed on a table (geometrical centre facing downwards) and the background was measured once for 3 minutes, once for 9 minutes and 3 times for 15 minutes. The data was sampled at a rate of 1 dp per 10s.

Table 4-3 shows that the dose rate levels are about 0.09 µSv/h, once an elevated dose rate was detected (0.14 µSv/h) probably due to statistics.

Table 4-3: Background measurements Polismart

	Dose rate [µSv/h]					
	15 min(1)	15 min(2)	15 min(3)	3 min	9 min	All
Min	0.08	0.08	0.08	0.09	0.09	0.08
Averaged	0.09	0.09	0.09	0.10	0.10	0.09
Max	0.09	0.09	0.09	0.10	0.14	0.14

4.b.2 Sample rate and sample time

In case of an emergency, the data collection shouldn't take a long time. And therefore the total measurement time was evaluated for a sample rate of 1 data point per minute for respectively 5 and 10 minutes with a ^{60}Co-source at $\dot{H}^*_{(10)}$ of 1 mSv/h.

When comparing the results from both measurements (Figure 4-25), it can be noticed that the difference between both sample times is minimal. To evaluate the dose rate, the dataset has to be cleaned up. This is done by isolating a plateau. First all measurements before and after the irradiation are excluded. Next all data points with a variation larger than 10% will be excluded. The data points that are left are used to calculate the averaged value and their standard deviation.

As can be seen in Table 4-4 the reconstructed dose rate for both measuring times are similar and overestimates the reference dose about 33±3%.

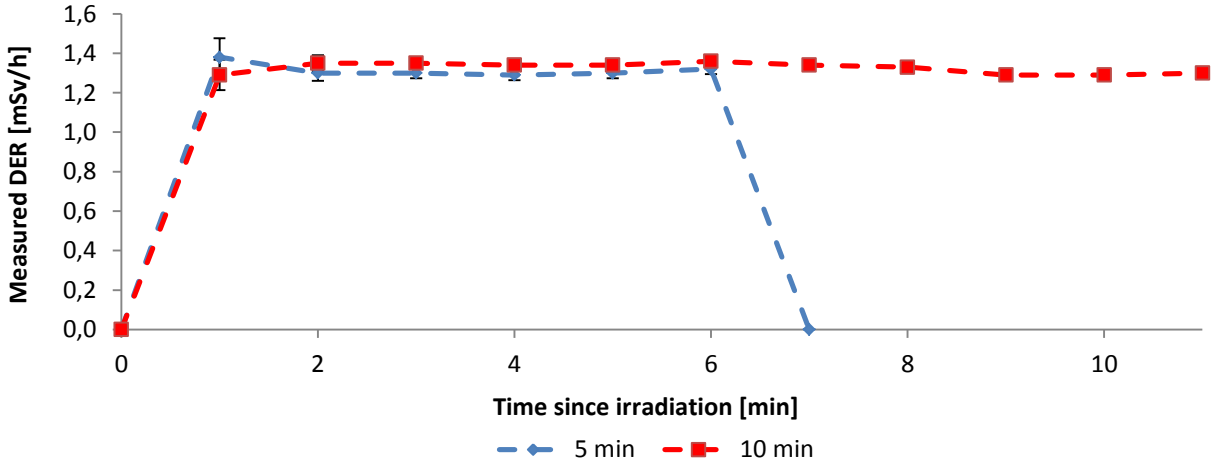

Figure 4-25: Polismart measurement time experiment. The iPhone with Polismart PM1904 was irradiated with ^{60}Co $\dot{H}^*_{(10)}$ = 1000 µSv/h. The sample rate was set on 1 data point per minute and irradiated respectively approximately 5 and 10 minutes. The Polimaster's variation has been used to construct the error bars

Table 4-4: Polismart measurement time experiment. Dose rate reconstruction by averaging the plateau values for different sample times while the uncertainty is the standard deviation of the same plateau values. Except for the reference value, which is computed at the LNK laboratory

	^{60}Co	
	DER [mSv/h]	Uncertainty [mSv/h]
5 min	1.32	0.03
10 min	1.33	0.03
Reference	1.00	0.03

Next the Polismart's sample rate is investigated with a ^{60}Co-source and an ambient dose equivalent rate of 10.0 ± 0.3 µSv/h. An irradiation of 5 minutes was chosen for the sample rate of 1 data point per second and an irradiation time of 10 minutes was chosen for the sample rate of 1 data point per minute in order to have more than 5 data points.

The results, as shown in Figure 4-26 and Figure 4-27, illustrates that a higher sample rate (1 dp/s) will have a smaller variation and a more stable signal compared with a lower sample rate (1 dp/min).

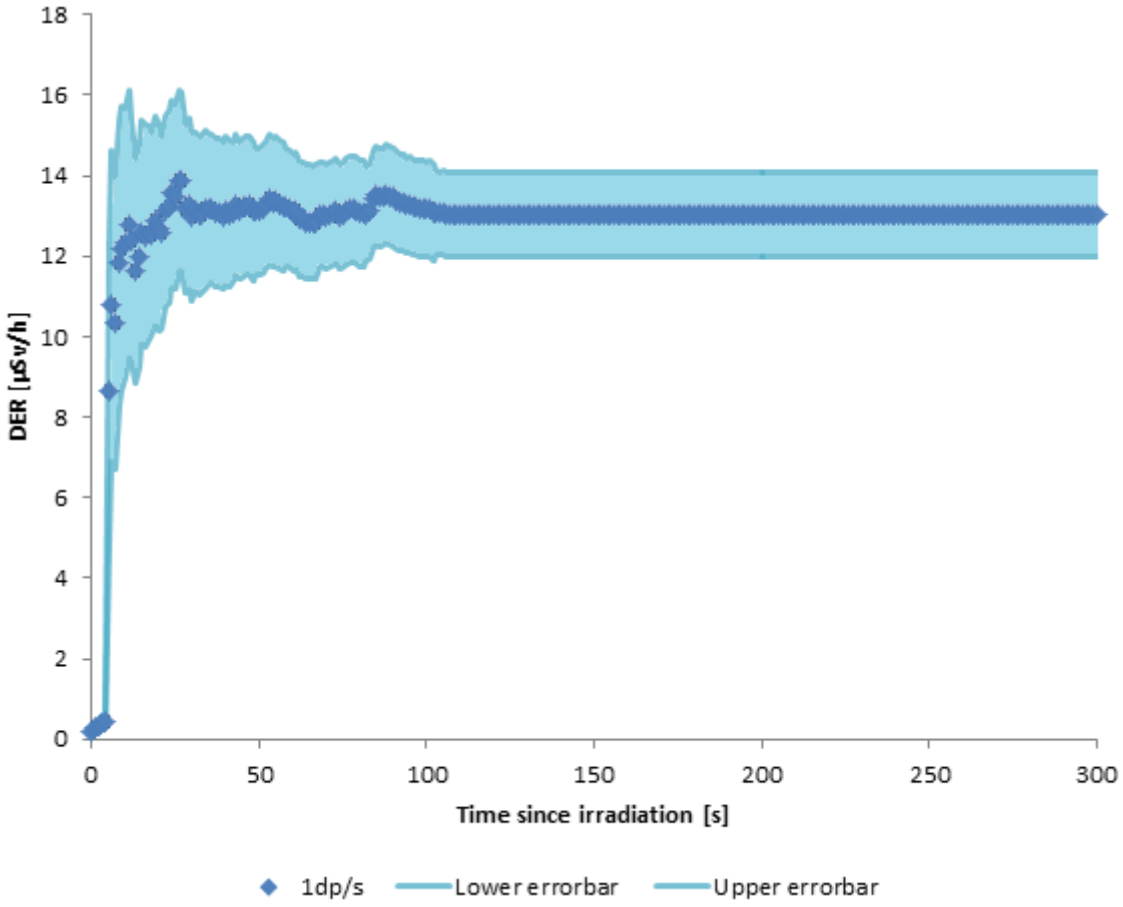

Figure 4-26: Polismart sample time experiment. The iPhone with Polismart PM1904 was irradiated with ^{60}Co $\dot{H}^*_{(10)}$ = 10.0±0.3µSv/h. The sample rate was set on 1 data point per second and irradiated about 330s. The Polimaster's variation has been used to construct the error bars

As can be noticed in Table 4-5, the reconstructed ambient dose equivalent rate is very precise when sampling at 1dp/s (uncertainty 0.1 µSv/h). However when sampling at 1 data point per second, the DER is overestimated about 31% (with an uncertainty of 1%), while otherwise the DER is overestimated with about 41% (with an high uncertainty of about 19%). A higher sampling rate would implement more data points and a flatter plateau level, which results in a better reconstructed DER-value (and DER-uncertainty).

Table 4-5: Polismart sample time experiment. Dose rate reconstruction by averaging the plateau values for different sample rates while the uncertainty is the standard deviation of the same plateau values. Except for the reference value, which is computed at the Calibration laboratory

	^{60}Co	
	DER [µSv/h]	Uncertainty [µSv/h]
1dp/min	14.1	1.9
1dp/s	13.1	0.1
Reference	10.0	0.3

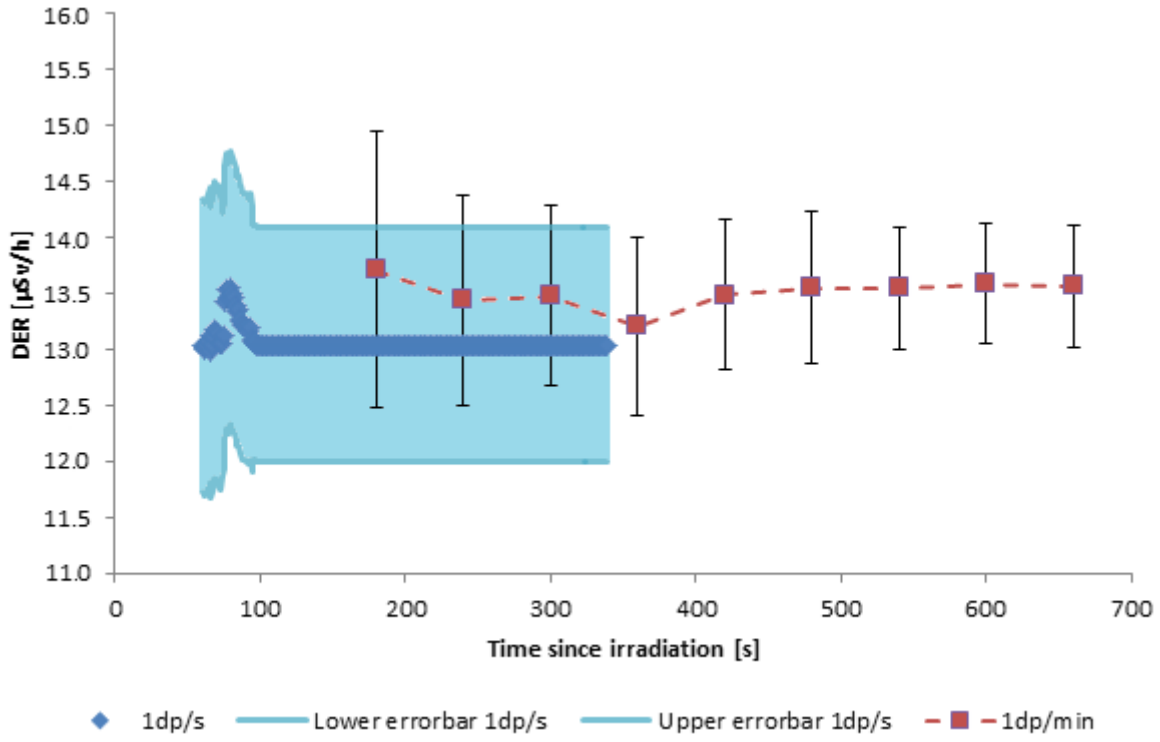

Figure 4-27: Polismart sample time experiment. The iPhone with Polismart PM1904 was irradiated with ^{60}Co $\dot{H}^*_{(10)}$ = 10.0±0.3µSv/h. The sample rate was set on 1 data point per second and 1 data point per minute and irradiated respectively approx. 330s and 540s. The Polimaster's variation has been used to construct the error bars. The raw dataset (of 1dp/s) was excluded from data before & after the irradiation and from values where variation > 10%

4.b.3 Dose rate dependency

When a dosimeter is exposed to ionising radiation, the displayed values should be independent from the dose rate, which can be translated into a linear dose rate response. The producer's manual specifies the DER measurement range between 0.01 µSv/h and 13 mSv/h [32]. We will try to validate this by characterising the detector's dose rate dependency with a ^{137}Cs and a ^{60}Co-source.

The detector has a linear dose rate response ($R^2 > 0.98$) but when comparing both trend lines (Figure 4-28 - Figure 4-29) we noticed a different slope for each line (1.1045 and 0.9444) meaning that the dose rate response for cobalt is about 16% higher than caesium, which is still below the maximum difference stated in the manual (Figure 3-10).

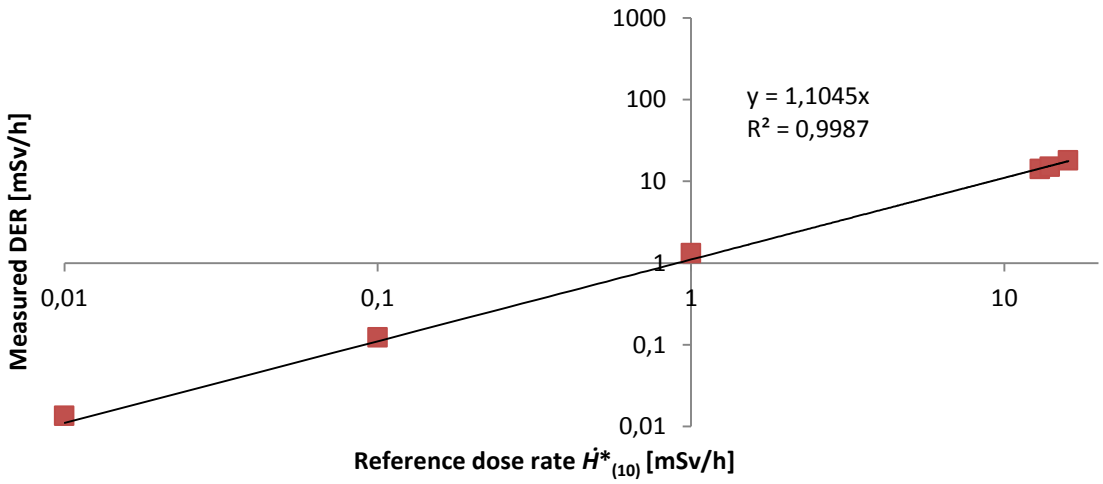

Figure 4-28: Polismart dose rate response for ^{60}Co.

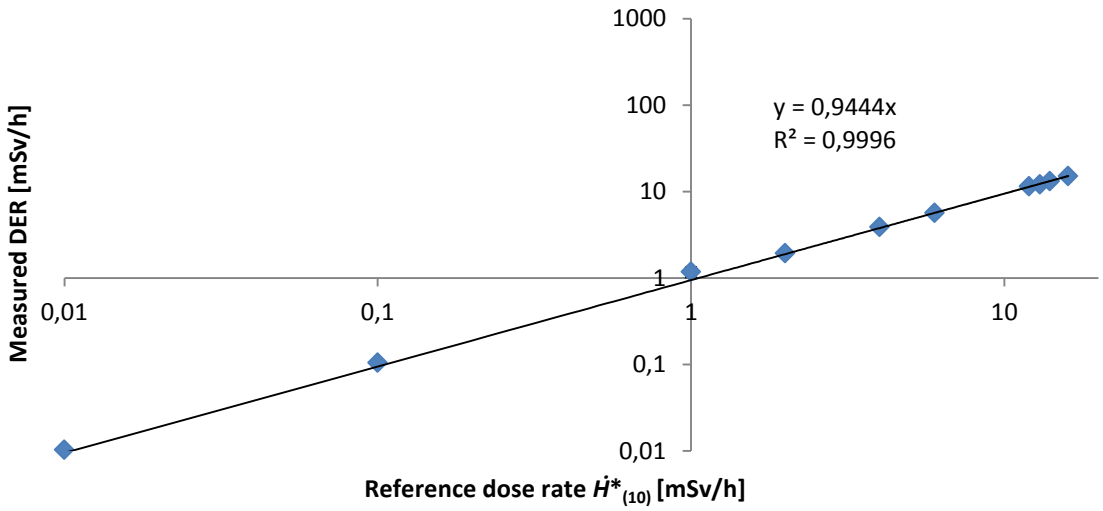

Figure 4-29: Polismart dose rate response for ^{137}Cs.

4.b.5 Effect of a high dose rate

Since some Geiger-Muller tubes can paralyse when exposed to high levels of radiations, it is in our interest to investigate the effect of a high dose rate on our detector. The DER measurement range was specified up to 13 mSv/h which was already exceeded with 3 mSv/h in last experiment. Now to make sure we would exceed this value significantly, we decided to measure at an ambient Dose Equivalent Rate of 100 mSv/h with a ^{137}Cs source.

The recovered signal (Figure 4-30) is fluctuating about 5% during the whole measurement and is displaying a dose above 100 mSv/h. We failed to paralyse the detector.

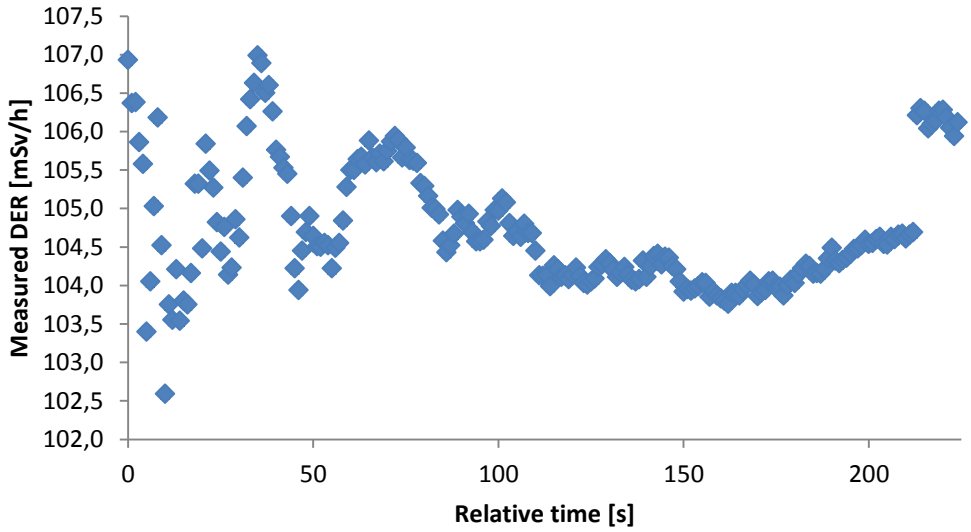

Figure 4-30: Effect of a high dose rate on the Polismart detector (^{137}Cs source with $\dot{H}^*_{(10)}$ = 100 mSv/h)

Assuming that the detector is still in DER measurable range, we can add our new found data to our dose rate dependence and we can see (Figure 4-31) that the new dose rate response curve is a bit more steeper (the slope is increased with a factor 1.10).

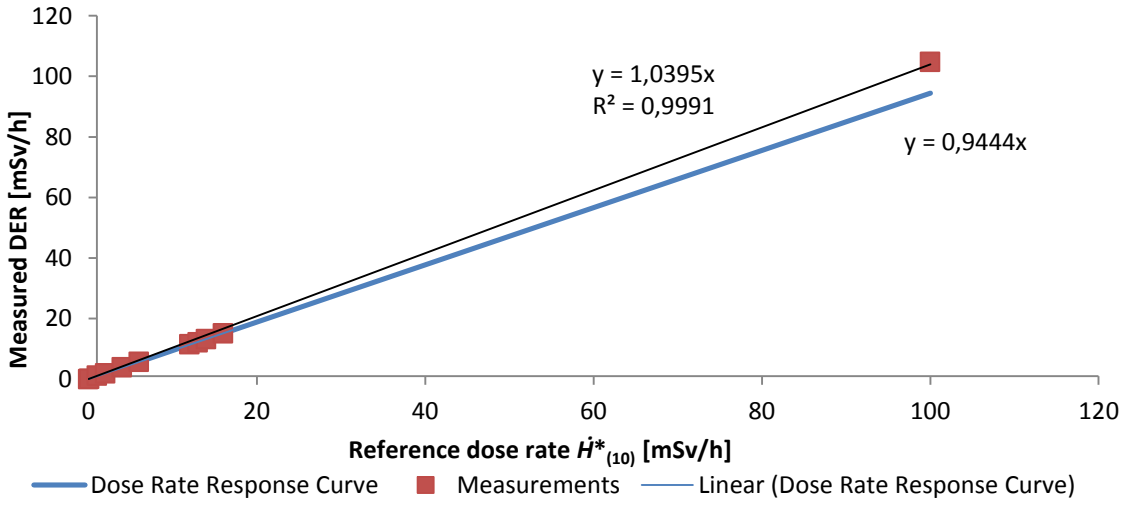

Figure 4-31: Old (blue) and new dose rate response for ^{137}Cs by including the result for $\dot{H}^*_{(10)}$ =100 mSv/h

4.b.6 Energy response

Until now we tested the PM1904 with caesium 137 (512 keV) and cobalt 60 (1173 and 1333 keV) but there are sources with much lower energies and the dosimeter's reading can be influenced. To see the effect of different energies on the reading, we performed an energy response with X-rays for a reference dose rate ($\dot{H}^*_{(10)}$) around 100µSv/h. Since the actual reference dose rate varies (93-223 µSv/h) for some of the measurements, the results were normalised over the actual delivered reference dose. For dose delivery we chose to use the narrow spectrum series (N-series) of X-ray beam confirm the ISO 4037-1 guidelines.

Table 4-6: Characteristics of narrow-spectrum series [39](p6)

N-series (Tube potential [kV])	Mean energy [keV]
30	24
60	48
80	65
100	83
120	100
200	164
250	208
300	250

The following figure (Figure 4-32) shows that the reference DER is over- and under-estimated at different energies. We should not take the N30 beam into account since its energy spectra is located beneath the Polismart's suggested energy range (60 keV). The under estimation of the N60 series can be accepted since its spectra ends around 60 keV (Figure 4-33).

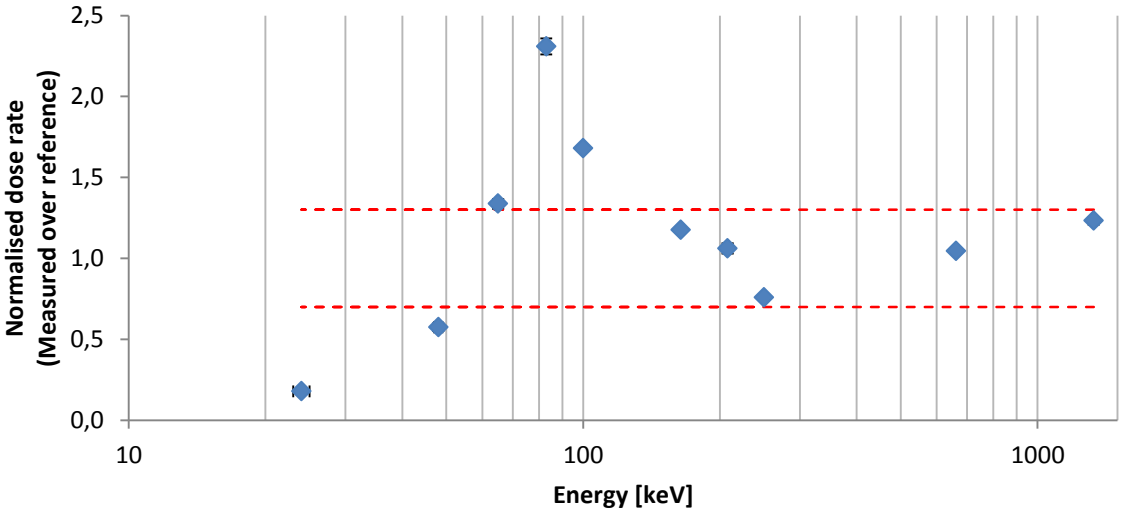

Figure 4-32: Polismart energy response with 2 border lines indicating 0.7 and 1.3

For all the other energies, we expected a normalised value around 0.70-1.30 since it was stated in the manual that the energy response relative to caesium-137 is no more than ±30% while ^{137}Cs has a normalised value of ~1 (in fact 1.04).

We can confirm this partly (Figure 4-32). X-rays with a mean energy of 65-100 keV (N80, N100, N120) are overestimated more than 30% while higher energetic radiation is within the expected derivation of 30%.

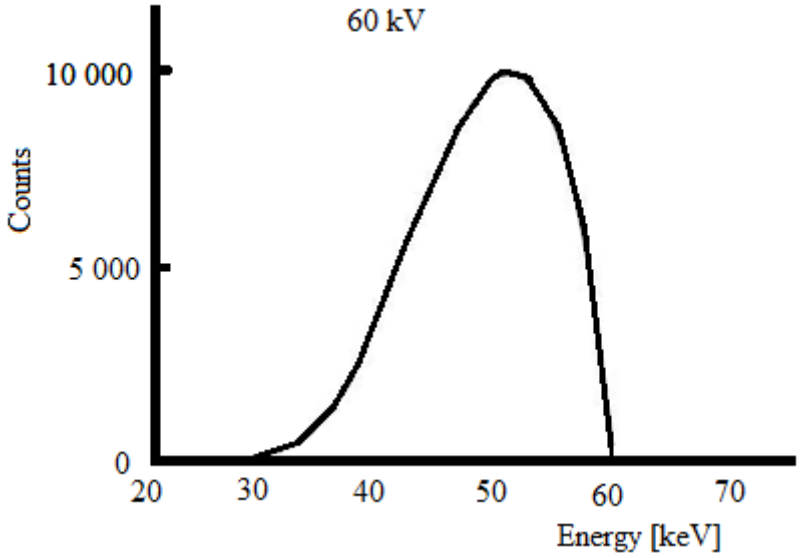

Figure 4-33: N60 X-ray spectra [39] (p26)

4.b.7 Angular response

After studying the dose rate and energy response it might be interesting to study the angular response. The angular response is the response of the dosimeter when it is being irradiated under another angle. We investigate the effect on DER readings with ^{137}Cs and a N80 X-ray beam by rotating the Polismart horizontally. We chose caesium for calibration purposes and N80 because the angular dependence is usually more pronounced for lower energies.

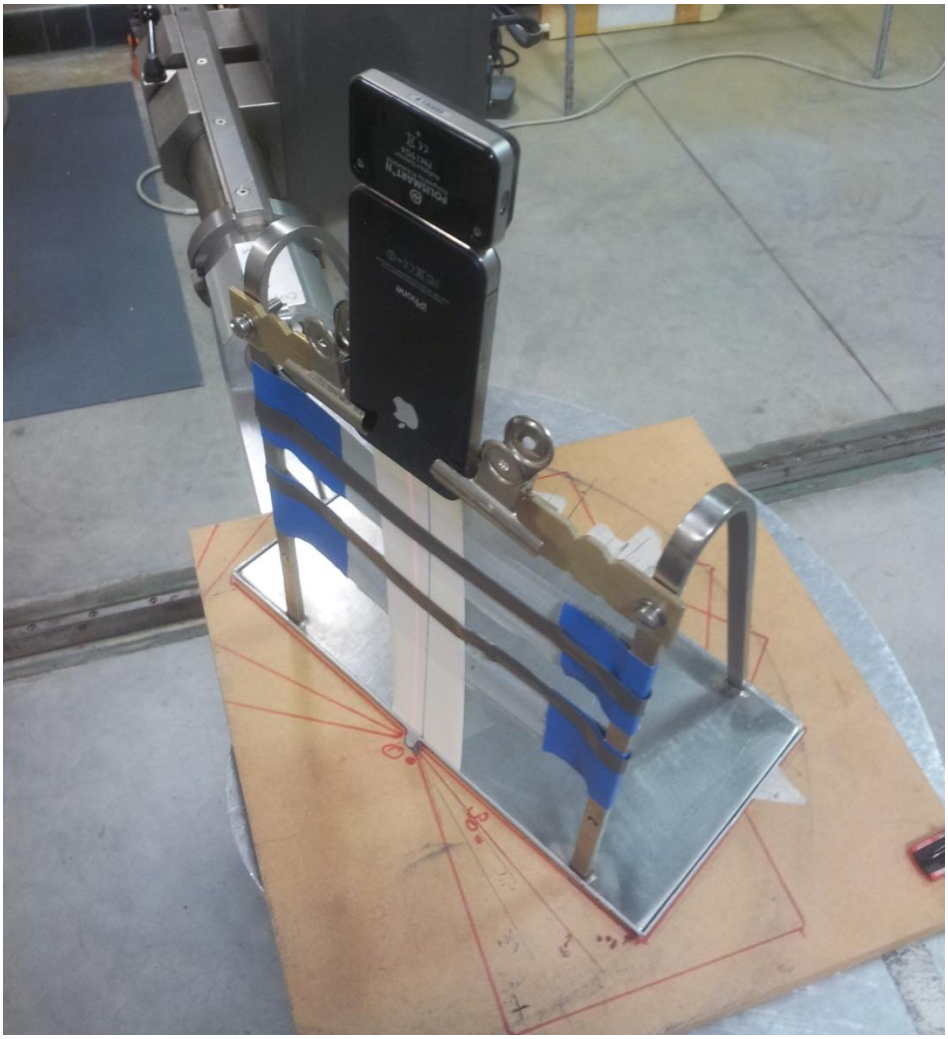

Figure 4-34: Experimental set-up for angular response

During the energy response experiment, we noticed that ^{137}Cs has a normalised value (reading over reference) of 1.04 while N80 had a value 1.34 for this experiment at an angle of 0°. This is expected as seen in the energy response experiments. We will also take this effect into account by normalising over the measured value at 0° instead of the reference value.

As can be seen in Figure 4-35, the effect of turning the detector has a significant effect on the restarted dose rate: A dose rate drop is noticed at ±90° and is high-likely due internal components which are placed at the sides of the detector. Just before we reach 270° we notice a strong signal increase of low energetic X-ray beams but these peaks are not confirmed by the ^{137}Cs-measurement.

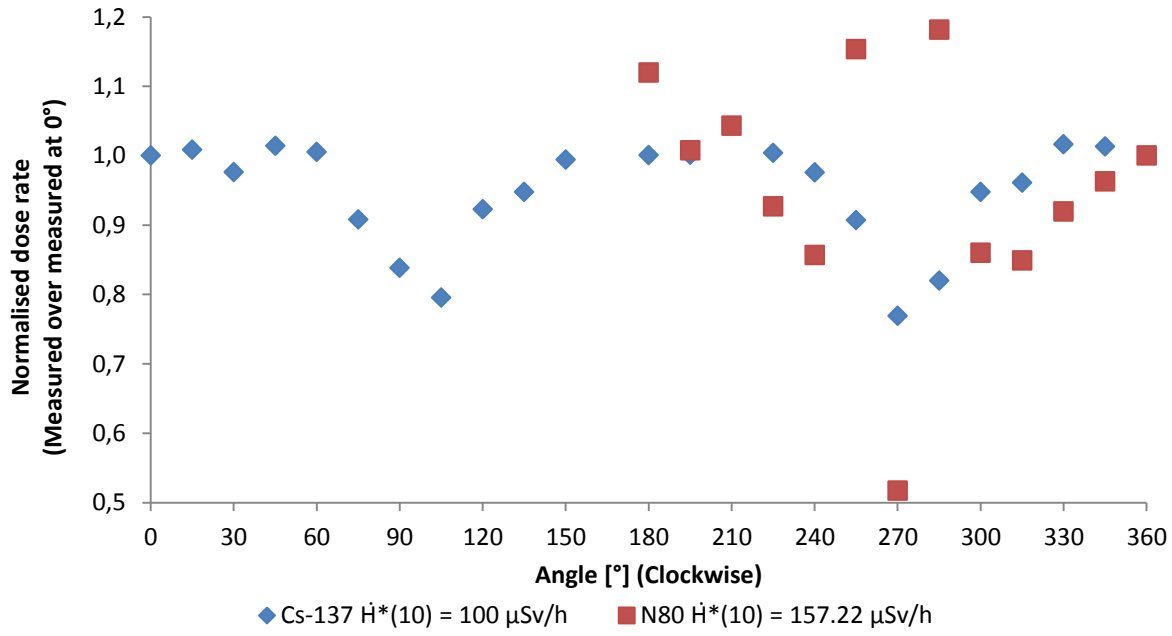

Figure 4-35: Polismart angular response, normalised over the measured dose rate at 0°

4.b.8 Additional comparison

While gathering the Polismart data at high dose rates (≥ 1 mSv/h for ^{60}Co and all for ^{137}Cs) we placed several iPhones with the Radioactivity Counter app next to it. Irradiations lasted for about 5 minutes (below stabilisation time of Radioactivity Counter) and the Polismart was positioned in the middle of the beam. It is possible that an iPhone camera was located outside or on the edge of the beam while irradiating the Polismart (see Figure 3-7). The high dose rates were delivered inside the bunker (panoramic set-up) while low dose rates were delivered with the horizontal setup.

We noticed that the Polismart scored best in the dose rate response and energy response. The performance of the Radioactivity Counter is less than expected (previous experiments), this is possibly due to a fast measurement (not stabilised) or due to bad positioning (outside the beam). Assuming that the iPhones were badly positioned and they didn't reach their stabilisation time, the Radiation Counter succeeded in measuring dose rates and to indicate their order.

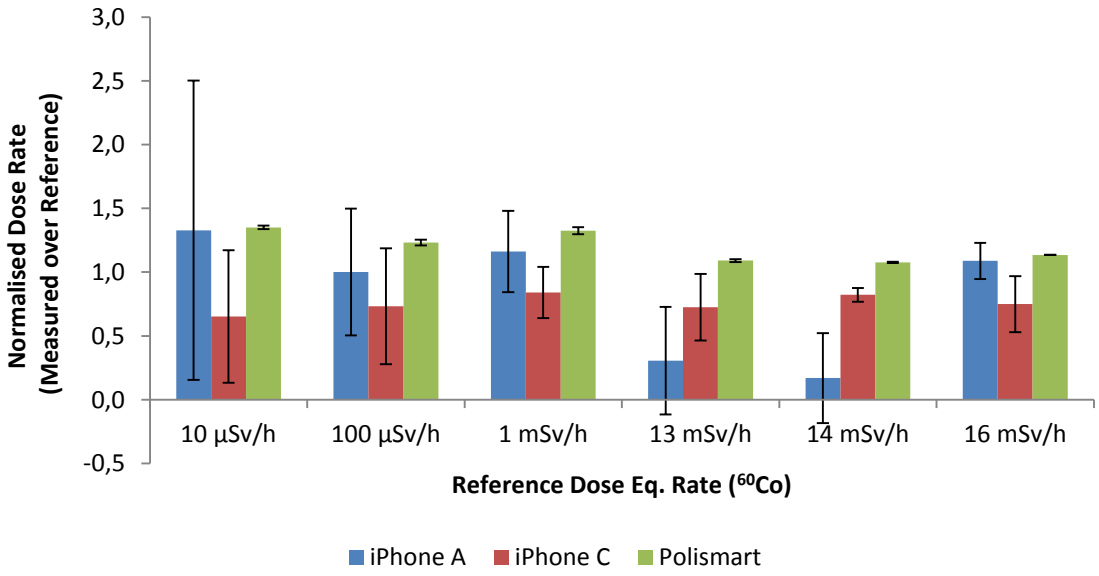

Figure 4-36: Comparison dose rate responses of ^{60}Co between Polismart with Radioactivity Counter

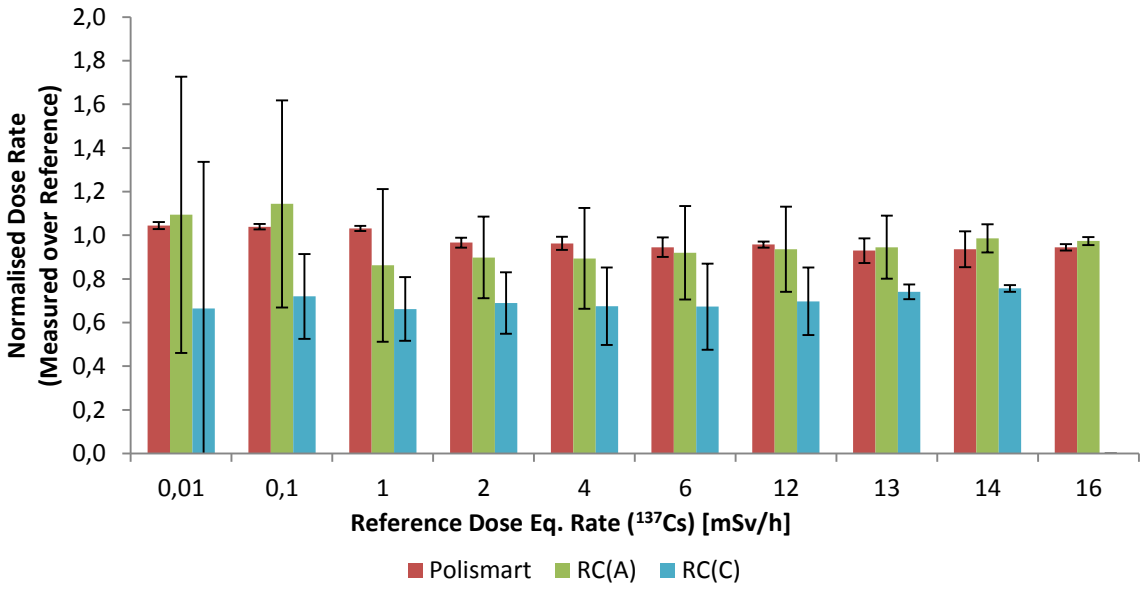

Figure 4-37: Comparison dose rate responses of ^{137}Cs between Polismart and Radioactivity Counter (RC) on iPhone A and iPhone C

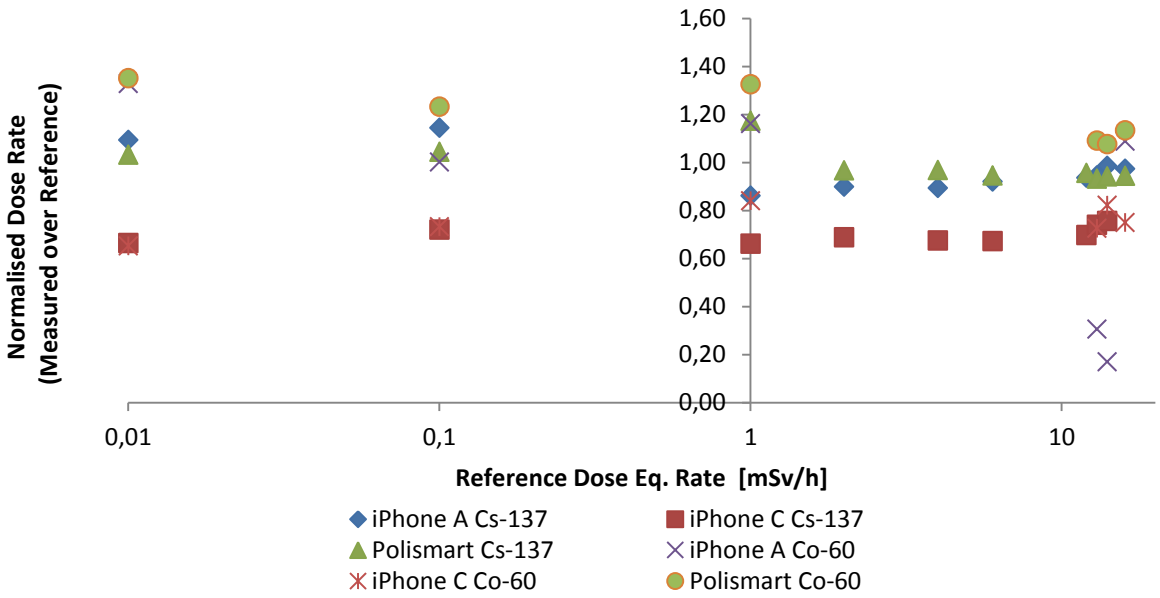

Figure 4-38: Comparing the dose rate response and energy response between Polismart and Radioactivity Counter

c. SIM cards

4.c.1 Shape of the OSL signal

The shape of the OSL signal can be observed in several ways[11], one method is to split the signal into several components, and another one is the peak-&-tail division.

Slow and fast components

The first option is to analyse the signal in a mathematical way. The mathematical analysis will be limited to a curve fitting of a double or triple exponential function where the relaxation time τ can be used to determine the time window of the fast, middle-fast and slow components [7, 33]. These three different components indicates that there are different kind of optically stimulated traps responsible for the OSL signal.

$$I_{\mathrm{OSL}} = \mathrm{A}\exp\left(-\frac{t}{\tau_1}\right) + \mathrm{B}\exp\left(-\frac{t}{\tau_2}\right) + \mathrm{C}$$

$$I_{\mathrm{OSL}} = \mathrm{A}\exp\left(-\frac{t}{\tau_1}\right) + \mathrm{B}\exp\left(-\frac{t}{\tau_1}\right) + \mathrm{C}\ \exp\left(-\frac{t}{\tau_1}\right) + \mathrm{D}$$

Equation 4-1: Double and triple exponential function [7]

Peak and Tail

The OSL signal can be divided in two parts, respectively the peak and the tail Figure 4-39. The peak is that part of the signal used to calculate the signal peak P for Posl while the tail contains information about the signal-background B for Posl calculations.

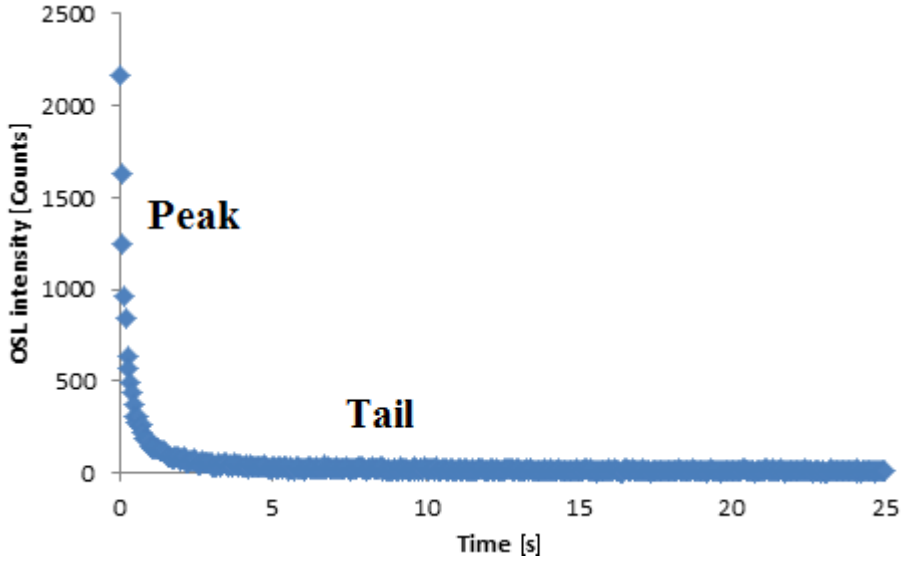

Figure 4-39: Example OSL signal of sample SC2 set 004 SIM card with a dose of 360 mGy

[11] In this master's thesis we don't study the components but we use the peak and tail method for Posl calculations.

A first indication or a good parameter to determine is the peak and the tail of the OSL-signal. As can be seen the peak of a tested chip card (Figure 4-39) is very small compared to the total signal

Having a closer look (Figure 4-40) will reveal that for some samples the peak last less than 0.5 seconds but we can clearly see that the first 4 data points are part of the peak and thus we used them to calculate the P-value in Posl (Equation 3-3).

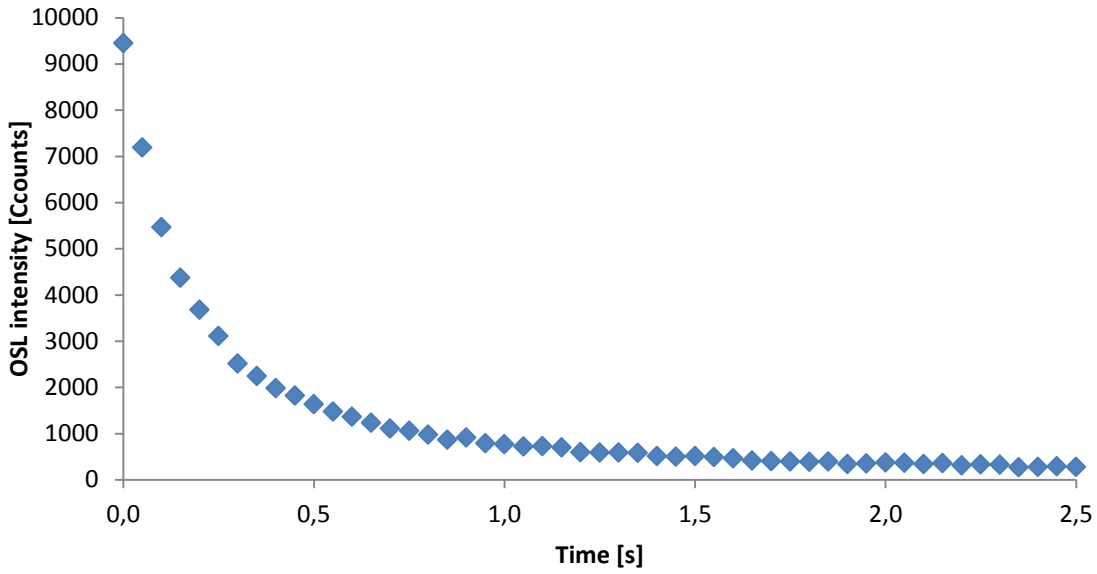

Figure 4-40: Example OSL peak of a Delo 698/4670 chip with a dose around 1 Gy

After an irradiation of 360 mGy (set002-007), we noticed for all SIM cards and SIM modules, a high Posl value except for the SLE cards (Figure 4-41). When comparing the signal shape we noticed that all cards have a decaying OSL signal but the SLE card didn't express this behaviour as can be seen in Figure 4-42 (p 85). Therefore, it was concluded that all except the SLE card samples have an OSL sensitive signal and can be investigated further on.

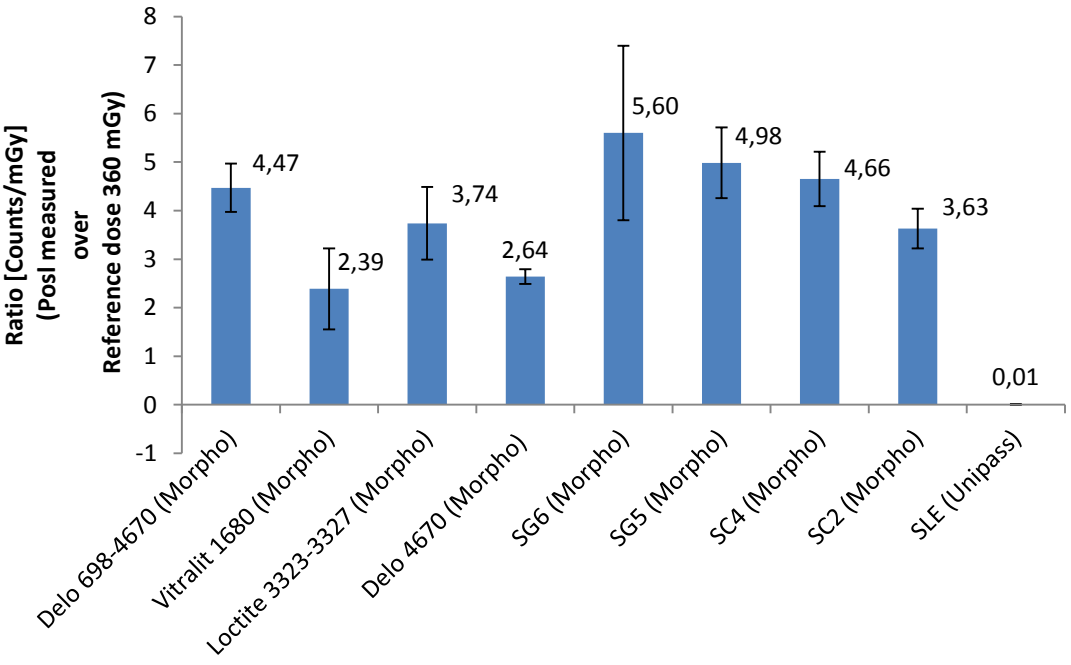

Figure 4-41: Results of analysing the signal shape with Posl

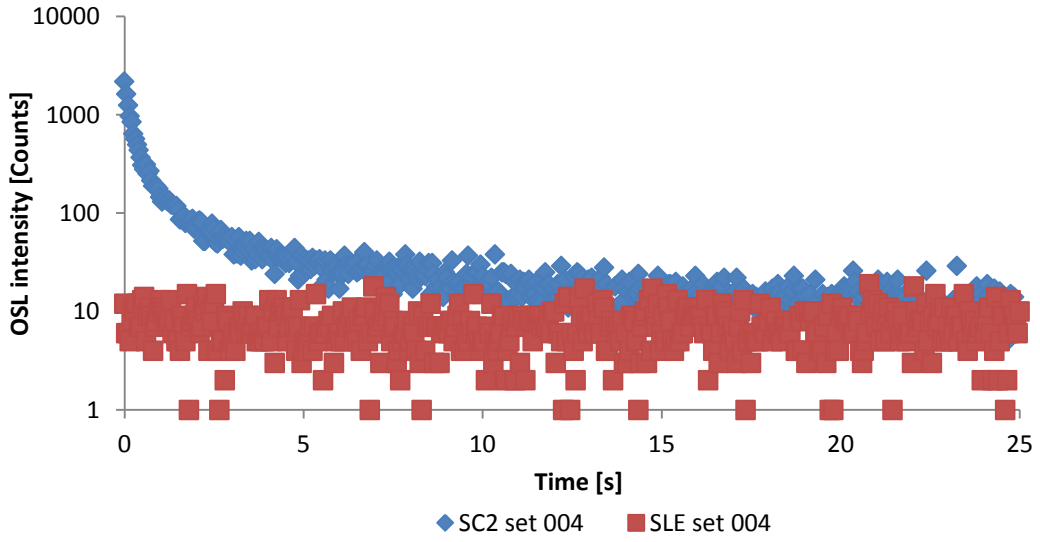

Figure 4-42: Results for an OSL-sensitive (SC2) and non-OSL-sensitive (SLE) material. Irradiated with a reference dose of 360 mGy

4.c.2 Minimal Detectable Dose

Before we mentioned that OSL materials have some lower limits related to traps. The minimal detectable dose (MDD) is also a lower limit. It is the lowest dose that can be detected. To study this lower limit we used fresh and non-irradiated SIM cards. The samples are directly measured with OSL and next they are calibrated by irradiating them with a known dose rate of 72 mGy/h for 5 seconds (total of 360 mGy).

Directly after this irradiation, the OSL signal is read-out again, enabling us to link the first measured signal with a known dose.

After a one-point calibration using the Posl value, we reconstructed the initial or minimal detectable dose on the sample. We tested several samples from each type of card and noticed (Figure 4-43) that the reconstructed dose is about 2 mGy but in some cases the reconstructed dose is higher (~8mGy). For calculating the MDD we should make the sum of the average and standard deviation of the reconstructed dose of all samples. The MDD when taking the negative values into account is at 2.15 mGy (~ 2 mGy) and when taking the absolute values into account the MDD is at 2.90 mGy (~3 mGy). But for safety reasons we define the minimal detectable dose as the maximum of the reconstructed doses (7.88 mGy) plus the standard deviation of all absolute values (1.38 mGy) which is in total 9.26 mGy. So for safety reasons we defined the minimal detectable dose at 10 mGy but knowing that for most samples the MDD is about 2-3 mGy.

Another thing that has to be mentioned is that several cards have a negative reconstructed dose, this is because the signal-background was higher than the signal-peak. This means that there wasn't a typical OSL decaying signal in these cards at that moment. After irradiating and reading these cards again, the typical OSL signal was present.

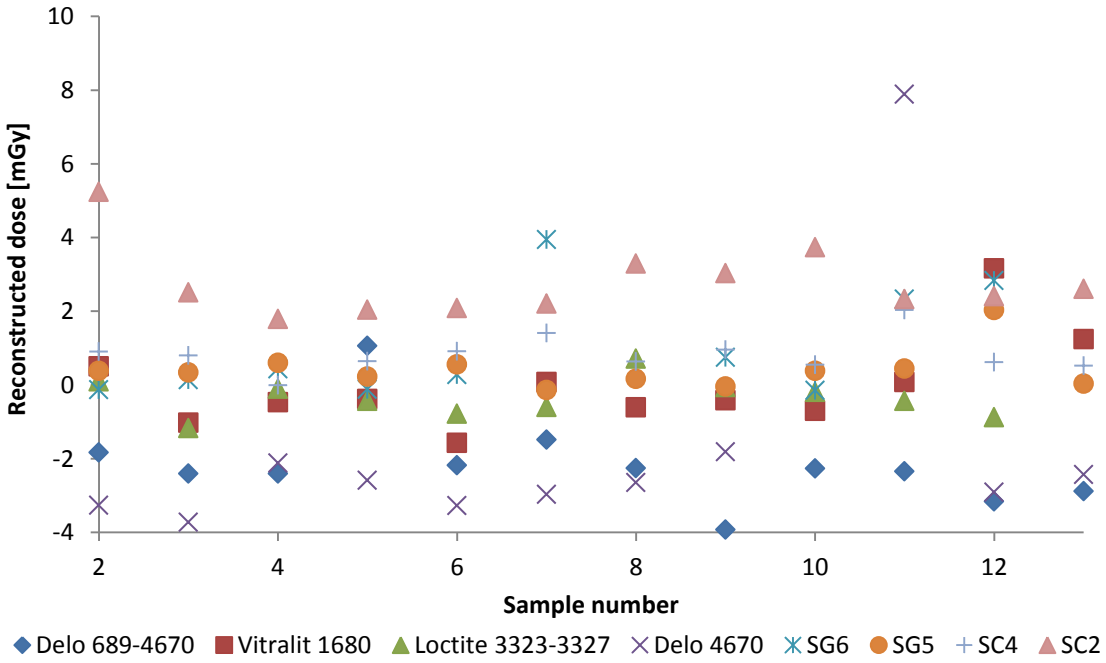

Figure 4-43: Minimal detectable dose reconstructed by a one point calibration

4.c.3 Reproducibility

After analysing the results of the minimal detectable dose, we found that all tested SIM cards are suitable for further investigation. One of the experiments we will conduct is to investigate the dose response by irradiating and reading the samples multiple times. One of the problems that could be faced during such experiment is that the sample has a residual signal from previous irradiation. Therefor we need to investigate the effectiveness of our OSL reading in emptying the traps. This experiment is also being used to investigate the reproducibility of our samples.

The samples are first being bleached by an OSL reading (and not by the specific build-in bleaching option) to eliminate any residual dose from previous experiments. After that the sample will be irradiated and read-out for the first time (Times 1) and this irradiation-reading is repeated another 4 times. In total 6 samples per SIM-type (set 002-007) have been irradiated (360 mGy[12]) and analysed with Posl.

Figure 4-44 shows the findings of this test, the Posl values were averaged and normalised over the Posl value of the first radiation-reading. Large standard deviations have been found between different samples of the same card type. This is probably due differences in the amount of silica in the sample. Each sample can have slightly different amount of epoxy encapsulant and the composition of the silica inside the epoxy can also be slightly different.

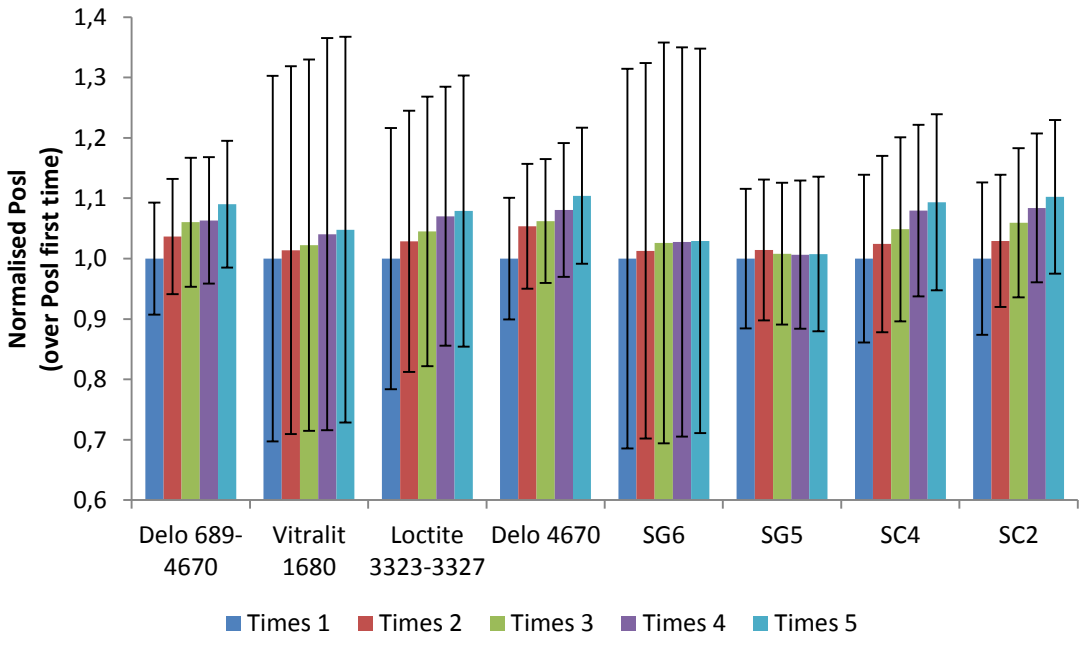

Figure 4-44: Reproducibility of SIM cards. Set 002-007 irradiated with 360 mGy. Results shown the average and the standard deviation (error bars) from sets 002 up to 007

[12] The $^{90}Sr/^{90}Y$ source inside the Risø has a dose rate of 72 mGy/s and irradiated the samples for 5 seconds so that the effect of opening/closing the source shielding would be minimalised.

As mentioned before, the samples might have a different amount of silica particles which can leads to different Posl values. Table 4-7 shows the difference in normalised Posl values of the first and last irradiation-reading. In this table the maximum increase is ~17% for a certain SC2 and Delo 4670 sample. This maximum value can be seen as an out-shouting event since the overall median value of all card types is equal or below 10%, this is also confirmed by our results in Figure 4-44.

Table 4-7: Reproducibility between different sets of the same card type

	Difference Posl (Times 5 - Times 1)			
	Max	Averaged	Min	Median
Delo 689-4670	0.10	0.09	0.08	0.09
Vitralit 1680	0.08	0.05	0.02	0.05
Loctite 3323-3327	0.12	0.08	-0.01	0.10
Delo 4670	0.17	0.10	0.06	0.10
SG6	0.05	0.03	0.01	0.04
SG5	0.04	0.01	-0.02	0.01
SC4	0.12	0.09	0.07	0.09
SC2	0.16	0.10	0.07	0.09

4.c.4 Dose response

When an ideal dosimeter is irradiated their reading should be linear to the received dose, if not, the reading should be corrected. Since our SIM card is far out not a dedicated dosimeter it is important to investigate its dose response. The dose response is tested by first bleaching the sample and then irradiating and reading the sample again and again with an increasing dose. The delivered doses are in the range from 72 mGy [13]up to 4.3Gy[14]. Figure 4-45 shows that our averaged Posl results (of set 001-007) are increasing linear with the dose. As can be noticed on the same graph, the values of e.g. Vitralit 1680, are not perfectly situated on the dose response curve. This is due variation in Posl values between different samples of the same type.

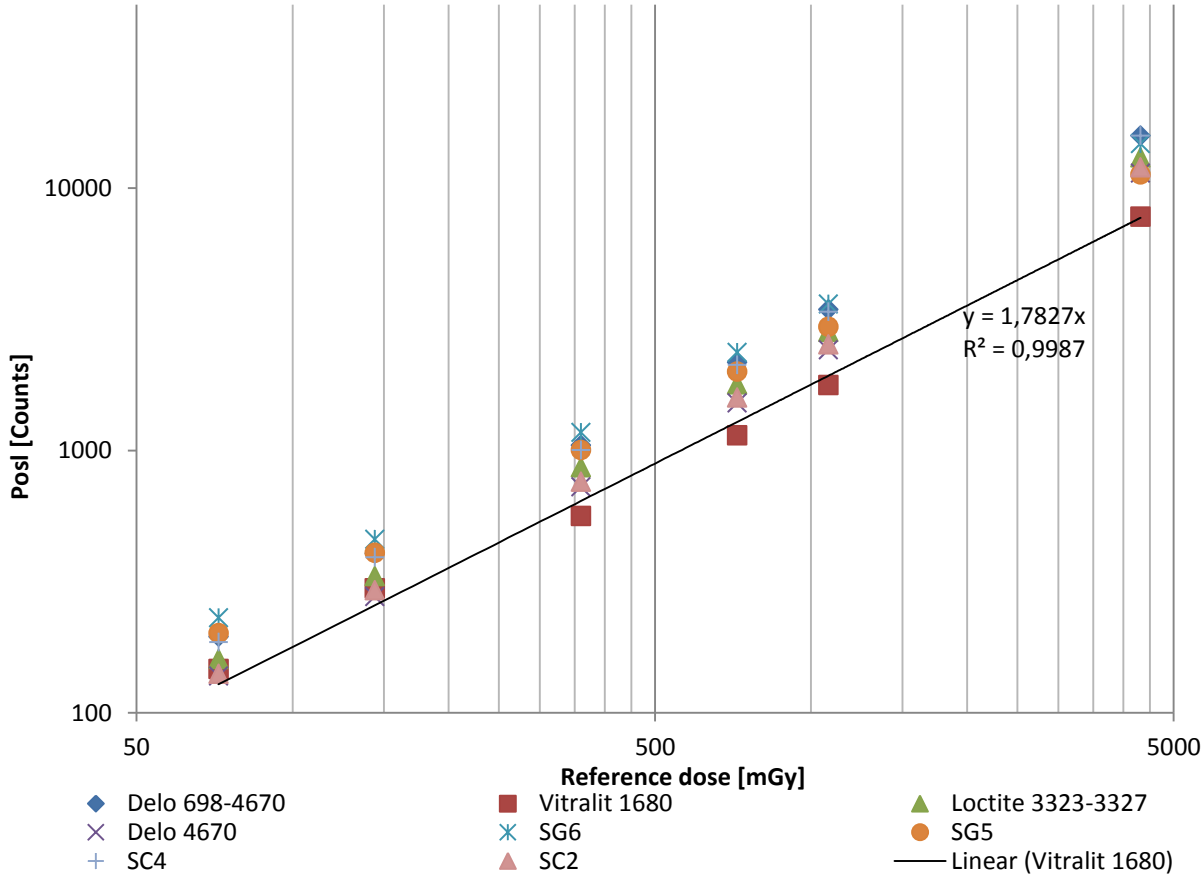

Figure 4-45: Dose response for SIM cards. The test was performed with set 001 – 007 for each card type in which each sample is irradiated and analysed over the whole dose range

[13] The minimal dose that can be delivered by the Risø is 72 mGy.

[14] For a normal healthy adult human, the lethal dose (for half of the exposed individuals) within 60 days, is around 4 Gy midline dose (ICRP 103).

The SIM cards have a linear but not perfect dose response (Figure 4-45). In order to reconstruct the absorbed dose we need to evaluate the relationship between Posl and the reference dose. The Posl (of all samples) are normalised over the reference dose and plotted in Figure 4-46. We notice that the normalised readings differ between type cards and between doses. Therefore each tested SIM card should be tested additionally on its dose response.

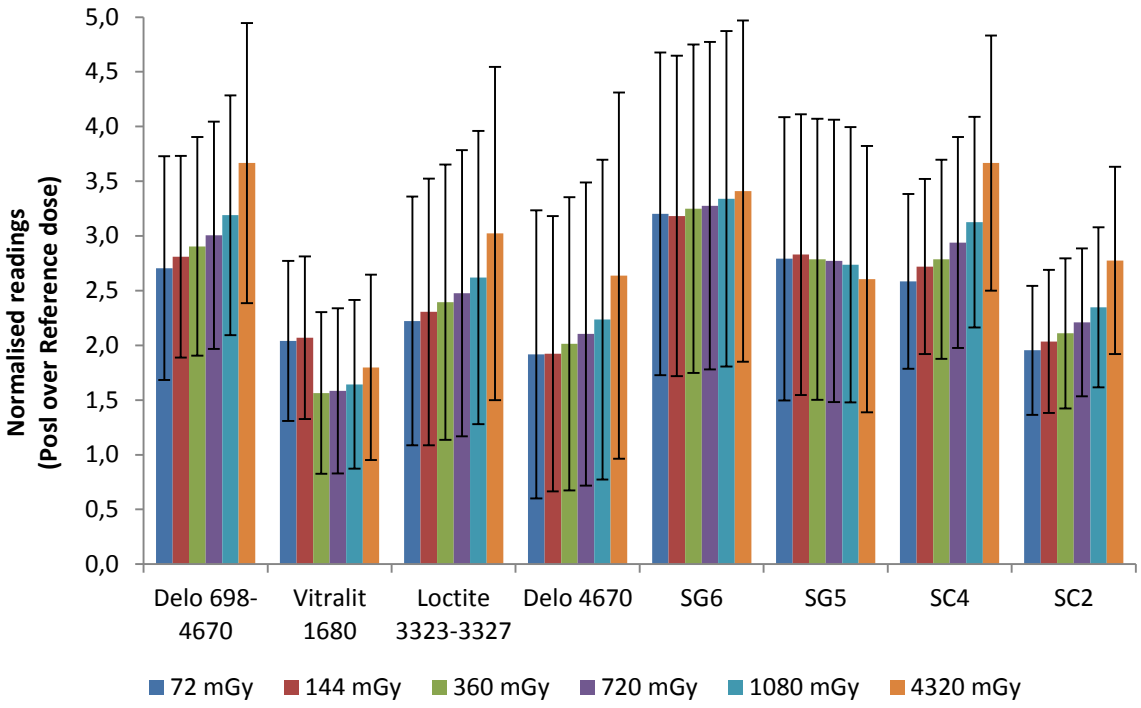

Figure 4-46: SIM card dose response averaged Posl (set 001-007) and their standard deviation (error bars) normalised over reference dose. The large standard deviations are due the fact that every SIM card has different amounts of silica which leads to different amount of registered OSL counts and thus a different in Posl values

4.c.5 Fading

In case of an accident there is always a certain time span between exposure to ionising radiation and to the actual read-out of the SIM card. During this time span, the electrons can escape their traps and recombine resulting in a lower OSL signal. This effect (Signal fading) must be studied in order to preform dose reconstructions. The tested time span consists of 2 parts. The first part is the effect of signal fading is studied at a fading time of 5, 10 and 20 minutes with 8 samples per card. The second part has been tested in larger time intervals (hours – weeks) with only set 001. We assumed from previous results, that the effect for all SIM cards would be similar except their Posl values would vary due different silica composition.

In each measurement the samples are first bleached, secondly irradiated (360 mGy), thirdly a pause is held (representing the fading time), next the OSL signal is measured and after this a new irradiation is preformed and directly afterwards the OSL signal is measured again. This enables us to find a ratio between the Posl measured after fading and the Posl measured directly after irradiation. This ratio (Fading ratio) seems to be decaying logarithmic in function of time as shown in e.g. Figure 4-47.

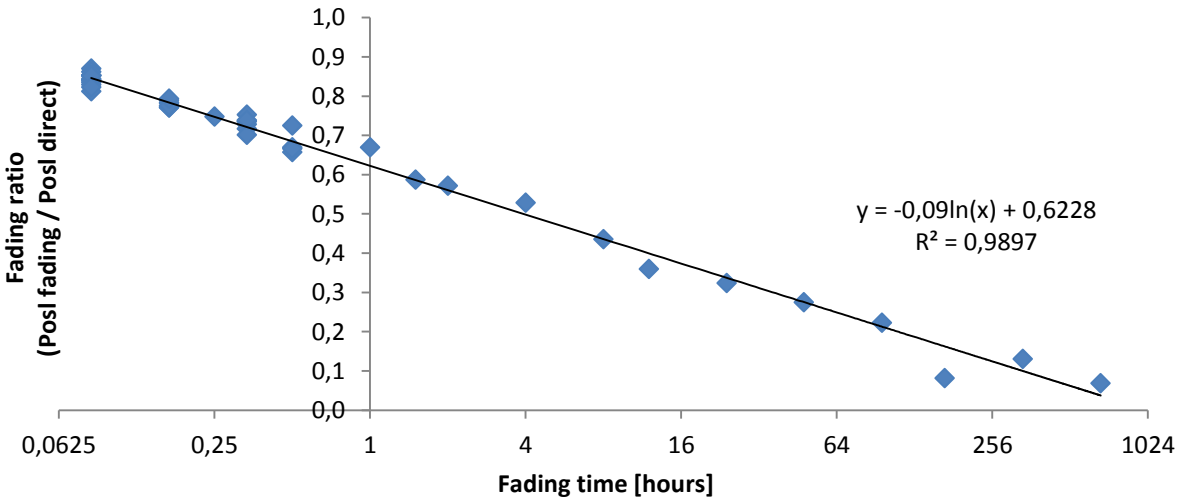

Figure 4-47: Signal fading for Delo 689-4670 seems to be a logarithmic decay in function of time.

For all the tested SIM cards it can be remarked that the cards should be measured as soon as possible. The signal drop after a couple of hours (0.5 – 4) is already about 50% , after a day the signal dropped with about 75% and after a week only 10% of the original signal remains, leading to the conclusion that SIM cards should be measured as fast as possible (Figure 4-48).

The biggest problem of fading is not the signal decay but that the fading differs significantly from sample to sample, making it impossible to have a universal correction curve.

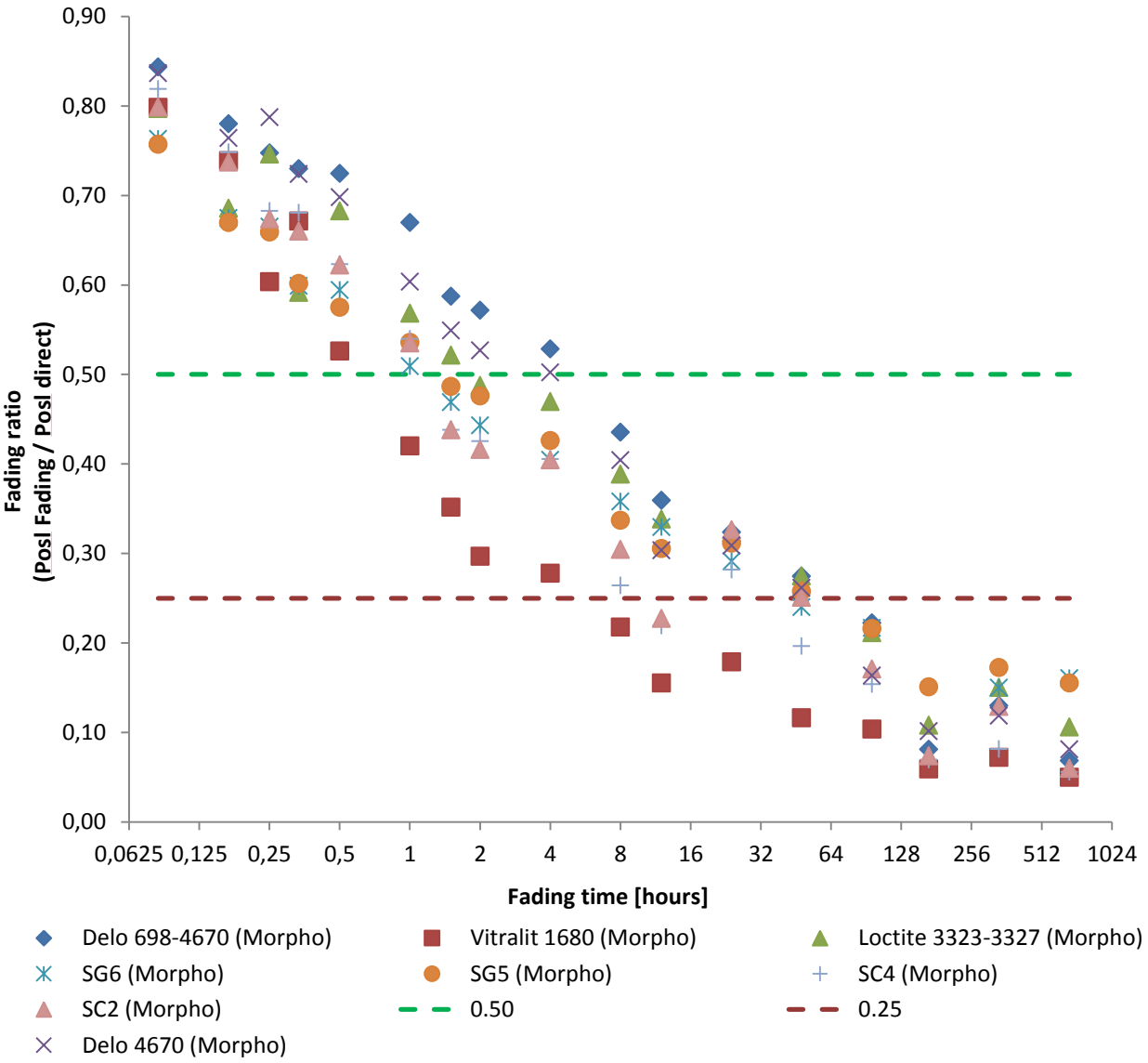

Figure 4-48: Signal fading for SIM cards

Table 4-8: Hours to time conversion

Hours	Time
0.0625	3,75 min
0.125	7,5 min
0.25	15 min
32	1 day 8h
64	2 days 16h
128	5 days 8h
256	1,5 weeks
512	~3 weeks
1024	~6 weeks

4.c.6 Accident simulation low dose and fast response

After studying the minimal detectable dose, the dose response and the fading we decided to irradiate several new SIM cards with a ^{137}Cs source at the calibration lab. The cards were placed on a water equivalent phantom to mimic the human body and a dose of 10 mGy (air kerma) was delivered in 1 hour without correction for backscatter.

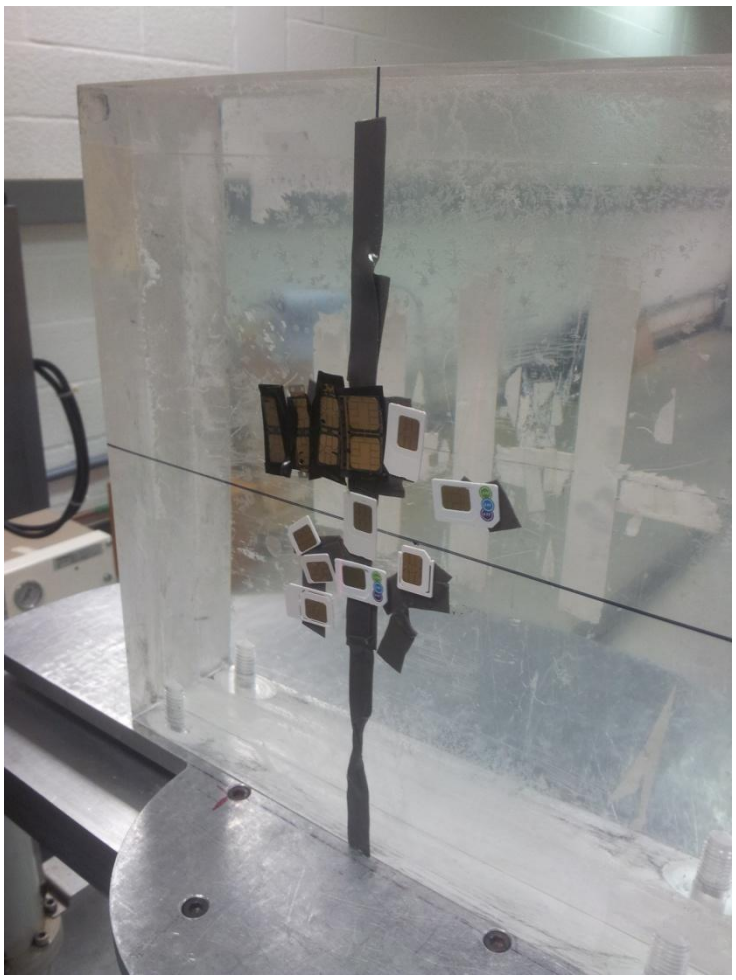

Figure 4-49: Experimental set-up for irradiations of the samples on a water phantom

After irradiation the cards they were transported, extracted and analysed. The analyses started with reading the reading the OSL signal (originating from the "accident"), irradiating-&-reading them again with a known dose (72, 360 and 720 mGy) by use of a 3 point calibration, the accident dose was first reconstructed without any corrections for e.g. fading.

First lets recall that we defined a MDD of 10 mGy but that we noticed that most SIM cards have a MDD about 2 mGy. In this experiment we delivered the MDD (10 mGy) to see its effect and we noticed in Figure 4-50 that a majority of the SIM cards registered an uncorrected reconstructed dose about 3 mGy.

For correcting these doses, they have been divided through the signal-fading ratio at that fading time. The ratios are calculated with the help of the logarithmic decay curve represented in Equation 4-2. The a and b components are gathered from the fading experiments[15] are inserted in this equation and used to correct the dose.

$$\text{Fading ratio} = \text{a}\ln(t) + \text{b}$$

Equation 4-2: Logarithmic decay function.

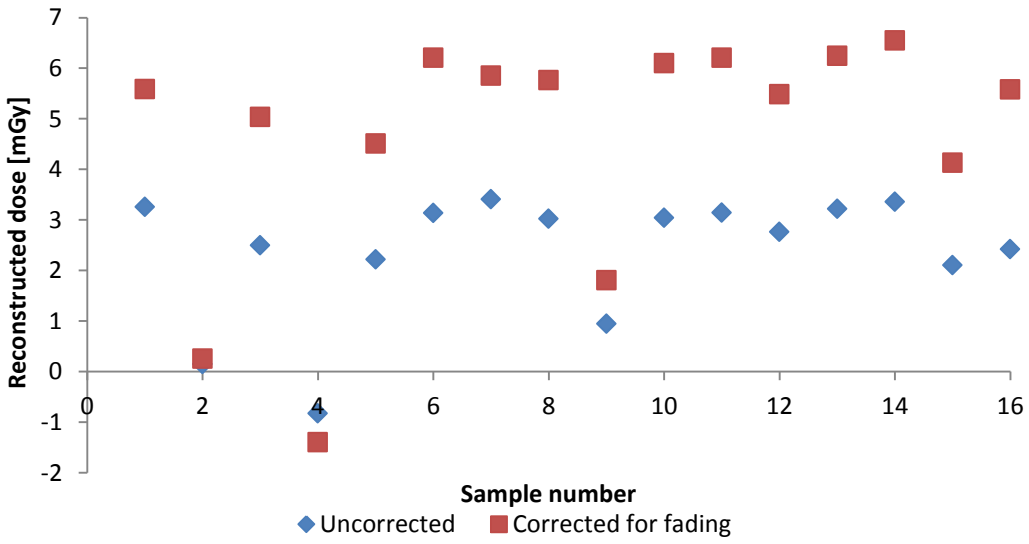

Figure 4-50: Accident simulation, with a delivered dose of 10mGy (^{137}Cs 10mGy/h) and analysed after a minimal time span of 1 hour

After applying this correction for signal fading, the reconstructed dose reaches about 6 mGy. The for fading corrected dose still underestimates the reference dose. This can be explained due differences in our experimental set-up and the accident.

With our Risø reader we irradiated the epoxy and not the chip card as happened during the "accident". We also irradiate with another source and a much higher dose rate. All these and other factors can lead to an underestimation of the delivered dose during the accident.

[15] The samples used for experiments in *"4.c.5 Fading"* are different from the ones used in this experiment.

Table 4-9: Uncorrected and fading corrected doses for accident simulation (10 mGy ^{137}Cs, fading 1h)

Number	Type	Uncorrected dose [mGy]	Dose corrected for fading [mGy]
1	Delo 4670	3.26	5.59
2	Delo 4670	0.15	0.26
3	Vitralit 1680	2.50	5.03
4	Delo 689-4670	-0.82	-1.39
5	Vitralit 1680	2.22	4.51
6	SG6	3.14	6.21
7	Delo 689-4670	3.41	5.86
8	Loctite 3323-3327	3.03	5.76
9	Loctite 3323-3327	0.95	1.81
10	SG6	3.04	6.10
11	SG5	3.14	6.21
12	SG5	2.77	5.49
13	SC4	3.22	6.25
14	SC4	3.36	6.55
15	SC2	2.10	4.13
16	SC2	2.42	5.58

4.c.7 Accident simulation low dose and slow response

We carried out a similar accident but now the time span accident-reading is one week, mimicking a slow response. As in previous simulation, the SIM cards were placed on a phantom and irradiated, this time with a dose of 20 mGy (air kerma without correction for backscatter) in 5 minutes.

The SIM cards were collected directly and stored in a dark room for a week and then the cards were prepared and analysed. The calibration was conducted with a one-point calibration (72 mGy).

As can be seen in Table 4-10, the uncorrected dose is below 2 mGy (MDD), a correction for fading could be applied, but even some SIM cards gave doses between 10-30 mGy we are not able to discriminate if this dose is coming from the accident or from noise.

Table 4-10: Uncorrected and fading corrected doses for accident simulation (20 mGy ^{137}Cs, fading 1 week)

Number	Type	Uncorrected dose [mGy]	Dose corrected for fading [mGy]
1	Delo 689-4670	-2.72	< 0
2	Delo 689-4670	-2.68	< 0
3	Vitralit 1680	0.63	31.20
4	Vitralit 1680	0.65	32.15
5	Loctite 3323-3327	1.87	12.18
6	Loctite 3323-3327	0.48	3.14
7	Delo 4670	-1.96	< 0
8	Delo 4670	-3.97	< 0
9	SG6	0.80	5.95
10	SG6	0.27	1.97
11	SG5	1.05	7.79
12	SG5	0.61	4.51
13	SC4	0.10	1.17
14	SC4	0.23	2.81
15	SC2	1.27	11.73
16	SC2	2.13	19.62

4.c.8 Fading no light / red light experiment

In this chapter we study the effect of signal fading when the epoxy is exposed to red light during sample preparation. The samples are first being irradiated then exposed (to red light or to no light) for 30 min and after this they are read-out. Directly after this reading we irradiate and read them again to determine the fading ratio. This fading due red or no light will be compared with each other to link the effect of the big red lights during sample preparation.

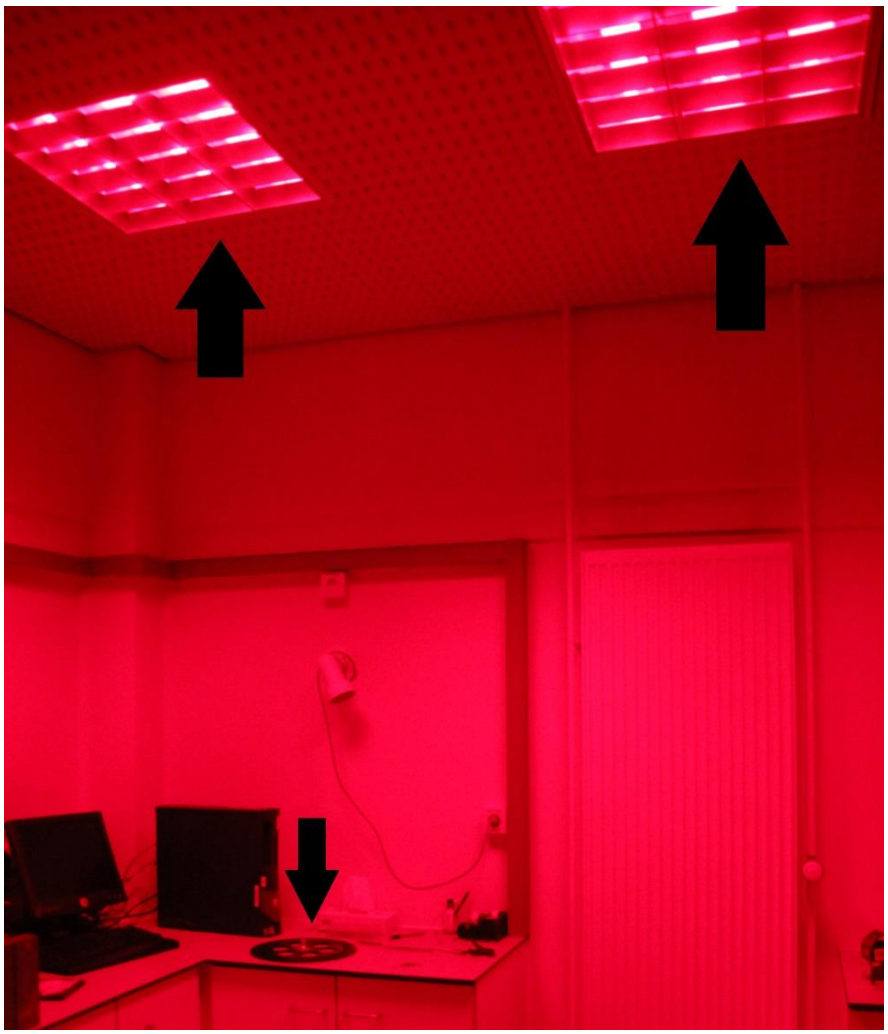

Figure 4-51: Situation "Fading under red light"

Since a lot of samples are being irradiated at once, the fading time consists out of 2 parts. A first part is while they are being waiting for being irradiated or being analysed (1h) and the part that they are deliberately exposed to the fading effect (30 min being exposed to either no light or only red light). The red light experiment is conducted with 13-14 samples per card type and the no light experiment is conducted with 4 samples per card type.

First the fading ratios when not exposed are compared with previous fading results and only Delo 4670 and SC4 card types seems to have a significant lower averaged signal than expected (Table 4-11).

Table 4-11: Signal fading ratios for previous experiment (4.c.5 Fading) and current experiment

	Fading ratio (Posl fading / Posl direct)		
	Previous Fading experiment	No light experiment	Red light experiment
Delo 689-4670	0.59	0.58	0.51
Vitralit 1680	0.35	0.32	0.32
Loctite 3323-3327	0.52	0.50	0.49
Delo 4670	0.55	0.46	0.47
SG6	0.47	0.46	0.45
SG5	0.49	0.50	0.48
SC4	0.44	0.35	0.40
SC2	0.44	0.39	0.43

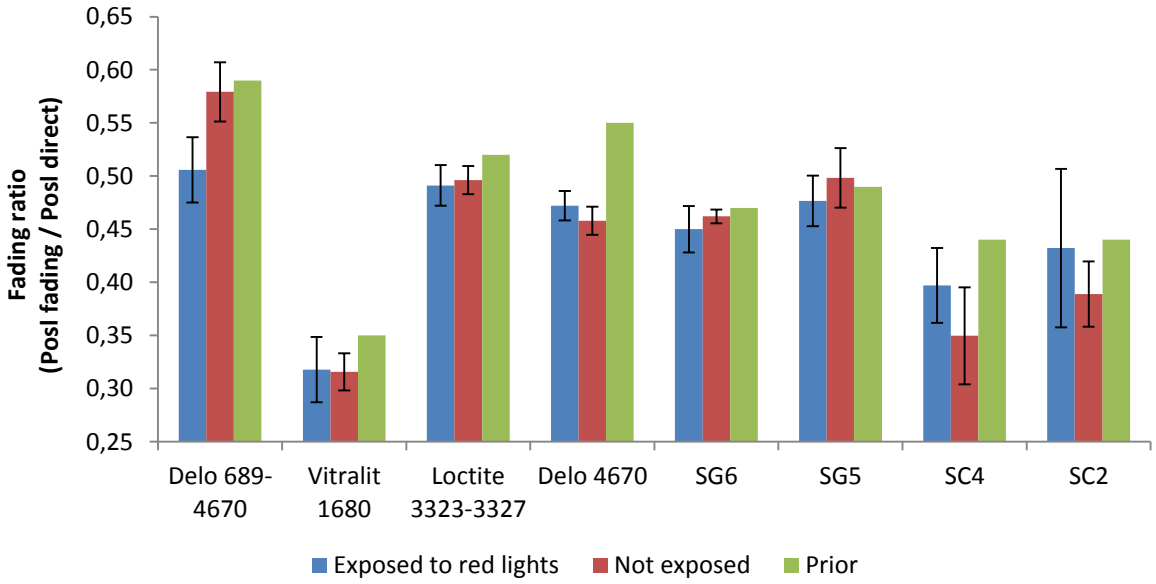

Figure 4-52: Fading ratio when SIM is exposed to red lights and when not. Posl values are averaged over the results of the samples and their deviation is displayed as error bars. The total fading time is split up into a standard fading time of 1h and a (un) exposed fading time of 30 min. Note that only 1 set was used for prior results and thus no error bars (deviation) are added

Secondly the effect of red light vs. no light is been studied. We expect that when a sample is exposed to light, the signal loss will be larger than when not exposed to light, so the ratio is expected to be smaller than 1. Table 4-12 shows that this isn't the case for every sample (probably due statistics) and that the effect of exposing 30 min to red light is minimal (a few per cent) except for Delo 689-4670 (23% underestimation).

Table 4-12: Results for the Red-No light fading experiment

	Ratio (Ratio Red / Ratio no light)
Delo 689-4670	0.87
Vitralit 1680	1.01
Loctite 3323-3327	0.99
Delo 4670	1.03
SG6	0.97
SG5	0.96
SC4	1.14
SC2	1.11

4.c.9 Effect of preheat

The effect of pre-heating a sample before reading it, was tested by first bleaching the samples, then irradiating them with a dose of 360 mGy then a pause (fading) followed by a preheat (10s) , a small pause of 10 s (cool down) and an OSL measurement. After this measurement the sample was irradiated again and directly pre-heated and read. This was been done to calculate the fading ratio (Posl fading over Posl direct).

Since we don't know what the actual epoxy melting temperatures are, we heated one sample from each type outside the Risø to a temperature of 200°C in steps of 20°C. We noticed that some samples could stand heats up to 200°C while others began to decompose at 120/140°C. Therefore we investigated the effect of preheat at temperatures of 30, 50 and 100°C. The samples that were heated up to 200°C were afterwards excluded from any further study.

Figure 4-53: Simulation of the Risø heating plate by a controllable heating plate (RET digi-visc from IKA Labortechnik, SCK serial number 002484)

Fading at room temperature was carried out earlier in the scope of the fading experiment. There for we re-use these data (set 002-007) and neglecting the effect of the 20s pause. For the pre-heating at 30°C, 50°C and 100°C we used 5 samples per type (set 002-007).

To have a global view on the fading effect we averaged all fading ratios and plotted them in function of the fading time. From these averaged the effect of preheating with 30°C seems minimal (compared with no preheat) while the effect of 50°C is higher and pre-heating with 100°C gives significant higher fading ratios which means that the signal fades slower (Figure 4-54).

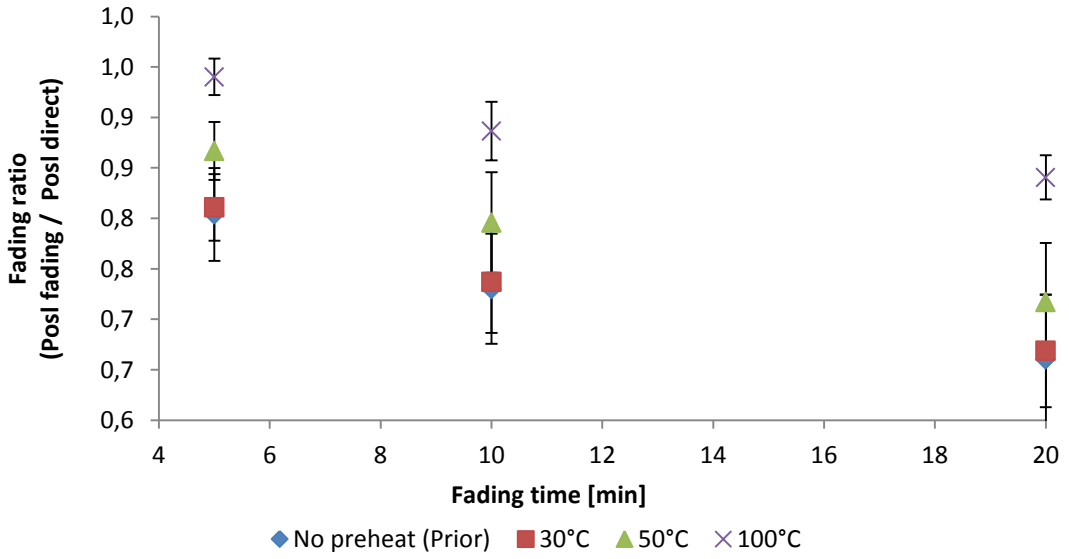

Figure 4-54: Effect of preheat on fading ratio (averaged over several sets) and their error bars (standard deviation on the averaged value)

Table 4-13: Fading ratio (Posl fading over Posl direct) for different SIM cards at different pre-heat temperatures for different fading times

Fading ratio	Averaged over all SIM cards			Stdev of all SIM cards		
	5 min	10 min	20 min	5 min	10 min	20 min
No preheat (Prior)	0.80	0.73	0.66	0.05	0.05	0.06
30°C	0.81	0.74	0.67	0.03	0.05	0.06
50°C	0.87	0.80	0.72	0.03	0.05	0.06
100°C	0.94	0.89	0.84	0.02	0.03	0.02

When observing the fading ratio per sample type per fading time, we can see the expected trend of a decreasing fading ratio. However the ratio seems to decrease faster at lower pre-heat temperatures than with higher pre-heat (Figure 4-55 to Figure 4-57).

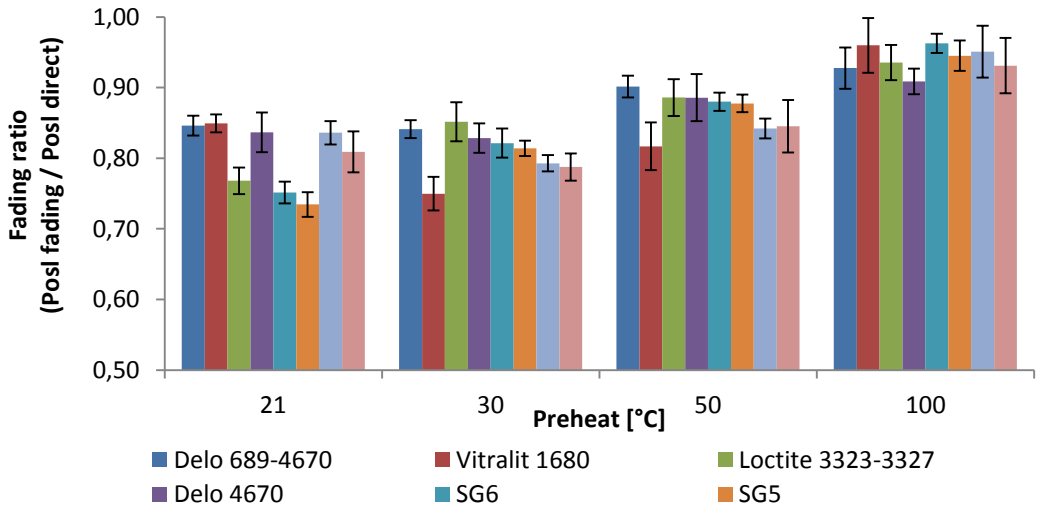

Figure 4-55: Effect of pre-heat on fading ratios at a fading time of 5 minutes

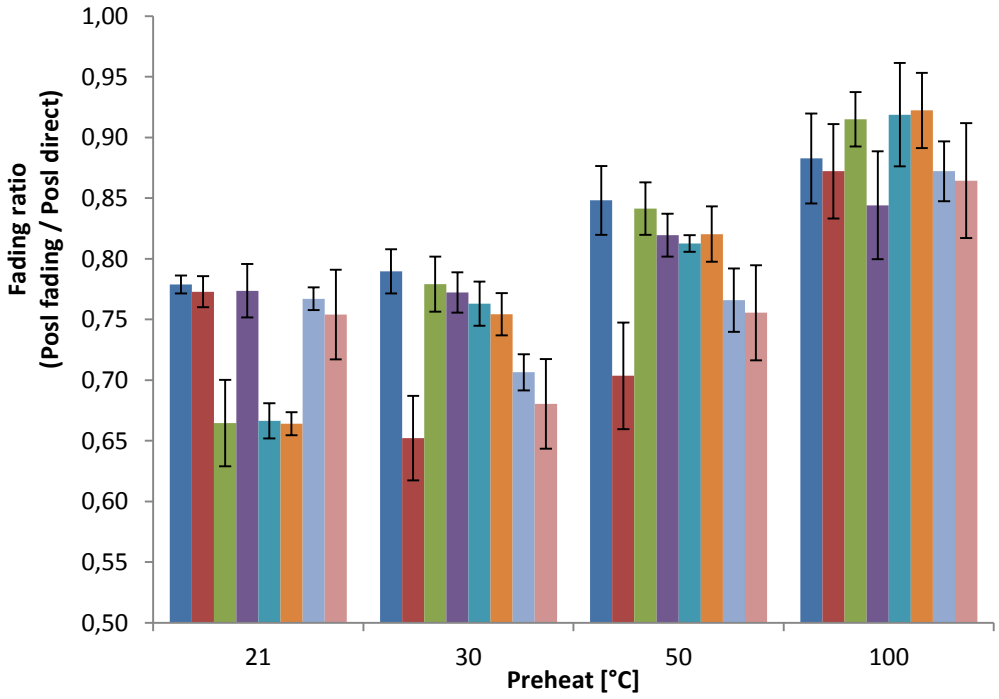

Figure 4-56: Effect of pre-heat on fading ratios at a fading time of 10 minutes

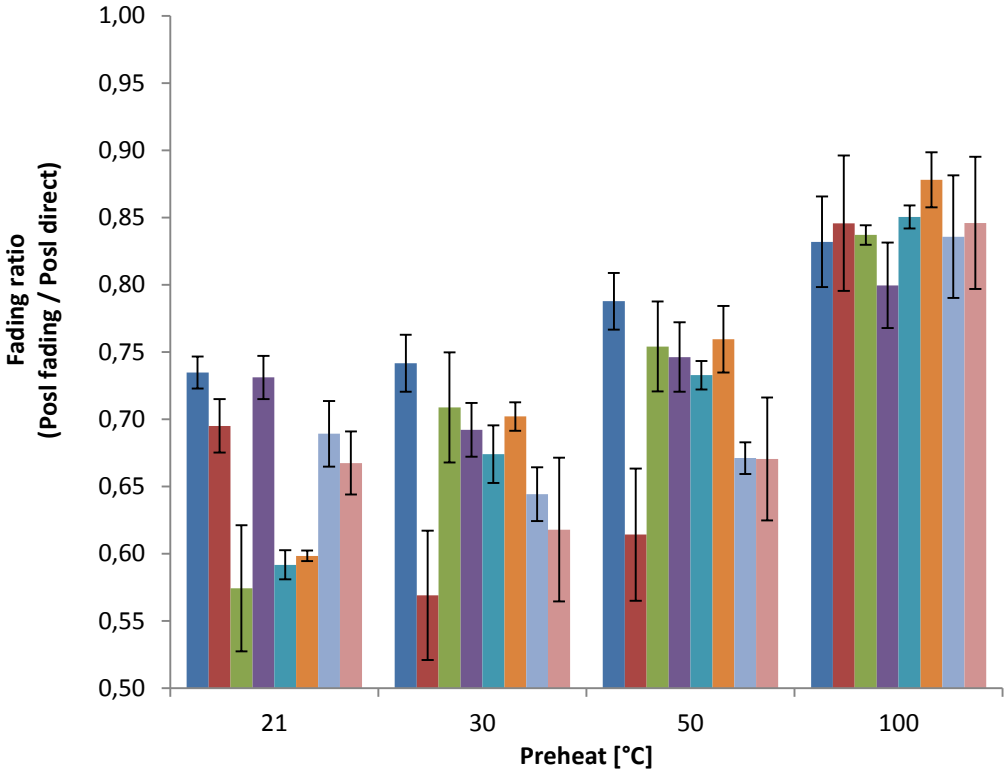

Figure 4-57: Effect of pre-heat on fading ratios at a fading time of 20 minutes

4.c.10 Effect of heated OSL

Last experiment investigated use of pre-heat; another option is to heat the sample while performing the OSL measurement (in order to keep the heated traps empty). By adding external heat during the measurement we are not really performing a "pure" OSL-measurement since we would detect luminescence originating from thermal and optical stimulation.

During this experiment 2 samples of each card (set 002 & 003) were irradiated, pre-heated (10s) and analysed with heated OSL. The results were averaged over all the cards and are displayed in Figure 4-58. As can be seen in this graph, it seems that the Posl for chip cards decreases at increasing temperature. This drop can be explained that troughs increasing the temperature at preheat, more electrons will escapes their trap which results in a lower OSL signal which is measured 10 seconds later.

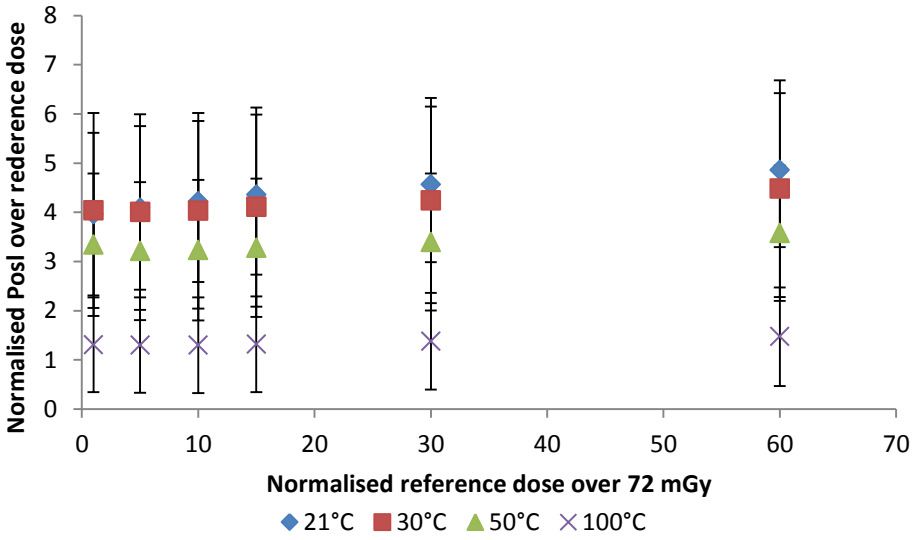

Figure 4-58: Dose response for OSL measurements while heated. Results plotted of the averaged over results of all cards and their standard deviation (error bars)

Table 4-14: Dose response for OSL measurements while heated

	Normalised average of all SIM cards over Reference dose					
Reference dose [mGy]	72	360	720	1080	2160	4320
21°C	3.96	4.09	4.22	4.36	4.57	4.86
30°C	4.04	4.01	4.03	4.11	4.24	4.48
50°C	3.34	3.21	3.23	3.28	3.40	3.58
100°C	1.31	1.30	1.30	1.32	1.38	1.47

Table 4-15: Dose response for OSL measurements while heated

	normalised standard deviation of all SIM cards over Reference dose					
Reference dose [mGy]	72	360	720	1080	2160	4320
21°C	1.65	1.66	1.64	1.63	1.58	1.56
30°C	1.98	1.99	1.99	2.02	2.08	2.21
50°C	1.45	1.40	1.43	1.41	1.39	1.37
100°C	0.96	0.97	0.97	0.98	0.98	1.00

5 Discussion – Pros & Cons

a. Smartphone apps

In the experiments we noticed that the smartphone's apps succeeds in detecting ionising radiation but in order to have stable readings, they need to measure at least for 10 minutes[16]. We noticed that readings for the same app can vary between different phones (of the same type) due differences in their CMOS sensor. When comparing different apps on the same phone we noticed that some applications are better than others. This is mainly due to 2 reasons; first each program has another detecting algorithm; and secondly their calibration mechanism.

We noticed that the Radioactivity Counter has the possibility to calibrate using the current background dose rates or previous recorded data, while others didn't supported this option.

For the Wikisensor we noticed that it had a bad calibration mechanism (static) and we didn't noticed any significant relationship between measured dose rate (or burned pixels / minute) and integration time. This last is since it only measures during a certain time interval and doesn't take any other previous measurements into account when displaying the dose rate.

We also noticed that the applications are not always measuring the delivered dose rate which can be due to its detection algorithm. Another possible explanation for this phenomenon is due to the system properties of the smartphone. A smartphone mostly runs only 1 program or task at the time, and if it runs a background program for a fraction of time, he has to stop running the code of the other apps. So when the smartphone is running a background task, he will stop for a short moment in time to run our detection app and this can result in an "no signal" reading.

For our tested applications we noticed that they request to cover the camera with black tape. Which is good since visible light is not affecting the readings. However not everyone will always tape off their camera or have some black tape with them.

[16] The stabilisation time for Radioactivity Counter, Wikisensor and iRad are respectively 10 minutes, unknown and 10-30 minutes. For the Wikisensor we noticed that a stabilisation time about 20 min when we reconstructed the mean values by hand afterwards.

b. Polismart

The Polismart PM1904 GM-detector is an add-on that can be attached to a smartphone and utilises it to show the dose rate levels. The detector has a linear dose rate response and preforms fine in the suggested range (0.01µSv/h – 13 mSv/h. When exposed to higher dose rates (100 mSv/h), the Polismart keeps registering the dose rate with a good precision.

The detector can be used to show readings directly but in these experiments the data points were saved every second and analysed later on. When exposing the detector to ionising radiation, we noticed a short and sharp increase of the dose rate values and a large uncertainty. After a few seconds the values gave a good indication of the dose rate level. After about half a minute, these values reached a plateau level, which means that these dose rates readings reached a variation below 10%.

After these experiments, the energy response was tested with several Narrow-series X-beams. It was suggested that Polismart's energy response (relative to 662 keV from ^{137}Cs) in the range of 60-1330 keV was no more than ± 30 %. We confirmed this for the range 100-1330 keV. For energies below 60 keV we noticed an under estimation and an over estimation for energies below 164 keV. This over- and underestimation seems normal for an energy compensated Geiger-Müller tube and is as what can be expected (Figure 2-4).

However the Polismart is relative expensive ($ 200) and must be delivered after purchase while the Polismart are inexpensive (free – a few dollars) and can be directly used after purchase. Another advantage of the apps is that you have them always with you (except the black tape!) and you can use them as long the smartphone has enough battery life. This is in contradiction with the Polismart which needs to be charged and carried with you while measuring. The Polismart however is a separate device which is plugged into the smartphone to see real-time measurements (and their variation). It can also be used as a standalone device however the readings can't be displayed at that moment.

Next to these practical dis- and advantages, the Polismart is preforming better on all topics than the camera apps.

c. SIM cards

Thanks to the silica particles inside the translucent epoxy encapsulent of SIM cards, we were able to measure useful OSL signals; this was not the case for the SLE card.

The typical logarithmic decay was noticed for all the 8 epoxy types in which a very steep and small (in time) peak was expressed. The SIM cards also have a flat dose response in the tested range of 72 mGy up to 4 Gy. Next the minimal detectable dose was tested and for most cards this is about 2-3 mGy, however due some higher values for several samples, we defined the minimal detectable dose at 10 mGy. These properties make SIM cards an interesting tool for dose assessments. However the signal fading is playing an important role on their usability. We noticed the signal dropped with 75% when the signal was analysed 24h after the irradiation and even with 90% when analysed after a week. This property of the SIM card is a very big disadvantage; however the effect of pre-heating (100°C) seems to minimalize this effect.

We also noticed that each SIM card (from the same type) can give different readings. This is due the different amount and composition of the epoxy (and so thus the amount of silica in each sample). In order to make dose assessments, each card should be tested and calibrated separately.

6 Proposal Protocol

With the collective knowledge of all the SIM-card experiments, we were able to construct a working protocol that can be utilised in case of an emergency. When the SIM card arrives at the lab, the OSL signal (originating from accident) should be read out as soon as possible, next the card needs to be calibrated in order to relate the OSL signal to absorbed dose. After that the card's dose response and fading behaviour must be checked in order to make dose corrections. This working protocol is presented in Figure 6-1.

The samples should be analysed for 120s with blue light OSL (470 nm) with an optically power of 90% which is around 40.5mW cm^{-2} and a sample rate of 0.05 seconds per data point. Next the signal should be checked to see if the OSL decay is present. And then the signal can be used to calculate Posl values by averaging the registered counts of first 0.2 seconds subtracted by the average counts of the 20-25 seconds of the signal. Before making an OSL measurement the sample should be pre-heated with a temperature of 100°C for 10 seconds.

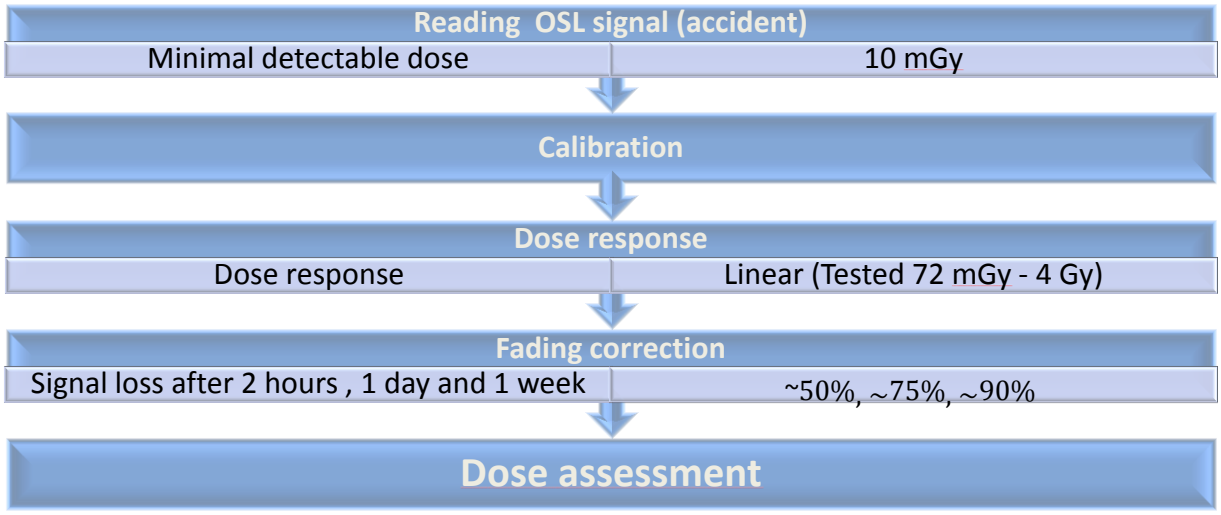

Figure 6-1: Schematic working protocol for OSL signal reading

Remark: When the mobile phone is collected at the accident site it is important to note where the phone was located (e.g. in his car, in his back pocket, inside the pocket of the jacket).

7 Conclusions

The goal of this research was to investigate the use of mobile phones to detect ionising radiation. We limited ourselves to study the mobile phone as an active dosimeter for reading dose rate levels in real time (apps and Polismart) and we also studied the use of the mobile phone's SIM card for dose reconstruction.

The smartphone applications Radioactivity Counter, WikiSensor and iRad succeeded in showing higher readings while being irradiated. They are not accurate enough and usable enough to replace professional detection devices. However they are usable for detecting ionising radiation and they can give promising good results when they have a good detection software and when they are used correctly.

We noticed that Radioactivity Counter (10 min) and iRad (10-30 min) need to measure at least 10 min before reaching a stable signal. During these stabilisation experiments we also noticed that WikiSensor underestimated the dose rate (10µSv/h) by a factor 10 whilst other apps over/underestimated the dose rate about 0.82-1.4. The WikiSensor seemed to have a bad calibration mechanism and therefor the burned pixels per second have been used to reconstruct the given dose rate resulting in relative better dose rate readings. The readings of the WikiSensor are not an average of the previous results but the reading of that moment. In order to determine the stabilisation time (and the dose rate) we had to calculate the mean values by hand. Afterwards we noticed that the WikiSensor also needed a stabilisation time of 20 minutes.

When the iPhone was connected with the PM1904 Polismart II detector (a dedicated GM-tube) we noticed a relative short stabilisation time compared to the applications. The Polismart directly registers detection and soon reaches a stable signal (< 2 min). The detector has a good dose rate linearity (tested in the range 1 µSv/h – 16 mSv/h) and didn't paralyse at a high dose rate of 100 mSv/h (5 min). The detector also expressed a good energy response (max over/under estimation compared with ^{137}Cs: ±30%) for energies in the range 100 – 1330 keV mean energy. The GM-tube tends to over/under estimate more severe at lower energies. We also noticed that the detector has a good angular response except for angles around ±90° from the geometrical centre.

If we put the results from the Polismart PM1904 and the Radioactivity Counter app next to each other we can see (for ^{137}Cs and ^{60}Co) that the Polismart detector is far more superior thanks to a better dose rate and energy response. Also the uncertainties from the PM1904 are much smaller than those from the Radioactivity Counter app.

After these real-time measurements, we also investigated the SIM card for its use for dose reconstruction and dose assessments. The silica particles inside the epoxy encapsulant are radiosensitive and can be measured by means of OSL.

A total of 9 different cards have been tested. One (SLE from Unipas) didn't had any epoxy and thus none OSL signal could be measured. The other 8 types gave positive results but each

sample from each type gave different results, probably due different amounts of silica in each sample. Non-irradiated cards were used to determine the minimal detectable dose about 2-3 mGy for most of the cards. However some cards had a higher MDD (about 9 mGy) and therefor, for safety reasons we assumed that the minimal detectable dose is 10mGy.

The SIM cards were also tested on their dose response which is linear in the tested range of 72 mGy up to 4 Gy. Having a low minimal detectable and a linear dose response makes the SIM cards interesting for dose assessments. However in case of an accident the SIM cards are not analysed directly and signal fading will become an important factor on the usability of the detector. Reading the cards a couple of hours after the accident will lead to a signal drop about 50% after one day only 25% of the remaining signal remains and 10% remains after a couple of weeks and this is due the fact of electron escaping from shallow traps. This effect of fading can be minimalized by using a pre-heat of 100°C before preforming an OSL measurement. We also found that exposure to red light (during sampling) has almost no influence on signal loss compared to fading without red light.

In overall we can conclude that the mobile phone can be used to detect ionising radiation:

1) Smartphone applications using the phone's camera are not always accurate and often require stabilisation times that are longer than 10 minutes. But they succeed in warning the user for the presence of ionising radiation.

2) The external GM-tube (PM1904) of Polismart is a dedicated detector that uses the phone to display their readings. It is an interesting tool to transform the phone into an accurate detector.

3) The epoxy encapsulant of the SIM cards can be used for dose assessments; however the signal fading will limit its precision. In case of an accident the cards should be collected as soon as possible with a working protocol that covers the reading of the OSL signal (accident) followed by a calibration. Next the protocol should also cover a dose response and the fading test in order to make dose corrections. This whole protocol should be repeated for each sample due difference in their amount of silica.

Outlook

This master's thesis investigated the use of 3 tools to detect ionising radiations but there are more tools available that might be worth for investigation in future works. But these 3 tools can also be investigated future more. Following small list will propose some possible subjects that could be studies in the future.

First for our smartphone applications using the camera:

- Repeating the preformed measurements (statistics & reproducibility);
- stabilisation measurements for other dose rates;
- the effect of using the wrong camera while measuring (angular response);
- testing more and different types of apps and phones;
- the effect of high dose rates on reading values (saturation);
- the "zero reading" effect during irradiation;
- the effect of running programs in the background;
- the effects of the different weather situations (hot/cold/rain/…);
- and many more.

Secondly for the PM1904 Polismart II detector:

- Repeating the preformed measurements (statistics & reproducibility);
- the effect of even higher dose rate level on the detector;
- measuring the dead time of the GM-tube;
- the effects of the different weather situations (hot/cold/rain/…);
- and so on …

Thirdly for the SIM cards:

- Repeating the fading experiment with more samples for time windows of days-weeks;
- investigating the effect of gamma sources on SIM cards;
- dose rate response;
- energy response;
- angular response;
- irradiation with SIM card inside phone;
- studying more and different types of SIM cards;
- creating a model for dose response based on amount of epoxy;
- effect of electricity ("using the SIM card") on the OSL signal;
- effect of punching (heat/shock) on the stored OSL signal;
- effect of lower (< 72 mGy) and of higher doses (> 4.3 Gy);
- effect of exposing the SIM card to visible light before sampling;
- …

References

[1] Polimaster."Personal communication with Polismart helpdesk", Personal Communications.

[2] ICRP, "The 2007 Recommendations of the International Commission on Radiological Protection. ICRP Publication 103. Ann. ICRP 37 (2-4)," ICRP2007.

[3] K. Beerten, F. Reekmans, W. Schroeyers, L. Lievens, and F. Vanhavere, "Dose reconstruction using mobile phones," *Radiation Protection Dosimetry,* vol. 144, pp. 580-583, Mar 2011.

[4] J. I. Lee, J. L. Kim, A. S. Pradhan, B. H. Kim, and J. S. Kim, "Retrospective Accident Dosimetry using OSL of Electronic Components of Mobile Phones " presented at the Transactions of the Korean Nuclear Society Spring Meeting, May 29-30, 2008, Gyeongju, KoreA, 2008.

[5] K. Beerten, C. Woda, and F. Vanhavere, "Thermoluminescence dosimetry of electronic components from personal objects," *Radiation Measurements,* vol. 44, pp. 620-625, May-Jul 2009.

[6] H. Y. Goksu, "Telephone chip-cards as individual dosemeters," *Radiation Measurements,* vol. 37, pp. 617-620, Dec 2003.

[7] V. Cauwels, "Het gebruik van chipkaarten binnen de ongevaldosimetrie," Master, Toegepaste ingenieurswetenschappen - nucleaire technologie, xios Hogeschool Limburg, Diepenbeek, 2010.

[8] A. Nagao and L. F. Nascimento, "SCK CEN Internship Report - Radiation Detection Properties of Smartphones", unpublished.

[9] V. Cauwels and S. Alexia, "SCK CEN Internship Report - Testing the possibilities of smartphones as active radiation detectors", unpublished.

[10] A. Marques and V. Cauwels, "SCK CEN Internship Report - Radiation Detection Properties of Smartphones", unpublished.

[11] E. b. Podgorsak, *Radiation Oncology Physics: A Handbook for Teachers and Students*. Vienna: IAEA, 2006.

[12] IAEA, "IAEA INCIDENT AND TRAFFICKING DATABASE (ITDB), Incidents of nuclear and other radioactive material out of regulatory control, 2014 Fact Sheet," I. A. E. Agency, Ed., ed. Vienna: IAEA, 2014.

[13] IAEA, *The radiological accident in Nueva Aldea*. Vienna: International Atomic Energy Agency, 2009.

[14] C. Rojas-Palma, A. Liland, N. J. A., G. Etherington, M. Del Rosario Pérez, T. Rohola, *et al., TMT handbook - Triage, Monitoring and Treatment of people exposed to ionising radiationg following a malevolent act*. Østerås: Lobo Media AS, 2009.

[15] C. Woda, "Retrospective dosimetry concepts for triage / emergency situations - Status and future needs," ed: Eurados, 2013.

[16] G. F.Knoll, *Radiation Detection and Measurement*, 4 ed. vol. Editon 4: John Wiley & Sons, 2010.

[17] L. Bøtter-Jensen, *Development of Optically Stimulated Luminescence Techniques using Natural Minerals and Ceramics, and their Application to Retrospective Dosimetry*: Risø National Laboratory, 2000.

[18] Unknown, "Light spectrum," increasing-energy-wavelength-visible-light-graph.jpg, Ed., ed, Unknown.

[19] T. DALSA. (Unknown, 17 Sept 2014). *CCD vs CMOS*. Available: http://teledynedalsa.com/imaging/knowledge-center/appnotes/ccd-vs-cmos/

[20] E. Cruz-Zaragoza, I. P. Lopez, and Iop, "CMOS sensor as charged particles and ionizing radiation detector," *Vii International Congress of Engineering Physics*, vol. 582, p. 5, 2015.
[21] K. Brown, "The Photoelectric Effect," Springfield Public Schools2011.
[22] L. Dosiek and P. D. Schalk, "Passive radiation detection using optically active CMOS sensors," *Mobile Multimedia/Image Processing, Security, and Applications 2013*, vol. 8755, p. 14, 2013.
[23] P. Siegel. (Unknown, 11 May 2015). *Introduction to Geiger Counters*. Available: https://www.cpp.edu/~pbsiegel/phy432/labman/geiger.pdf
[24] G. Gache. (2008, 11 May 2015). *How Geiger Counters Work*. Available: http://news.softpedia.com/news/How-Geiger-Counters-Work-89087.shtml
[25] Dougsim. (2012, 16 May 2015). *File : GM tube compensation*. Available: http://en.wikipedia.org/wiki/File:GM_tube_compensation.gif
[26] L. Bøtter-Jensen, S. W.S. McKeever, and A. G. Wintle, *Optically Stimulated Luminescence Dosimetry*. Amsterdam: Elsevier, 2003.
[27] A. Eipert, "Optically stimulated luminescence (OSL) dating of sand deposited by the 1960 tsunami in south-central Chile," Carleton College2004.
[28] SCK-CEN. (27 May 2015). *Nuclear calibrations*. Available: http://science.sckcen.be/en/Institutes/EHS/RDC/Nuclear_calibrations
[29] SCK-CEN. (27 May 2015). *Dosimetry Calibrations*. Available: http://science.sckcen.be/en/Services/RDC/Dosimetry_calibrations
[30] O. Van Hoey, F. Vanhavere, V. Cauwels, L. F. Nascimento, S. Alexia, A. Marques, *et al.*, "Radiation dosimetry properties of smartphone CMOS sensors (draft)", unpublished.
[31] Polimaster. (Unknown, 19 Jan 2015). *Radiation Detector PM1904*. Available: http://www.polimaster.com/products/electronic_dosimeters/pm1904/?print=true
[32] Polimaster, "Quick start operation guide - Radiation detector PM1904 Polismart II," Unknown.
[33] J. H. Barkyoumb and V. K. Mathur, "Epoxy encapsulant as serendipitous dosimeters during radiological/nuclear events," *Radiation Measurements*, vol. 43, pp. 841-844, Feb-Jun 2008.
[34] V. K. Mathur, J. H. Barkyoumb, E. G. Yukihara, and H. Y. Goksu, "Radiation sensitivity of memory chip module of an ID card," *Radiation Measurements*, vol. 42, pp. 43-48, Jan 2007.
[35] Risø_National_Laboratory, "Guide to "The Risø Single grain lase OSL system"," Risø National Laboratory, Roskilde2007.
[36] A. G. Wintle and A. S. Murray, "Quartz OSL: Effects of thermal treatment and their relevance to laboratory dating procedures," *Radiation Measurements*, vol. 32, pp. 387-400, Oct-Dec 2000.
[37] O. Van Hoey. (16 Jan 2015),"Chip cards", Personal Communications.
[38] Unipas. (Unknown, 18 Sept 2014). *pasjes*. Available: http://www.unipas-online.nl/pasjes.php
[39] ISO, "International Standard ISO 4037-1: X and gamma reference radiation for calibrating dosemeters and doserate meters and for determining their response as a function of photon energy - Part1: Radiation characteristics and production methods," 1 ed, 1996.
[40] L. Froment, "MDECAY - Radioactive Decay," ed: Ondraf - Niras, 1997.
[41] E. Rault, S. Vandenberghe, S. Staelens, and I. Lemahieu, "Optimization of Yttrium-90 Bremsstrahlung Imaging with Monte Carlo Simulations," *4th European Conference of*

the International Federation for Medical and Biological Engineering, vol. 22, pp. 500-504, 2009.
[42] Apple. (Unknown, 16 Sept 2014). *Technische specificaties van iPhone 4s*. Available: http://www.apple.com/benl/iphone-4s/specs/
[43] Phonearena. (Unknown, 16 Sept 2014). *Apple iPhone 4s*. Available: http://www.phonearena.com/phones/Apple-iPhone-4s_id5257
[44] L. Photography. (2011, 19 Sept 2014). *iPhone 4S Camera Specifications, A quick Look*. Available: http://www.lifeatf8.co.uk/blog/2011/10/a-look-at-apple-iphone-4s-camera-specification/
[45] C. Sorrel. (2011, 17 Sept 2014). *What's Inside: The iPhone 4S Camera*. Available: http://www.wired.com/2011/10/whats-inside-the-iphone-4s-camera/
[46] Touchcom. (Unknown, 17 Sept 2014). *Apple iPhone: iPhone 4S*. Available: http://www.touchcom.ie/Special_Offers/iPhone_4S/2436.html
[47] Apple. (Unknown, 17 Sept 2014). *iTunes*. Available: https://www.apple.com/itunes/

Annex A

In this section we added the technical data about the used materials. First a short table with the source information is added (Table 0-1). This table provides additional information about the nuclear sources such as which particles they emit and their energies. The source half life time and decay products are also included.

Next the technical information about the iPhone model (Table 0-2) and its camera (Table 0-3) was gathered. Followed by a list of the app's versions (Table 0-4) and their latest versions (Table 0-5).

At the end, two tables (Table 0-6 and Table 0-7) were joined providing more information about the used samples from Morpho.

Table 0-1: Source information

Source	Particles	Half life time	Beta Energy [MeV]	Gamma Energy [MeV]	Decay products	Reference
Co-60	β^- gamma	5.27 years	0.318	1.173 1.333	Ni-60 (Stable)	[40]
Sr-90	β^-	28.60 years	0.546	x	Y-90	[40]
Y-90	β^- & infrequently gamma	64.10 hours	(0.523) 2.284	1.7 (0.01%)	Zr-90 (Stable)	[40, 41]
Cs-137	β^-	30,17 years	0.512 1.173	X	Ba-137m & Ba-137 (Stable)	[40]
Ba-137m	β^- gamma	2.55 min	0.004 0.624 0.656 (0.660)	(...) 0.662	Ba-137 (Stable)	[40]

Table 0-2: iPhone technical information

	iPhone A	iPhone B	iPhone C	iPhone D
Producer	Apple			
Product name	iPhone 4S			
Version	5.1 (9B179)	5.1 (9B179)	5.1 (9B179)	8.1.3 (12B466)
Model	MD235NF	MD235NF	MD235NF	MD235NF/A
Serial number	DNXHCLEUDTC0	DNXHCLDZDTC0	DNXHCLXTDTC0	DNXHCM1WDTC0
Firmware version	2.0.10	2.0.10	2.0.10	5.4.00

Table 0-3: Technical aspects of the iPhone 4S [42-46]

	Back Camera	Front Camera
Name	iSight Camera	FaceTime-camera
Quality	8 MP (Megapixels)	0.3 MP VGA-resolution
Diaphragm	f/2.4	
Lens	Consist of 5 elements	
Filters	Hybrid IR-filter	
Focal length	4.3 mm (equivalent to 35.00 mm)	
Camera sensor size	1/3.2"	
Camera type	BSI CMOS sensor (3264x2448 pixels)	
Features	Back-illuminated sensor (BSI) Digital image stabilization, Temporal Noise Reduction, full well capacity, …	

Table 0-4: Application specifications

	Producer	iPhone A Version	iPhone B Version	iPhone C Version	iPhone D Version
iRad	antier	2.0.0	2.0.0	2.0.0	2.0.0
WikiSensor	WikiSensor	Unknown	Unknown	Unknown	Unknown
Radioactivity Counter	Dipl.-Ing. Rolf-Dieter Klein	Rev 1.1	Rev 1.1	Rev 1.1	Rev 1.1

Table 0-5: Release date and version of the chosen applications [47]

	Last released version and its release date (At research start)
iRad	V2.1.0 (08-09-2013)
WikiSensor	Removed from app store (iTunes)
Radioactivity Counter	V1.3 (21-01-2014)

Table 0-6: Chip modules from Morpho

Tag	Material	Film tape	Encapsulation	Notes
Delo 698/4670	Delo 698/4670	E1H	UV-Dam&Fill	
Vitralit 1680	Vitralit 1680	E17	UV-Glob top	
Loctite 3323/3327	Loctite 3323/3327	E2L	UV-Dam&Fill	Module not used anymore in the future
Delo 4670	Delo 4670	E18	UV-Glob top	

Table 0-7: SIM-cards from Morpho

Tag	Name	Encapsulation	Card material
SG6	SG6-16-E18	UV-Dam&Fill	ABS-card body – Laser able white
SG5	SG5-41-E17	UV-glob top	ABS-carboy – Laser able white
SC4	SG4-00-E18	UV-glob top	ABS-carboy – Not laser able white
SC2	SC2-00-E1F	UV-glob top	ABS/PVC-mix carboy – Laser able printed

Auteursrechtelijke overeenkomst

Ik/wij verlenen het wereldwijde auteursrecht voor de ingediende eindverhandeling:
Accident dosimetry with mobile phones: Real-time measurements by means of mobile phone applications & Post-accident dose reconstruction with SIM cards

Richting: **master in de industriële wetenschappen: nucleaire technologie-nucleaire technieken / medisch nucleaire technieken**
Jaar: **2015**

in alle mogelijke mediaformaten, - bestaande en in de toekomst te ontwikkelen - , aan de Universiteit Hasselt.

Niet tegenstaand deze toekenning van het auteursrecht aan de Universiteit Hasselt behoud ik als auteur het recht om de eindverhandeling, - in zijn geheel of gedeeltelijk -, vrij te reproduceren, (her)publiceren of distribueren zonder de toelating te moeten verkrijgen van de Universiteit Hasselt.

Ik bevestig dat de eindverhandeling mijn origineel werk is, en dat ik het recht heb om de rechten te verlenen die in deze overeenkomst worden beschreven. Ik verklaar tevens dat de eindverhandeling, naar mijn weten, het auteursrecht van anderen niet overtreedt.

Ik verklaar tevens dat ik voor het materiaal in de eindverhandeling dat beschermd wordt door het auteursrecht, de nodige toelatingen heb verkregen zodat ik deze ook aan de Universiteit Hasselt kan overdragen en dat dit duidelijk in de tekst en inhoud van de eindverhandeling werd genotificeerd.

Universiteit Hasselt zal mij als auteur(s) van de eindverhandeling identificeren en zal geen wijzigingen aanbrengen aan de eindverhandeling, uitgezonderd deze toegelaten door deze overeenkomst.

Voor akkoord,

Willems, Ruben